THE PML PROTEIN IS NOT ESSENTIAL FOR TELOMERE MAINTENANCE BY THE ALTERNATIVE
LENGTHENING OF TELOMERES PATHWAY (ALT) AND ITS DELETION MODIFIES ALT BIOMARKERS

By

Walter Thomas Barry

A dissertation submitted to Johns Hopkins University in conformity with the

requirements for the degree of Doctor of Philosophy

Baltimore, Maryland

December, 2017

Abstract

All cancers must maintain their chromosomal ends (telomeres) in order to continue to proliferate indefinitely and to prevent intolerable levels of chromosomal instability. In ~95% of cancers, telomeres are maintained, or extended, through the reactivation of the telomerase enzyme. For the remaining 5% of cancers, a homologous recombination-dependent mechanism called alternative lengthening of telomeres (ALT) is utilized. ALT has several associated characteristics, but no one biomarker is defining. It becomes necessary then to examine a body of data on the presence of these characteristics to confirm a cancer as having ALT as a telomere maintenance mechanism (TMM). One such characteristic is the presence of large ultra-bright telomere DNA foci visible by fluorescence in situ hybridization (FISH), and the co-localization of these foci with immunoaffinity signals for the promyelocytic leukemia protein (PML) which together are referred to as ALT associated PML bodies (APBs). Repeated reports of this phenomenon in the literature, coupled with experiments demonstrating that large ultra-bright telomere FISH foci are a likely site of significant ALT-associated activity have elevated the level of interest in APBs. The body of work described in this thesis addresses the question of whether PML is required for the ALT mechanism and the related question if the presence of APBs is a defining ALT characteristic. CRISPR/Cas9 was used to generate PML knockouts in the ALT-positive human cancer-derived cell lines U2OS and SAOS2. Cell viability and maintenance of telomeres over long term culture, the presence of telomere DNA c-circles, homologous recombination at telomeres, and the absence of telomerase activity were all tested. The results were consistent with ALT representing a TMM in PML-knockout U2OS and SAOS2 cells. Large telomere ultra-bright foci still formed in cells lacking PML, and were found to co-localize with the APB components SP100 and DAXX. However, the extent to which SP100, DAXX and large telomere foci co-localized relative to the total number nuclear bodies formed by each of these proteins was found to be significantly reduced. Therefore, while it is not required for ALT, PML does

significantly impact the frequency of co-localization between SP100, DAXX and large telomere foci, which suggests that the function of PML in ALT is as a mediator of nuclear trafficking at APBs.

Thesis Advisor: Alan K. Meeker, M.A.T., Ph.D.

                    Associate Professor, Dept. of Pathology, Oncology, Urology

Second Reader: Fred Bunz, M.D., Ph.D.

                    Associate Professor, Department of Radiation Oncology and Molecular Radiation Sciences

Committee: Fred Bunz, M.D., Ph.D. (chair)

                    Angelo DeMarzo, M.D., Ph.D.

                    Kathleen Burns, M.D., Ph.D.

Acknowledgements

The following people had a significant impact on this thesis: Alan Meeker, Christopher Heaphy, Angelo DeMarzo, Fred Bunz, Srinivasan (Vasan) Yegnasubramanian, Jacqeline Brosnan-Cashman, Mindy Graham and of course Anthony (Tony) Rizzo. I am very grateful for your help.

The following people provided significant material support: Hugh Giovinazzo, Ajay and David Esopi. Their timely help was critical.

The following people are my friends who helped me along the way: Benjamin Blumberg, Tony Cook, Kristen Barry, Jim Machamer, Nina Martin and Cara Cook.

I would like to give special thanks to Colleen Graham without whom this thesis would not have happened.

Table of Contents

List of Tables

List of Figures

Introduction

Part 1 Telomere

In humans, the sequence of a linear chromosome begins with the nucleotides TTAGGG and ends with CCCTAA. These complementary sequences exist at the termini as a hexanucleotide repeat of approximately 10 kb in length, on average. [1] The function of the telomere is to protect the end of the chromosome from degradation and prevent the recognition of the end of the chromosome as a DNA double strand break. [2] Chromosomes are not blunt ended. There is, in mammals, a single stranded length of the 3' TTAGGG repeats that is between 50 and 200 nucleotides long. [3] This is referred to as the 3' overhang. Electron microscopy of mammalian telomeres has shown the presence of a duplexed lariat structure at telomere ends. [4] These are referred to as telomere-loops (T-loops). [5] They form as a result of strand invasion of the 3' overhang to a site in cis of the telomere. Formation of the loop acts to sequester the end of the chromosome. [6]

Telomere sequences are complexed to the six proteins of shelterin. The shelterin complex is bound along the length of the telomere as a repeating unit of the six proteins, and is composed of the proteins TRF1, TRF2, RAP1, POT1, TIN2, TPP1. [2] Shelterin contributes to the chromosome end protection function of the telomere. The TRF1 and TRF2 components confer telomere repeat sequence binding affinity. [7, 8] Occupation of the telomere repeats sequesters the sequence from other nucleoplasmic proteins. Experimental inactivation of TRF1 causes gaps in telomere DNA and robust activation of the DNA damage response pathway (DDR). [9] [10] Likewise, TRF2 also suppresses the DDR pathway by inhibiting the DNA double-strand break sensor protein ATM. Experimental deletion of TRF2 can result in multiple chromosomes fusing together at their telomeres.[11-13] RAP1 deletion can cause increased telomere recombination and fragility.[14]The shelterin proteins also have a demonstrated function in assembly of the architecture of the telomere. POT1 is responsible for the binding and creation of the T-Loop.[15] TPP1 cooperates with POT1 and acts as a shelterin organizing center.[16-18]

1

A long non coding RNA referred to as TERRA (telomere repeat RNA) binds TRF2 and is considered a part of the shelterin complex.[19] TERRA is the product of the transcription of the C strand of telomeres.[20] There is no detectable transcription from the telomeric G strand, as assessed by QPCR and Northern blotting. TERRA is, on average, 300bp but can range from 100 bp to over 1 kb. [21] Transcription of TERRA is carried out by RNA pol II and begins in the subtelomeric region and proceeds into the telomere sequence. Within the subtelomeric region, a sequence of bases occurring as a repeating pattern of 61 bases, followed by 29 bases, followed by 37 bases, were identified as a TERRA promoter sequence.[22] Since it is made up of G-rich telomere repeats, TERRA can potentially form G-quadruplexes. [23] TERRA is critical for stability of the shelterin complex, with its knockdown leading to DNA damage responses, senescence, and telomere shortening - which is typical of experiments where shelterin components are disrupted.[20, 24, 25] It also plays a role in the replication of telomeres by cooperating with hnRPA1 to regulate the RPA to POT1 switch.[26] Furthermore, TERRA promotes heterochromatin formation through recruitment of HP1a to telomeres.[19] TERRA is produced throughout the cell cycle, but its abundance peaks at the start of S phase and is at a nadir at the start of G_2.[21, 27]

Dividing human somatic cells have steadily decreasing telomere lengths over time. [28] The biochemical explanation for this phenomenon is referred to as the "end-replication problem", as shown in figure S1-1 [29]. DNA polymerases require a 3' hydroxyl group on the deoxyribose ring of DNA for the catalysis of the phosphodiester linkage between two adjacent nucleotides. DNA polymerases therefore cannot synthesize entirely new strands without a 3' hydroxyl for use as a primer. This hydroxyl is supplied by a short RNA primer sequence bound to, and transcribed from, the template strand being replicated. In the so-called lagging strand, the primer is later degraded and replaced by DNA polymerized from an upstream DNA fragment (Okazaki fragment). (figure S1-1) At the 3' overhang a short complementary RNA primer can be generated. Due to this primer sequence being at the terminus

of the chromosome when the primer is degraded the sequence cannot be replaced through extension of

an adjacent Okazaki fragment. This results in a shortened 5' strand. The solution for the maintenance of

telomere lengths in humans is the reverse transcriptase enzyme telomerase.[30-33]

Telomerase, a ribonucleoprotein reverse-transcriptase, can add telomere repeats de novo to the

3' end of the chromosome. Telomerase is composed of two parts, the protein component TERT, and the

RNA component TERC. A single telomere repeat is present in TERC at the active site of TERT. TERC acts

as a template for base addition. Study of telomerase activity indicates that addition occurs in 6 bp single

telomere repeat intervals.[34] The extension of the available template for the 5' strand compensates for

the loss of the sequence due to the end replication problem. (figure S1-1) Human stem cell

compartments require telomerase to replenish their telomeres. Patients with defective components of

the telomerase pathway have pathologies relating to stem cell failure. Bone marrow failure, pulmonary

fibrosis, and increased age-related diseases are all known consequences of telomerase dysfunction.[30,

35, 36] In contrast to stem cells, most human somatic cells do not express telomerase. [37]

The Hayflick limit describes the growth of human somatic cells over time in tissue culture

settings. [38] As these cells undergo rounds of replication, they will eventually enter senescence and fail

to divide further. Research suggests that this limit is connected to the progressive telomere shortening

that occurs during every replication cycle. [28, 34] Human cancer cell lines are not subject to the Hayflick

limit, and are capable of presumably indefinite replication cycles. For a cancer to accomplish indefinite

replication they must have an active telomere maintenance mechanism (TMM). In approximately 95%

of cancers, telomerase expression is activated.[39] Examples of changes to cancer cells that serve to

activate telomerase expression include, but are not limited to, changes in telomerase gene methylation

status, genomic translocations of the telomerase gene or, modifications in transcriptional networks

regulating telomerase expression.[40-45] It is important to note that telomerase activity is measurable

but the protein itself is not. It is thought that there are fewer than 100-200 telomerase complexes in a

cancer cell. At these levels, telomerase is generally not detectable by immunohistochemistry or western blot.[32, 33]

Part 2 Alternative lengthening of telomeres

If a cancer cell line or tumor isolated from a patient has a TMM but no telomerase activity, it is designated as containing an alternate lengthening of telomeres (ALT) pathway. These samples are designated as ALT positive (+) cells. At present, the literature states that approximately 5% of cancers utilize ALT.[46-50] Initial discovery of ALT was suspect due to the fact that the concept of telomerase was still fairly new and it is difficult to measure telomerase activity, thus false negative assay results were a distinct possibility. [51, 52] Over time however, a body of convincing evidence was established in support of ALT as a bona fide TMM.[39, 46, 50, 53-58] This work established characteristics associated with ALT (+) cells, some of which are now considered ALT biomarkers.

First and foremost a cell line designated as ALT (+) must be able to be passaged (grown) continually, long-term, without undergoing replicative senescence. During this time, these cells also must maintain their telomere lengths through replication cycles. This is established by analyzing the cell line's telomere lengths at time points of low and high number of population doublings.[51, 52] Telomere lengths and their distribution are measurable by the terminal restriction fragment assay (TRF).[59] This assay relies on the fact that there are no restriction enzyme sites in telomere sequences. Thus, when genomic DNA is isolated and cut with a high cutting frequency restriction enzyme, the only large segments of DNA remaining should be the telomeres. Separation of these lengths on an agarose gel followed by Southern blotting with a telomere sequence probe allows for TRF analysis.[52, 59] Continuous growth and constant telomere lengths implies circumvention of the Hayflick limit and the presence of a TMM. These passages must also be negative for telomerase activity.[39, 53, 56, 60]

Telomerase activity is measurable by the telomere repeat amplification protocol (TRAP).[61] In TRAP, cell lysates are incubated with a suitable DNA substrate for telomerase elongation activity; yielding a laddering of the aforementioned 6 bp telomere repeats if telomerase is active. Visualization of the elongated substrates is carried out by first amplifying the elongation products with the polymerase chain reaction, followed by acrylamide gel electrophoresis separation of the PCR products. No laddering implies no telomerase activity.[61] Prolonged continuous growth in vivo, having a TMM, and lack of telomerase activity represent the essential requirements for defining a cell line as ALT(+).[51, 52, 62, 63] Beyond this requirement there are other ALT associated characteristics described below. In lieu of the aforementioned in vivo requirements, these associated characteristics (biomarkers) are used to support the designation of a sample as ALT (+), (e.g. when live cells are not available) and also provide potential clues to the mechanism of the ALT pathway.

ALT(+) cells have been recorded as having homologous recombination (HR) events at their telomeres, events that are absent at telomeres of ALT(-) cells. Telomeric HR events are measurable by the chromosome in situ hybridization (CO-FISH) assay.[53] [63]This assay is outlined in figure S2-1. In addition, homologous recombination at telomeres was identified by an experiment in which a tagged sequence cassette was inserted in one of the telomeres of an ALT utilizing line.[63] The cassette could be tracked using PCR and southern blotting and over time the cassette spread to other telomeres of the cell. Knockdown of components of homologous recombination, such as the MRE11/NBS1/RAD50 complex, cause senescence and apoptosis in ALT(+) cells, implicate DNA damage signaling and homologous recombination as important for the continued replication of ALT(+) cells.[55, 64, 65] These publications contribute to the current understanding of the mechanism of the ALT pathway to be based on homologous recombination. The overall telomere lengths in an ALT cell line as measured by Southern blotting are extremely heterogeneous, typically ranging from below 1 kb to above 10 kb. [56] Unequal

recombination events leading to one telomere being extended while another is shortened may be contributing to the source of this heterogeneity.

The presence of extrachromosomal circles of telomere DNA is another biomarker of ALT (+) cells and their formation may be linked to ongoing homologous recombination at telomeres. [66] Because the telomere sequence is repetitive, and therefore homologous along its length, intra-telomere recombination can occur which can result in the excision of a circle of telomere DNA, a schematic of which is provided in figure S2-2. [67] A circle of telomere C strand DNA is aptly referred to as a C-circle. The assay for the presence of C-circles is outlined in figure S2-3. [66] The C-circle assay utilizes the phi29 processive polymerase. This polymerase will continuously polymerize if template is available and is capable of DNA strand displacement. Research suggests that at least a fraction of C-circles are partially double stranded.[66, 68] Thus, fragments of G rich telomere DNA strands are hybridized to the covalently linked circle of C rich telomere standand can therefore serve as a primer for DNA polymerization by phi29 polymerase. Because the template is circular, phi29 can continuously polymerize. What results is significant amounts of DNA complementary to the C-circle. The products can then be dot blotted onto a membrane and visualized by hybridizing a labelled G-rich telomere sequence probe to the membrane. A sample is considered positive for c-circles if any signal is detected from this reaction, thus the c-circle assay is used as a binary marker for ALT-positivity.[66]

ALT (+) cells contain a nuclear structure referred to as an ALT associated promyelocytic leukemia protein (PML) body (APB). These are PML nuclear bodies with telomere coincidence that may also include other ALT associated contents such as the components of the homologous recombination repair pathway.[54, 69, 70] Determination of the presence of APBs in whole cells on a microscope slide is carried out by combined fluorescent in situ hybridization (FISH) using a telomere sequence specific fluorescently labelled probe and immunofluorescence (IF) for the PML protein. Telomere signals co-localizing with signals from PML are, in combination, considered APBs. The other protein contents of

6

APBs are determined through a similar co-localization analysis utilizing IF. It is not that PML forming a nuclear body is specific to ALT, but rather the ALT specific contents of these bodies that links PML to ALT. PML readily forms nuclear bodies in ALT negative cells.[71-78] The next section provides an in depth look at PML, followed by further explanation of the potential role of PML in ALT.

Part 3 The Promyelocytic Leukemia Protein

The promyelocytic leukemia protein was initially discovered as a protein that is overexpressed in promyelocytic leukemia as a product of a recurrent 15;17 translocation. Here, PML is the N-terminal half of the oncogenic fusion protein PML-RARa; the C-terminus encodes the retinoic acid receptor. The PML promoter is constitutive, so it drives high levels of the fusion protein, which acts as a dominant negative in this leukemia. The primary driver of the disease is the retinoic acid receptor because it has lost the regulatory domains of the N-terminus. [79-82] Interestingly, at first because of this association, PML was thought of as an oncoprotein. [83] It would only later be identified as a tumor suppressor through over expression studies and animal models.[72, 84]

The PML protein has eleven recorded isoforms of varying sizes from 48 kDa to 91 kDa .[85] When it is assayed by western blotting, a ladder of these different isoforms is observed. PML is a member of the tripartite motif protein family (TRIM), comprised of a RING-B-Box-Coiled-coil (RBCC) domain in exons 1-3 and a SIM (SUMO interacting motif) in exon 7 (see figure S3-1). [75, 86] PML is mostly a nuclear protein but isoform 1 does have a nuclear export signal which allows this isoform to shuttle from the nucleus to the cytoplasm and back.[87] PML was present in the ancestor of all chordates and is expressed in all human cells. The function of PML is partly connected to its structural roles in the nucleus.[88]

PML will oligomerize into hollow spheres that can be of many sizes. These spheres, referred to as PML nuclear bodies (PML-NB), are dynamic and change based on stress, position in the cell cycle,

DNA damage and differentiation status.[74, 76, 83, 89-94] The PML-NB is often described as a storage

depot of nuclear proteins. Examples of PML body resident proteins include SP100, DAXX, ATRX and BLM.

The PML-NB may be considered as a storage depot because DNA is not often found within the sphere,

and it is believed PML exerts its role mostly through protein-protein interactions.[73, 95]. The functions

of the example PML body resident proteins, on the other hand, have so far been identified as occurring

at or with DNA sequences.[46, 94, 96-98] PML therefore may sequester these proteins from the DNA

until their appropriate time and place of action.

It is as a result of the diversity of potential interactions that research on the precise function of

PML has proven challenging. Often when investigating the existing published literature on PML, one

finds research on one of the PML interacting proteins, with an enzymatic or DNA binding domain of the

interacting protein being the primary focus and its subsequent connection to PML although being

secondary, heavily referenced in terms of the function of PML. Exemplifying this difficulty is the fact the

PML knockout mouse has no gross phenotype. PML connects with many proteins but apparently itself is

not vital in mice.[71, 72] It is of note that the database *Online Mendelian Inheritance of Man* (OMIM)

lists no human genetic diseases directly linked to mutations only in the PML gene.[99] However, PML is

essential for induced pluripotent stem cell differentiation of human cells.[78] It is important to bear in

mind that PML sits within a large web of interactions with no immediate discernable consequence to its

total loss based on prior data. This fact alone makes PML an attractive target for further basic research.

PML has mostly been studied in terms of the PML-RARa oncofusion; while exploration of its intimate

connection to the ALT pathway has been comparatively under explored.

The ALT associated PML body or APB is widely considered to be one of the defining features of

ALT. APBs were discovered early in the history of ALT in 1999, while ALT had first been described as such

in 1997. The connection between the two was made as a result of the striking uniqueness of the IF for

TRF1 and telomere FISH stains of ALT cells.[69] Together they form a ring or a disc. This disc is, as one

could imagine, the cross section of a sphere observed in cut tissue sections. PML was previously recorded as forming this unique shape in PML bodies. When co-staining, these rings were found to be are coincident between all three of these protein species. These overlying rings of telomere, TRF1, and PML are only found in telomerase-negative cells. Through later work, the ALT specific components of APBs were determined to be the coincidence of telomere DNA, shelterin components and components of the homologous recombination repair pathway, including Rad51, BRCA1/2, BLM, WRN, MRE11/NBS1/RAD50. [54, 55, 69, 100-103] Interestingly, a full study of ALT cell lines characterizing APB prevalence has not been performed. Each cell line or patient sample will have a unique APB pattern. Such variation makes it challenging to make broad statements about APB frequency and its potential significance to ALT. Most will simply define an APB as any coincident telomere and PML focus.[101] A subset of cells within an ALT-positive population is typically seen to harbor relatively large amounts of telomere DNA sequences in discrete intra-nuclear foci. These large aggregates of telomere DNA often, though not always, co-localize with PML protein. It is also possible to have large telomeric FISH foci and have no PML co-localization.[50]

The functional significance of APBs to the ALT pathway may involve the purported designation of the APB as the site of the homologous recombination underlying the mechanism of ALT.[54, 64, 65, 70, 101-107] The APB is extremely unusual. The telomere signal found at APBs can be much more intense than a single chromosomal telomere. This could mean that it represents either the association of many telomeres, or a concentration of continuously replicating extra-chromosomal telomere DNA sequences. This replication could be the result of dysfunctional S-phase, ongoing homologous recombination or another repair process, and a variety of extra-chromosomal telomere DNA species have been identified in ALT-positive cells.. It has been reported that APBs form during G2.[54] That indicates this is a post-replicative process, and since homologous recombination is supposed to occur in G2 it lends credence to the possibility that the APB is the site of telomere homologous recombination

9

(HR). This is further supported by the presence of many HR proteins at APBs. RAD51, RAD52, RPA, RAD51D, BLM, WRN, RAP1, BRCA1, MRN complex and many others have been identified.[54, 57, 58, 69, 108] These coincidences have been supported by the live cell imaging of ALT telomeres which were shown to cluster to APBs once damaged.[64, 101, 103, 104, 106] These same references support the proposal that the APB is the site of the HR believed to be the basis of the ALT pathway.

In order to determine if there are direct requirements between the presence of the PML protein and the mechanism of the ALT pathway, the CRISPR/Cas9 genome editing system was used to introduce nonsense mutations into the PML gene of the well-characterized ALT (+) human cell lines U2OS and SAOS2. Long-term viability of these cell lines without the PML protein indicates that PML is not required for these cell lines to survive. This fact alone does not establish that ALT as a TMM is ongoing in these PML knockout (KO) cell lines. As outlined in part 2, each of the characteristics of ALT as a TMM must be assessed by their designated assays in order to provide a rigorous and informed designation of ongoing ALT. Once ALT status has been established as ongoing, the impact of PML KO on the number and frequency of co-localization of the PML body resident proteins SP100 and DAXX was assessed by IF. A change in the number of nuclear bodies formed by SP100 and DAXX was contradictory between the two cell lines; however, the frequency of co-localizations between the two proteins was decreased in both lines. Both SP100 and DAXX are found with telomere DNA foci in APBs. The analysis of nuclear bodies in PML KO cells was therefore extended to also include the ultra- bright telomere signals also found in APBs. Study of these three bodies provides insight into APB formation in the absence of PML. It was found that co-localizations between these three entities were decreased. This implies that the function of PML in ALT (+) cells is in nuclear trafficking at APBs.

Materials and Methods

Cell Culture, Plasmids and transfection

The following cell lines used in this study were obtained from American Type Culture Collection, Manassas, VA: U-2 OS (HTB-96), Saos-2 (HTB-85), SJSA-1 (CRL-2098), MG-63 (CRL-1427). HEK293T packaging line was provided by the laboratory of William Nelson (Johns Hopkins School of Medicine, Baltimore MD). U-2 OS, Saos-2, HEK293T were maintained in DMEM, high glucose, pyruvate supplemented with 10% fetal bovine serum (FBS) and 100 units/ml penicillin and 100ug/ml streptomycin (ThermoFischer, Waltham, MA). SJSA-1 was maintained with RPMI supplemented with 10% FBS 100 units/ml penicillin and 100ug/ml streptomycin (ThermoFischer, Waltham, MA). MG-63 was maintained with MEM supplemented with 10% FBS 100 units/ml penicillin and 100ug/ml streptomycin (ThermoFischer, Waltham, MA). All cell lines were maintained at 37°C and 5% CO_2. The following plasmids were obtained from Addgene Cambridge, MA: pSpCas9(BB)-2A-GFP PX458 (#48138), lentiCRISPRv2 (#52961), psPAX2 (#12260), pCMV-VSV-G (# 8454), pLJMI-EGFP (#19319), pLPC-Flag-PML-IV (# 62804), pDsRed2-N1 (#54493). The HR and NHEJ reporters were a kind gift of Vera Gubernova (University of Rochester, NY)[109]. The FLAG-PML gene from pLPC-Flag-PML-IV was cloned into pcDNA3.1 (ThermoFischer Waltham, MA). Transfections were carried out with cationic liposomes (Lipofectamine 3000 #L3000001, Thermo Fischer, Waltham, MA)

Genome Editing by CRISPR/Cas9

A wild type cas9 based genome editing strategy was devised for the PML gene. All known isoforms of PML have an identical N-terminus diverging at the fourth exon, thus in order to ablate all isoforms a target site for the second exon was designed using CRISPRdirect (http://crispr.dbcls.jp/). Guide RNAs were synthesized by Integrated DNA Technologies (Coralville, IA) gPML340 5'-CGAAGCTGCTGCCTTGTCT- 3'. Two CRISPR delivery methods were utilized. The first utilized transfection

to deliver pSpCas9(BB)-2A-GFP, with the above guide sequences inserted, to the U2OS cell line. A cell

sorting procedure based on GFP was then used to isolate transfectants. Cells were plated onto 150 mm^2

round dishes. Once clonal colonies reached at least 3 mm in diameter they were isolated with cloning

cylinders and re-plated into individual wells of a 24-well plate. Clones were screened for loss of PML

expression via immunofluorescence (IF) and western blotting. The second method utilized lentiviral

delivery of lentiCRISPRv2 with the above inserted guide sequences. The remaining cell lines proved

difficult to transfect and necessitated a lentiviral approach. Virus was produced in the HEK293T

packaging cell line by transient transfection with the plasmids psPAX2, pCMV-VSV-G, and

lentiCRISPRv2(PML). The supernatant from three days post transfection was used for transduction with

8 ug/ml hexadimethrine bromide. Transduction was carried out with enough of this supernatant such

that 10% of transduced cells were positive for inserted cas9 expression. Transduced cells were placed

under 2 ug/ml puromycin selection three days post transduction. Colonies were picked and clones

initially screened for loss of PML expression via IF. In order to confirm genetic disruption clones were

sequenced at the cas9 target site through a two-step process. First PCR was performed on genomic DNA

isolated from clones with primers flanking the cas9 target genome site. Forward:

CGAAGCTGCTGCCTTGTCT Reverse: CTCGTGCTTGAGGAACCACT. Then PCR products were TOPO cloned

and transformed into TOP10 competent *e. coli* (cat. K450001, Thermo Fischer, Waltham, MA).

Transformants were plated overnight at 37°C; colonies were picked and grown overnight in Lysogeny

Broth at 37°C. Plasmid DNA was isolated using the Qiagen miniprep kit (cat. 27104, Qiagen,

Germantown, MD). Plasmids were then sequenced by Eurofins (Lousiville, KY) using stock primers for

the TOPO plasmid construct. In addition, clones were assayed for PML expression at the protein level by

Western blotting (below).

Cells were plated with fresh media at 5000 cells per well according to Coulter Counter

measurements (Beckman Coulter, Brea, CA) in a 96 well plate. These were then placed in the Incucyte

system (Essen Bioscience, Ann Arbor, MI) to grow under standard growth conditions for seven days. This

system is essentially a camera mounted in an incubator that takes detailed images of every well.

Confluency measurements were taken automatically every four hours. Confluency curves were

generated using IncucyteZoom software (Essen Bioscience, Ann Arbor, MI).

Microscopy and Image Analysis

Two microscopes were used in this thesis for capturing images. For section 1, 2, 3 and 5 slides

were imaged with a Nikon 50i epifluorescence microscope equipped with X-Cite series 120 illuminator

(EXFO Photonics Solutions, Mississauga, ON, Canada) and appropriate fluorescence excitation/emission

filters. Grayscale images were captured using Nikon NIS-Elements software version 2.30 and an attached

Photometrics (Tucson, AZ) CoolSNAP EZ digital camera, pseudo-colored, and merged.

Images in section 4 were captured using the Tissuegnostics TissueFAXS fluo automated

fluorescent microscope with accompanying light sources and appropriate fluorescence

excitation/emission filters. This also included Tissuegnostics branded imaging software. Use of this

microscope was particularly useful because it provided hundreds of images collected in a consistent

manner.

Images from both sources were analyzed in the same manner for number of puncta and number

of co-localizing puncta. Images were loaded into the imageJ analysis software. Background was

subtracted using a rolling ball algorithm using the same parameters for all images. This removes auto

fluorescence of cells. Images were then thresholded for brightness such that all but the faintest puncta

were included. This is to remove potential background from nonspecific antibody binding. Each channel

was thresholded separately and threshold parameters were kept the same for each single stain across experiments. The process of thresholding turns the images into binary signals, as once the brightness is set the intensity is no longer required for the next step. The images could then be analyzed with a tool in imageJ to count the number of events (puncta) across an image which is referred to as a field of view in this thesis. For co-localizations between channels involves the same steps except after thresholding the images are overlaid. The program identifies overlapping pixels using the co-localization plugin tool for imageJ available from: https://imagej.net/Colocalization_Analysis. These events are then counted using the same tool for single image counting.

Immunofluorescence and Western Blotting

Cells were grown on chambered cell culture slides (# 154534, ThermoFischer Waltham, MA) for at least 24 hours and then fixed at room temperature in formalin, neutral buffered, 10% (# HT501128, Sigmaaldrich, St. Louis, MO) for 20 minutes followed by a permeability buffer of .5% triton-x (# 9002-93-1, Sigmaaldrich, St. Louis, MO) in pH 7 PBS for 15 minutes. Slides were then blocked for ten minutes using Dako serum free protein block (X090930-2, Agilent, Santa Clara, CA). Primary antibody diluted in antibody dilution buffer (251-018, Ventana, Tucson, AZ) was applied for an overnight incubation at 4 °C followed by Molecular Probes Alexa-Fluor fluorescently labelled secondary antibodies in PBS-Tween20 for 30 minutes at room temperature (ThermoFischer, Waltham, MA). Before mounting with ProLong Gold antifade reagent (P36931, ThermoFischer) slides were incubated with 4',6-diamidino-2-phenylindole (DAPI) for five minutes (ThermoFischer, Waltham, MA). Monoclonal primary antibodies used in this study: anti-PML (#sc-966, Santa Cruz, Dallas, TX and, ab200200 Abcam, Eugene, CA), anti-SP100 (ab167605, Abcam, Eugene, CA), anti-DAXX (#HPA008736, ThermoFischer, Waltham, MA), anti-phospho-Histone-H2A.X Ser139 (#05-636-I, Millipore, Billerica, MA), anti-TRF2 (NB110-57130, Novus Biologics) and anti 53BP1(Novus #NB100-305A-1). For Western blotting cell pellets were harvested from log phase growth cultures and proteins were extracted using RIPA buffer (#9806, Cell Signaling, Danvers,

MA) with protease inhibitor cocktail (#04693159001, Roche, Basel, Switzerland). Concentration of protein was determined by the BCA assay (#23225, ThermoFischer, Waltham, MA). 30 ug of protein were loaded into each lane of a stacking 4-15% Mini-Protean TGX gels (#4561081, BioRad, Hercules, CA). An electrical potential of 150V was applied to the gel via a cassette suspended in a bath of 25mM Tris, 192mM glycine, .1% SDS pH 8.3. A wet transfer onto a nylon membrane (#Z670197, Sigma-Aldrich, St. Louis, MO) with transfer buffer 25mM Tris, 192mM glycine and 20% methanol was carried out overnight at 10mA. Primary antibody was diluted in TBS-Tween20 with 5% dry nonfat milk and added to the membrane for an overnight incubation at 4°C. Membranes were washed three times for 5 min with TBS-Tween20. HRP conjugated secondary antibodies diluted in TBS-Tween20 with 5% dry nonfat milk were incubated with the membrane for one hour at room temperature (#7076S, Cell Signaling, Danvers, MA). After three washes with TBS-Tween20 for five minutes ECL substrate (#1705061, BioRad, Hercules, CA) with photosensitive film (#3409, Fujifilm, Japan) were used to visualize western blot results according to the manufacturer's instructions.

Telomere DNA FISH

Telomere specific fluorescent in situ hybridization was performed using a Cy3 labeled PNA probe with the N to C terminus sequence of CCCTAACCCTAACCCTAA. [110]This PNA probe was synthesized by Panagene, Daejeon, South Korea. This sequence is complementary to the mammalian telomere repeat sequence corresponding to the G-rich strand. For FISH alone, or combined with immunofluorescence, chamber slides were fixed and permeabilized as described above followed by steaming in citrate buffer for 35 minutes (Vector Laboratories, GA). Slides were then dehydrated stepwise in increasing concentrations of ethanol and water, 70%, 90%, 90% for five minutes at a time ending in air drying. The FISH probe hybridization mix used consists of 70% formamide, 30% water, 10 mM Tris-HCl pH 7.5. Telomere probe was added to the mix for a final concentration of 0.3 ug/ml. Enough of the probe in hybridization mix was added to cover the slide followed by a coverslip. Slides were incubated at room

temperature for two hours in a humidified chamber and then washed twice for 15 minutes with a PNA

wash solution of 70% formamide, 30% water, 10 mM Tris-HCl pH 7.5. Slides were rinsed briefly in PBS

and stained with DAPI. Prolong Gold anti-fade mounting medium was then applied and slides were

cover slipped. Immunofluorescence and telomere FISH protocols can be combined on the same slide for

combination FISH and immunofluorescence. Telomere FISH is first carried out to the PBS rinse step after

the PNA wash and then the (above) immunofluorescence protocol is followed starting from protein

blocking until coverslipping.

Telomere RNA FISH (TERRA)

TERRA-specific FISH is similar to telomere DNA FISH, except for the use of locked nucleic acid

probes instead of PNA and there is no denaturation.[111] These also require different hybridization

conditions to maintain telomeric DNA in its native double-stranded form, so as to avoid undesired probe

hybridization to telomere DNA species, rather than the desired binding to telomere RNA species

(TERRA). The TERRA LNA probe sequence

is:FAM/CCCTA+AC+CCT+A+AC+CCTAACCCT+A+ACCCT+A+ACCCT+A+ACCCT+AA-FAM with FAM being a

green fluorescent probe label and the + sign indicating the following base as a locked nucleic acid. The

opposite strand probe is TAM/GGGT+TAGGG+T+TAG+GGTTAGGG+T+TAGGG+T+TAGGG/TAM with TAM

being a red fluorescent probe label. Both were ordered from Exiqon in Denmark. Cells grown in chamber

slides were fixed and permeabilized as outlined above. For hybridization, slides were dehydrated

stepwise as outlined above. The TERRA FISH or opposite strand probe hybridization mix is 2xSSC, 50%

formamide, .2% BSA, 10 ug yeast tRNA (Thermo FischerAM7119) and 200 nM of probe. The mix is

incubated on the slide for 1 hour in a humidified chamber at 37 °C. Wash follows with .1x SSC for 15

minutes at 60 °C then 2x SSC for 5 minutes. Slides are DAPI stained and mounted as outlined above. For

RNAse treatments 200 ug/ml of RNAse A (#10109142001, Sigma Aldrich) in PBS was applied to the slides

before the dehydration step for 30 minutes at 37°C. Denaturation treatments use the citrate steam outlined above for telomere DNA FISH before dehydration steps.

Telomere COFISH

The telomere-specific chromosome orientation fluorescence in situ hybridization (COFISH) assay [112] was performed by first supplementing the media of logarithmically growing cell cultures at 70% confluency with 7.5 uM bromodeoxyuridine and 2.5 uM bromodeoxycytidine (B5002 and COM448648460, Sigma-Aldrich, St. Louis, MO). 24 hours later the media was exchanged for fresh pre-warmed media containing 100 ng/ml colcemid (15210040, Thermo Fischer, Waltham, MA). After a two hour incubation under normal growth conditions, cells were trypsinized (25300054, Thermo Fischer, Waltham, MA) and neutralized with pre-warmed growth media. Cells were centrifuged at 800x g RCF for five minutes and washed once with 1x PBS and pelleted again. The pellet was then suspended in 15 ml of a hypotonic solution of .07 M KCl and incubated in a water bath at 37°C for 30 minutes. Cells were carefully pelleted at 800x g RCF for five minutes. The hypotonic solution was aspirated to 100 ul remaining and one and a half volumes of fresh iced fixative solution of 3:1 methanol: glacial acetic acid was added (~400 ul) resuspending the pellet. This was incubated on ice for 30 minutes. Cells were centrifuged at 800x g RCF for five minutes, placed on ice, supernatant was aspirated, and cells suspended in 500 ul of iced fresh fixative. Positively charged microscopy slides (16004-406, Randor, PA, VWR) were prepared for metaphases by soaking slides for 30 minutes in a solution of ethanol and .5% (v/v) concentrated HCl. Slides were then rinsed in ice water and placed on a moistened stack of paper towels. A transfer pipette was used to drop suspended cells onto the slides. After dropping, slides were briefly rinsed in fresh iced fixative and placed on a rack to air dry overnight.

Prepared metaphase slides were rehydrated in PBS and treated with 0.5 mg/ml RNase A (A797C, Promega, Madison, WI) in PBS for 20 minutes at 37°C. Slides were rinsed in PBS. Slides were then

incubated in 0.5 ug/ml Hoechst 33258 (861405, Sigma Aldrich, St.Louis, MI) 2x SSC for 15 minutes at

room temperature. Slides were then placed in a shallow tray of 2x SSC and exposed to 365 nm UV light

for $5.4 \times 10^3 J/m^2$. Slides were then treated with 10 U/ul exonuclease III in supplied buffer (M0206, New

England Biolabs, Ipswich, MA) for 30 minutes at 37°C followed by a 5 minute PBS wash and dehydration

by graded ethanol series. Two telomere specific PNA probes were used for FISH. A Cy3 labelled N to C

telomere sequence CCCTAACCCTAACCCTAA "TelC" and a FITC labelled N to C telomere sequence

GGGATTGGGATTGGGATT "TelG". FISH was then performed according to the procedures outlined above

with first the TelG probe followed by washes and then the TelC probe followed by washes. Slides were

incubated with DAPI for 5 minutes before a PBS rinse and coverslipping with Prolong Gold mounting

solution. Images of individual metaphases were taken manually (see microscopy). Scoring of telomere

exchanges was carried out by first recording the total number of clearly identifiable and complete sister

chromatid pairs. Then the fluorescent channels specific to the TelG and TelC probes were overlaid. Each

identified chromatid pair was scored positive for an exchange if on a single chromatid arm there were

coincident TelG and TelC signals.

Terminal restriction fragment (TRF) measurement

Following an overnight digestion at 37 °C of cell pellets with at least 5 x10^6 cells with 100 ug/ml

proteinase K (# 3115887001 Sigma-Aldrich) Phenol/chloroform (#7761 Sigma-Aldrich) was used to extract

high molecular weight genomic DNA from frozen cell pellets of at least 5 x10^6 cells.[59] Genomic DNA

from the aqueous fraction of the phenol/chloroform extraction was precipitated with 70% ethanol and

.2 M sodium acetate and then suspended in water. The entire sample of genomic DNA was digested

with 50 U of MboI (NEB# R0137L) and AluI (NEB# R0147L) overnight at 37 °C. DNA concentration was

then measured with the Qubit using the HS dsDNA kit according to manufacturer's instruction (#Q33851

Thermo-Fischer). Each sample was loaded equally at 2 ug per well of a 1% agarose gel made from TAE

(#15558026Thermo-Fischer). Gel electrophoresis at 100V for 4 hours was carried out. The gel was

bathed with .25N HCl for 30 minutes for depurination following electrophoresis. The gel was then

denatured with denaturation solution (0.5M NaOH 1.5 M NaCl) for 30 minutes. The gel was then

neutralized with neutralization solution (2.5 M NaCl, 1.5 M Tris base) for 30 minutes. The gel was then

bathed in 20x SSC with gentle agitation for 30 minutes. Downward transfer with 20x SSC (#15557036

ThermoFischer) overnight was used to transfer DNA to a positively charged nylon membrane (

#11209299001, Sigma-Aldrich). The membrane was crosslinked to the DNA by UV light using the

crosslink setting on a Stratalinker which was followed by a 2x SSC wash. A DIG labelled DNA telomere

repeat (CCCTAA 24bp) probe was then hybridized at 2nM to the membrane using DIG easy hyb

(#11603558001, Sigma-Aldrich,) overnight at 42 °C in a rolling bottle. The membrane was washed with

first 2xSSC + 0.1% SDS for 5 minutes at room temperature then .2x SSC + 0.1% SDS for 30 minutes at 50

°C. The membrane was blocked with 5% milk for 30 minutes. Anti-DIG-AP Fab fragment (#11093274910,

Sigma-Aldrich) in 5% milk at a 1:10000 dilution was applied to the membrane for 30 minutes at room

temperature. The DIG easy hyb wash and buffer set (#11585762001, Sigma-Aldrich,) was used to wash

the membrane for 30 minutes with wash buffer and equilibrate the membrane for detection with

detection buffer for 5 minutes. CDP-Star-ready-to-use (12041677001, Sigma-Aldrich) was used as

substrate for chemilluminescence. Images of the membrane were captured using the Chemidoc Imaging

System from Bio-rad.

C-circle assay

Genomic DNA was isolated from frozen cell pellets using the DNAeasy Qiagen kit (#69504)

according to the manufacturer's instructions.[66] Using 50 ng of this DNA the phi polymerase reaction

was carried out. The reaction consists of 10 mM TTP, GTP, ATP, final 1x buffer of included with the phi29

polymerase, 2 U of phi29 polyermase (#M0269S, NEB) with the thermal cycling program of 30 °C for 8

hours, 65 °C 20 minutes with a 4 °C hold. This reaction was loaded onto a positively charged nylon

membrane in a Schleicher & Schuell Minifold-1 dot blot apparatus, according to manufacturer's

directions. The membrane was UV crosslinked with a Stratalinker. A DIG labelled DNA telomere repeat (CCCTAA 24bp) probe was then hybridized at 2nM to the membrane using DIG easy hyb (#11603558001, Sigma-Aldrich,) overnight at 42 °C in a rolling bottle. The membrane was washed with first 2xSSC + 0.1% SDS for 5 minutes at room temperature then .2x SSC + 0.1% SDS for 30 minutes at 50 °C. Membrane was blocked with 5% milk for 30 minutes. Anti-DIG-AP Fab fragment (#11093274910, Sigma-Aldrich) in 5% milk at a 1:10000 dilution was applied to the membrane for 30 minutes at room temperature. The DIG easy hyb wash and buffer set (#11585762001, Sigma-Aldrich,) was used to wash the membrane for 30 minutes with the wash buffer and equilibrate the membrane for detection with the detection buffer for 5 minutes. CDP-Star-ready-to-use (12041677001, Sigma-Aldrich) was used as substrate for chemilluminescence. Images of the membrane were captured using the Chemidoc Imaging System from Bio-rad.

Telomeric repeat amplification protocol (TRAP)

Cell pellets of 1x 10^6 were lysed in a 1% NP-40 (#28324B, Thermo-Fischer) lysis solution. Lysis solution: 10 mM Tris-HCl pH 8.0, 1 mM $MgCl_2$, EDTA 1 mM, .25mM Sodium deoxycholate, 10% glycerol, 5 mM NaCl and .1 mM AEBSF (4-(2-aminoethyl)-benzenesulfonyl-sluoride-hydrochlorine) (#A8456, Sigma-Aldrich). [61] After 30 minutes on ice, 2500 cell equivalent of this lysate was used in a telomerase-dependent primer extension assay having a PCR-based readout. The buffer solution contains 200mM TrisHCl, 15 mM $MgCl_2$, 630 mM KCl, tween 20 .5% (v/v), 10 mM EGTA. This buffer contains a primer mix and .2 U Taq DNA polymerase and 10mM dNTP. Primer sequences used: Downstream TRAP: GCGCGGCTTACCCTTACCCTTACCCTAACC, Upstream TRAP AATCCGTCGAGCAGAGTT, Internal standard AATCCGTCGAGCAGAGTTAAAAGGCCGAGAAGCGAT reverse standard: ATCGCTTCTCGGCCTTTT to a final 2uM of each primer. Reaction mix was then thermal cycled with the following program: 30 °C for 30 min, heat inactivation at 94 °C for 10 minutes, denatured at 94 °C for 30 s

with a 72 °C extension of 45s. The whole reaction was run on a TBE precast acrylamide gel (#4545034

Novex) containing SYBR green dye for 140 minutes at 200 V and imaged using UV light.

Telomere Dysfunction Foci (TIF)

Combined telomere FISH and immunofluorescence for 53BP1 (#NB100-305A-1, Novus) were

performed as outlined above, and images were captured (see microscopy). [113] Using the image

analysis program imageJ, as outlined in microscopy, the number of co-localization events between

telomere FISH and IF for 53BP1 was determined. The number of co-localizations on a per cell basis was

determined using this program by marking nuclei from the DAPI stain as regions of interest (ROI) and

manually counting events per ROI.

Results

Part 1 TERRA

      The telomeres of mammalian cells have a DNA, a protein and an RNA component.[20, 114] The mechanism of the ALT pathway could potentially be the result of changes in any or all of these components. It is known that the RNA component is in part made up of the non-coding transcription of the C-rich strand of the telomere.[21] These telomere transcripts are known as TERRA. In order to examine potential changes in TERRA nuclear localization as a result of the presence of ALT, a protocol combining aspects of DNA fluorescence in situ hybridization (FISH) and RNA (FISH) had to be adapted for use in intact cells.[111] In order to visualize a target under a standard fluorescence microscope a single fluorochrome or epitope is not enough, there must be on the order of thousands. Traditional DNA FISH uses the double stranded DNA sequence of interest as the basis for the probe. The target sequence for such probes must be large, such as those contained in a bacterial artificial chromosome (BAC), resulting in probe binding all along the target's length, providing sufficient signal for chromogenic or fluorescent imaging. It is also necessary to denature the target cell sample (such as with boiling, steaming or microwaving) to unwind the DNA or otherwise reveal the target sequence for hybridization. In contrast, RNA FISH can be performed with much shorter probes because, while DNA targets are only present as two copies, RNA has many transcripts per cell to bind. Since RNA is single stranded no denaturation is necessary and is actually detrimental since the target sequence is also located in the source DNA and will also be detected by the RNA probe. Telomeres are a special case and complicate these procedures. The telomere sequence is repetitive and each of the 92 telomeres per cell can be over 10 kb in length. The telomere sequence probe takes advantage of this by being 18 bp in length; binding all along the repeat sequence it effectively becomes the large probe sequence outlined above. This is problematic for RNA FISH because this probe could theoretically hybridize and thereby visualize both RNA and DNA. It

22

becomes necessary then, when examining TERRA, to have a series of controls to make sure only telomere RNA is being detected.

The ALT positive U2OS cell line used in this study had not previously been examined for TERRA FISH at the time of the experiment (figure 1-1). Since ALT cells have unique telomere biology, I sought to look at changes in TERRA unique to ALT. TERRA is known to consist of UUAGGG repeats. Under native conditions no denaturation of DNA was performed so no telomere DNA should be detected. TERRA is a shelterin component so it appears as foci distributed throughout the nucleus mirroring the pattern of a telomere DNA stain.[19] Thus, for assessing TERRA by RNA FISH, to ensure signals are not actually originating from telomere DNA, another slide was treated with RNAse before hybridization. Here, the FISH signal was significantly reduced or almost eliminated after RNAse treatment (figure 1-1). Denaturation of DNA by steaming serves as a positive control for the hybridization reaction and demonstrates the pattern of telomere DNA staining that the TERRA stain mirrors (figure 1-1). To see if an ALT cell could have telomere RNA consisting of the opposite telomere strand, a hybridization to detect CCCUAA repeats was carried out under native conditions. No signal was detected in this instance, and this also implies that telomeric DNA is not significantly denatured and available for hybridization under these native hybridization conditions (figure 1-1). A denatured condition was performed to confirm that the probe was working as intended by binding its complementary DNA sequence (figure 1-1). After this protocol was fully working in the lab, a paper concerning a number of aspects of TERRA in ALT was published thereby, obviating a number of hypotheses.[107] Another TERRA-related effort attempted was development of a TERRA FISH stain in formalin-fixed tissue sections. Unfortunately, we concluded that the heating or other chemical exposures performed in creating paraffin sections prevented RNA only detection. Due to these issues, the primary focus of the thesis work was shifted to examining the role of the PML protein in ALT.

Part 2 Disruption of PML in ALT Positive Cells

PML has been implicated to be involved in ALT because the large telomere FISH foci that appear in cells utilizing the ALT pathway will frequently have co-localizing PML by IF. [69] This Co-incidence of the large telomere foci with PML protein are referred to as ALT associated PML bodies (APBs). In spite of this designation, the functional connection between the PML protein and the ALT pathway is underexplored. The present study seeks to elucidate the nature of this connection by comparing a model of the ALT pathway in the presence of PML to a model of the ALT pathway in the absence of PML. This involves first establishing stable PML expressing and non-expressing cell lines of identical background and second the assessment of ALT pathway activity in these two groups.

Two adherent cell lines that are commonly used and also maintain telomeres by ALT are the human osteosarcoma cell lines U2OS and SAOS2. Both have APBs and are mentioned as having such frequently in the literature.[70] An example of these distinctive bodies visible by combined PML IF and telomere FISH appears in figure 2-1. In APB, PML can form a ring or donut shape, while the associated telomere sequence DNA normally appear as solid puncta surrounded by PML. APBs are distinctive because of the close overlap between PML and telomere DNA with the ALT-associated large telomere DNA foci occurring in the center of this ring of PML. It would be reasonable then to hypothesize a functional connection between PML and telomeres in ALT based on the phenomenon of APBs. The CRISPR/Cas9 technology provides the means to efficiently generate the models required for this study. A targeting strategy using the double cutter Cas9 was designed (figure 2-2). This version of Cas9 forms double strand breaks at the target site as determined by a guide RNA located on the same plasmid that contains the Cas9 open reading frame (table 2-1). The specific target site was selected because it is early in the PML transcript (exon 2). This exon is common to all known isoforms of the PML protein, thereby preventing partial expression of PML through short isoforms. Since it is at the start of the transcript it greatly reduces the possibility of expression of a partially functional truncated protein.

24

Cas9 with and without the PML-targeted gRNA was transfected into U2OS and transduced into

SAOS2. Cas9 and its gRNA are located on the same backbone in both conditions. The samples treated

without the PML gRNA but with a functional Cas9 serve as empty vector (EV) controls for the influence

of the process of Cas9 expression itself and subsequent manipulations. Single cell cloning and screening

for PML expression was carried out for both cell lines. Cloning is important to ensure that populations of

cells are homogeneous, and no potential contaminating PML expressing cells will influence results. After

screening, clones were sequenced at the gRNA target site located in the PML gene (table 2-2). The

mechanism of action of Cas9 is demonstrated in the sequence of PML knockout clones. Cas9 introduced

insertions and deletions at the target site that result in nonsense mutations thereby preventing PML

protein expression. A total of three sequence-confirmed U2OS PML KO clones were selected and two

confirmed SAOS2 KO clones were also generated (table 2-2). SAOS2 proved to be challenging to work

with as a result of low transfection efficiency and poor cloning efficiency. IF for PML in U2OS knockout

clones is negative for signal (figure 2-3). IF for PML in SAOS2 knockout clones is also negative for signal

(figure 2-4). Western blotting for the PML protein is also negative in all KO clones, with GAPDH used as a

loading control (figure 2-5). PML is challenging to study partly because of the number of isoforms there

are. Each one could have different functions or localizations. This is reflected in the western blot results.

A "ladder" of isoforms is present in EV controls. The lack of these isoforms represents additional

confirmation that these clones are true PML KO lines.

Part 3 ALT is maintained in the absence of PML

Having completed the first step of establishing stable PML expressing and non-expressing cell

lines for comparison (U2OS EV vs U2OS PML KO and SAOS2 EV vs SAOS2 PML KO) it becomes necessary

then to assess ALT pathway activity in each of these groups in order to complete the modeling strategy

outlined in the previous section. Assessment of activity is carried out by analyzing several assays for the

known characteristics of the ALT pathway. A single metric is insufficient to confirm the presence of the ALT pathway.[53, 62, 63, 66, 69, 105]

Long term culture of the PML knockout lines was carried out to examine the long term effects of PML knockout out on cell viability and telomere lengths (table 3-1). Growth rates between parent EV and PML KO lines are similar for both U2OS and SAOS2, However, there is variability between the knockout clones in their growth rates, in particular SAOS2 KO 2 having a doubling time 20 hours longer than SAOS2 KO 1, but this could be explained by clonal variability. Notably, SAOS2 KO 1 has an identical doubling time as the parental (table 3-1). All knockout lines have proven capable of continuous long term culture over the course of more than two years. Regarding telomere dynamics, the mechanism of telomere shortening occurs slowly over time. As mentioned in the introduction, approximately 300 bp are lost per telomere, per replication cycle and assuming a 10 kb starting telomere length it would take 33 population doublings to erode the telomere. Here U2OS cells have reached over 200 calculated doublings and SAOS2 over 150 calculated doublings; thus, in both cell lines with PML KO, they have greatly exceeded the predicted number of cell divisions beyond which telomere loss would have become lethal (table 3-1). To determine the actual telomere length dynamics of knockout clones a terminal restriction fragment (TRF) assay was conducted. There are a number of ways to measure telomere lengths, but the TRF allows for determination of length and the heterogeneity of lengths present within a population. This technique exploits the fact that telomeres do not have any known restriction fragment enzymes targeting them. Therefore, if a combination of frequent cutters is used on genomic DNA it will theoretically leave only the telomere fragments intact. Once this is done the principles behind fragment separation in gel agarose electrophoresis can be relied upon to spread telomere lengths down a gel. Combined with Southern blotting, telomere lengths can then be visualized. One of the most defining characteristics of ALT is a wide distribution of telomere lengths from very short (1kb) to very large (30 kb); visible using this technique. In a telomerase positive cell line telomere

lengths are much more similar from chromosome to chromosome, which generates a less

heterogeneous distribution centered on a restricted range of sizes. Figure 3-1 is a TRF of side-by-side

low population doubling and high population doubling (PD) of each of the PML KO clones. EV low and

high PD are given for U2OS and SAOS2 as well. The distribution of telomere lengths between low and

high PD is similar for both EV and KO lines (figure 3-1). A signal ranging from above 23 kb to at least

below the 4.4 kb marker is present in all lanes. If any changes in telomere lengths had occurred, then

the distribution of sizes would also change. In particular, if telomere maintenance was disrupted by PML

loss, then significant attrition in telomere lengths across the entire distribution of lengths should have

occurred over the two years of continuous culture of these cell lines. Therefore, the observation that the

PML KO cells survive long term culture without evidence of significant losses in telomere length

distributions strongly imply ongoing ALT in the absence of PML. An investigation into biomarkers of ALT

activity of PML KO cells follows.

A widely used indicator of ALT activity is the C-circle assay. ALT cells have been shown to contain

extrachromosomal strands of telomere DNA sequence termed extrachromosomal telomere repeats

(ECTR). One such species is a covalently linked circle of partially double stranded telomere DNA, termed

C-circles. The assay to detect c-circles involves rolling circle amplification by the processive phi-29

polymerase from genomic DNA template samples. In C-circles, the C-rich sequence strand of the

telomere in its circular form is used as the target for amplification, primed by the partial double

stranded region of the C-circle. What results is a large amount of the G-rich strand telomere DNA

sequence products which are then detected using dot blotting. Although the amount of C-circles

present, and thus the amount of reaction product detected in the C-circle assay, varies widely between

different ALT-positive cell lines, C-circles have been shown to be ALT-specific, thus any positive signal

measured from this assay is scored as being positive for ALT activity.[66] Genomic DNA isolated from all

U2OS and SAOS2 cell lines produced a positive signal in the C-circle assay (figure 3-2). This is expected

from the U2OS and SAOS2 EV samples. The negative control is SJSA1, an osteosarcoma line which is telomerase positive and ALT negative. No C-circle assay signal was detected in this cell line (figure 3-2). To ensure no telomeric genomic DNA introduced from the initial template sample used in the reaction is detected (false positives), a reaction negative assay was conducted, showing no such false-positive signals were detected from genomic DNA (figure 3-2).

It is believed that the source of the C-circles is the excision product of ongoing telomere recombination in ALT. Most telomerase positive cell lines have no or almost no detectable homologous recombination at their telomeres.[53] Recombination at the telomeres is measurable by the chromosome orientation fluorescent in situ hybridization assay (COFISH; see methods for details). In this assay cells are grown for a single cell cycle in the presence of BrdU/C which labels newly synthesized DNA strands through incorporation. Metaphases of labeled cells are spread onto a microscope slide. Then the slide is treated with UV which creates breaks in the backbone of labelled strands. Nuclease treatment follows which results in the degradation of all labeled strands. What remains is the unlabeled DNA. A sequential hybridization reaction follows of first a telomere G strand sequence specific probe (green) and then a telomere C strand specific probe (red). Since DNA replication is semi-conservative these probes should be discrete with each labelling one arm of a chromatid pair. If an exchange has occurred or a strand has been translocated through some means through the course of a single cell cycle then a mixing of the two probes will occur. This is because the exchange has essentially cut and paste the hybridization target from one arm to the other. Figure 3-3 gives an example of the visualization of such an exchange. For each EV and KO cell line, metaphase spreads were generated and probed for exchanges. Then on a per metaphase basis the total number of chromatid pairs were recorded and the number of chromatid pairs that had an exchange in that metaphase were also recorded. Analysis was carried out by considering the fraction of chromatid pairs per metaphase that scored positive for an exchange (figure 3-4). For each line, over 1000 chromatid pairs scored. U2OS EV 1 had 10 metaphases

scored and all others had over 20 metaphases scored. To get an average population, the U2OS KO data were pooled (n> 60 metaphases) and the SAOS2 KO data were likewise pooled (n > 40 metaphases). Each of these were then compared against data from their corresponding EV using a t-test. KO of PML in U2OS was associated with a significantly increased fraction of sister chromatid pairs scoring positive for telomere exchanges, with an average value for EV of 5% (n=10 metaphases) and for KO 18% (n>60 metaphases) p<.01 (figure 3-4). In SAOS2, PML KO was also associated with a significantly increased fraction of chromatid pairs scoring positive for telomere exchanges, with an average value for EV of 42% (n>20 metaphases) and for KO of 56% (n > 40 metaphases) p<.05 (figure 3-4). The presence of these telomeric exchanges in KO cells is another indication of the preservation of ALT activity following PML KO. If exchanges were significantly reduced or eliminated that would argue against the ALT mechanism being maintained in these cells.

ALT is, by definition, an alternate to telomerase as a means of telomere maintenance. A cell must not have telomerase activity to be considered ALT-positive. To measure telomerase activity in the PML knockouts, the telomerase repeat amplification protocol (TRAP) was carried out. The readout indicates a positive signal when a laddering in increments of 6 bp appears after running the reaction out on a high resolution polyacrylamide gel. These 6 bp correspond to the 6 bp increments telomerase can add to a strand of DNA. Figure 3-3 shows this positive laddering in the telomerase positive cell line PC3. No laddering is seen in the EV and KO clones of either U2OS or SAOS2. The RNAse pre-treated sample is used to confirm that the laddering is the result of only telomerase activity, as the RNAse will degrade the RNA component of telomerase necessary for its activity.

Part 4 PML and the ALT Body

The PML protein forms discrete nuclear bodies that are often mentioned to be connected to the activities of other nuclear body proteins because these proteins will form co-localizing bodies with PML.

These are called "PML body resident proteins". How often these proteins actually co-localize with PML and how critical this localization is to their function is understudied. In order to help understand the potential organizing function of PML, the localization of two purported PML resident body proteins was examined: SP100 and DAXX. Since these proteins are also reported to be present in APBs, they intersect at the normal function of PML and the role of PML in ALT. [54, 104] In order to study this, we asked whether PML knockout results in changes in focus formation of these proteins, co-localizations between these two proteins, and their relationship to the large ALT-associated telomere foci that form the basis of our understanding of the ALT body.

First the assumptions underlying the above explanation must be tested. The established U2OS and SAOS2 cell lines described in the previous sections were utilized. Intact cells grown on chamber slides were image analyzed for localization and co-localization events using combined immunofluorescence for PML plus DAXX, and PML plus SP100. This dual immunofluorescence approach was necessary, as the species specificities of the antibodies used were incompatible in a triple stain. Image analysis through the program imageJ was used to avoid bias from manual counting. Important: all fields of view are from a 63x objective. Figure 4-1 contains an example staining of SP100 and PML in U2OS and SAOS2. Figure 4-2 contains an example staining of DAXX and PML in U2OS and SAOS2. To generate table 4-1 the image analysis data from the three U2OS EV clones (n = 8 fields of view each) and one SAOS2 EV clone (n= 8 fields of view) were used to generate standard deviations around the mean number of nuclear puncta per cell for each cell line. This standard deviation around the mean is the range provided in the table. Table 4-1 highlights that these three proteins form nuclear bodies in both U2OS and SAOS2 and that there are significant body formations in every cell. That is to say, you can expect bodies as indicated by fluorescent puncta in every cell examined. When the phrase "PML body resident protein" is used one would imagine this fits the description of a protein that spends most of its time in the PML body. Since in vivo imaging was not an option, it is instead necessary to infer this

dynamic from static images. If enough cells and puncta are counted, the prolonged residency of the

proteins SP100 and DAXX in PML bodies should be reflected in a high percentage of their puncta co-

localizing. Thus in Figure 4-3 the fraction of co-localizing bodies as a fraction of the total bodies of the

parent is given for each EV cell line (3 clones for U2OS and 1 clone for SAOS2). SP100 co-localizes with

PML on average 60% of the time across all cell lines (n= 4), whereas, DAXX co-localizes on average 72%

of the time with PML. Thus, the majority of nuclear punctae of SP100 and DAXX co-localize with PML

bodies in the SAOS2 and U2OS EV control clones..

Next, having confirmed a link between PML and the proteins SP100 and DAXX, the relationship

between SP100 and DAXX was examined. This was also examined in the context of PML status to see if

any relationship between SP100 and DAXX also has a dependency on PML. Figure 4-4 demonstrates in

U2OS EV that there are co-localizations between SP100 and DAXX (PML was the species limiting

antibody factor). The figure also demonstrates that there are co-localizations in the absence of PML as

well. Figure 4-5 demonstrates a similar relationship in SAOS2. In order to account for clone to clone

variation in total expression levels in the two proteins, or potential changes in expression as a result of

PML status, a denaturing western blot was performed on whole cell lysates with equal amounts of

protein loaded for each of the cell lines in question (figure 4-6). The major isoform of SP100 has a kDa of

54 but it runs anomalously at 100 kDa. This is why it is named SP"100". The doublet could potentially be

another isoform as there are six ranging from 50 kDa to 100 kDa. This staining pattern is consistent with

the antibody manufacturer's example blot, and both bands were considered when estimating total

SP100 protein levels. DAXX runs as a single band at 120 kDa, consistent with the manufacturers example

blot. GAPDH serves as a loading control at 40 kDa (figure 4-6). Densitometry analysis performed on the

blot is outlined in the next four figures. These results have been corrected for amounts of total protein

loaded by GAPDH signal and expressed relative to the first EV clone of either U2OS or SAOS2, as

indicated. Average adjusted relative levels of SP100 are unchanged in U2OS after PML loss (figure 4-7 t-

test, n=3 each condition). Average adjusted relative levels of SP100 are also similar in SAOS2 after PML loss (fig. 4-8). Average adjusted relative levels of DAXX are slightly, but significantly, less (15% reduction) in U2OS after PML loss (figure 4-9 t-test p<.0005, n=3 each condition). Average adjusted relative levels of DAXX are similar in SAOS2 after PML loss (figure 4-10).

With SP100 and DAXX co-stain and total protein levels established, the localization and co-localizations in terms of average puncta per cell of SP100 and DAXX were determined across all cell lines. Image analysis was carried out on U2OS for three separate EV and KO cell lines with 8 fields of view for each EV line and 8 fields of view for each KO line with a minimum 300 nuclei analyzed (figure 4-11). This was also carried out for SAOS2 with 8 fields of view for the EV and greater than 8 fields of view for the two KO lines with minimum 300 nuclei analyzed each (figure 4-12). These data are summarized in figure 4-13 in which samples were grouped by cell line and then PML status. The total fields of view for U2OS WT is the sum of the fields of view for the three EV control cell lines n=24. This was repeated for the other cell lines (figure 4-12). U2OS KO PML has n=24 fields of view, SAOS2 EV 1 has n = 8 and SAOS2 KO has n =16. In U2OS, the average number of SP100 puncta per cell was not significantly different between WT and KO. In contrast, the DAXX puncta and the corresponding co-localizations with SP100 are significantly decreased by fivefold and tenfold, respectively (t-test p<.0005) in the PML KO compared to EV (figure 4-12). In SAOS2 there is a significant increase in SP100 average puncta per cell from 4 in WT to 5.9 in PML KO (figure 4-12 t-test p<.0005). No significant change was seen in SAOS2 average DAXX puncta per cell between KO and EV (figure 4-12). As with U2OS, a significant decrease in SP100 and DAXX co-localizations was also seen in SOAS2 PML KO compared to SAOS2 WT (figure 4-12). The principal result then from both U2OS and SAOS2 is a decrease in the average number of co-localizations between SP100 and DAXX as a result of PML loss. This however can be difficult to interpret, as the drop in total puncta of either protein could influence the total number of possible co-localizations. To account for this, the data were reanalyzed as a fraction of the total number of nuclear bodies of either SP100 or

32

DAXX. Figure 4-14 details the fraction of SP100 puncta that co-localize with DAXX in terms of total SP100

punctae for either cell line using data from figure 4-13. A significant decrease in the fraction co-localizing

was seen for both cell lines in the PML KO with a decrease of 85% in U2OS and a decrease of 58% in

SAOS2(t-test p<.0005). Figure 4-15 details a similar manipulation but for DAXX, and it too has a

significant decrease in fraction co-localizing with SP100 - with a decrease of 23% for U2OS and a

decrease of 62% for SAOS2 (t-test p<.0005). These results indicate then that even when correcting for

the total number of bodies available for co-localization there is a significant drop in SP100 and DAXX

body co-localizations in response to loss of PML.

PML is connected to ALT primarily through its co-localizations with the large, ultra-bright

telomere DNA foci seen in a subset of cells in ALT-positive cell lines and human tumors. These large

telomere foci are often referred to as APBs, since they often (although not always) co-localize with PML.

In the course of investigating ALT positive cell lines it becomes clear that the number and size of foci can

vary drastically between cell lines. A comparison of the telomere FISH stain between U2OS and SAOS2

exemplifies this variability (figure 4-16). The telomere staining pattern in U2OS is consistent from cell to

cell and large outlying ultra-bright telomere foci are difficult to distinguish at low power (figure 4-16).

Additionally, U2OS has significant chromosomal telomere signals, making it difficult to determine on the

cellular level which signal is from a chromosome and which is from the APB foci, which are presumed to

be largely or exclusively composed of extrachromosomal telomeric sequence DNA. APBs could also

consist of some mix of these two that may be constantly changing. SAOS2, in contrast to U2OS, fits the

classic description of ALT telomere FISH. Here, most cells have a low baseline of telomere staining but

some cells have distinct nuclear foci far in excess of average telomere DNA content (figure 4-16).

Looking at a field of SAOS2 cells, as in figure 4-16, these large, ultra-bright foci are readily apparent

(asterisk indicated). One of the significant challenges in studying APBs is how to properly identify them.

This is also, in part, why this thesis came about. To avoid these confounding factors, studies on ALT body

formation were carried out in only SAOS2. Additionally, a high threshold of brightness for image analysis was established for telomere FISH signals in SAOS2. This high threshold should significantly exclude chromosomal telomere DNA signals and focus analysis only on these archetypical APBs. To confirm the assumptions behind calling these large telomere foci APBs, a combined telomere FISH and immunofluorescence for PML experiment was carried out with SAOS2 EV (figure 4-17). Two different antibodies against PML were employed to examine their potential use in experiments and to check for consistency of results. Both antibodies resulted in 20% of total PML puncta as co-localizing with large telomere foci in SAOS2 (figure 4-17 n= 8 fields of view FOV). A non-significant difference was apparent in the two antibodies for the fraction of large telomere foci co-localizing with PML (figure 4-17t-test not significant n= 8 FOV). In this case, the rabbit-derived PML antibody used gave 85% of large telomere foci as co-localizing with PML, while the mouse-derived PML antibody gave a 72% rate of co-localization between the two (figure 4-17 n= 8 FOV for both).

Having investigated the connection of SP100 and DAXX through PML, and the connection of PML to the large telomere foci characteristic of APBs, the connection between SP100, DAXX and large telomere foci was examined. SP100 and DAXX do co-localize with large telomere foci, both with and without PML in SAOS2 (figure 4-18). Next was asked if there was a change in the association of these bodies as a result of PML loss, that is, can APBs still form without PML; SP100 and DAXX co-localizing with large telomere foci being used here as a measure of ALT body formation. By definition, APBs rely on PML for their identification, but without PML co-localizations between ALT-associated telomere DNA foci, SP100 plus DAXX, this is the next best indicator that these structures are still able to form, even in the absence of PML. Telomere FISH and SP100 DAXX IF were performed on SAOS2 EV and SAOS2 PML KO 1 and 2. Image analysis was carried out for puncta co-localizations, with telomere thresholding as outline above so as to only assess the bright ALT-associated nuclear telomere DNA foci. (Figure 4-19, EV n= 8 FOV, KO1 n=12 FOV, KO2 n=16 FOV total at least 300 nuclei for each). Results indicate ALT-

associated large telomere foci are still present on a PML KO background and foci have co-localizations with SP100 and DAXX. The total EV was then compared to the total KO populations (Figure 4-20). We found that the number of large telomere foci do not change as a result of PML loss in SAOS2 (figure 4-20 t-test n.s. EV n=8 FOV, KO n=28 FOV). The number of co-localizations between telomere foci and SP100 was decreased from .9 to .4 puncta per cell, a 55% decrease, and the number of co-localizations between telomere foci and DAXX was also decreased from .9 to .4 puncta per cell, again, a 55% decrease (figure 4-20). The triple co-localization between telomere foci, SP100 and DAXX decreased from .8 puncta per cell to .1 puncta per cell, an 85% decrease (figure 4-20 t.test p<.0005 each comparison EV n=8 FOV, KO n=28 FOV). These results indicate that the telomere DNA ALT bodies still form without PML, although at a significantly reduced frequency. They also indicate that PML loss has reduced the association of SP100 and DAXX to the ALT body.

Part 5 PML and the DNA damage response (DDR)

Potential perturbations in the DDR as a result of PML loss were seen in the increased strand exchanges at telomeres (figure 3-3). PML is connected to ALT which is itself connected to the DDR through its postulated reliance on the mechanism of homologous recombination.[63] Because of this, and to examine any potential telomere dysfunction, an analysis for telomere dysfunction induced foci (TIF) was performed on the EV, PML KO cell lines outlined previously. TIFs are identified by any co-localizations of a DDR marker, typically yH2AX or 53BP1, with telomeres.[115] Combined telomere FISH and IF for 53BP1 is demonstrated in figure 5-1. Images were captured to cover at least 200 nuclei for each of the Cas9 clones and images were analyzed for puncta. Average TIFs per cell indicates a wide range of cell scores from a large number of cells with no TIFs and some with many (figure 5-2). Another way to examine TIFs is to consider them as a marker of cells experiencing significant telomere dysfunction. This involves looking only at cells that have multiple TIFs, and not just potentially incidental or insignificant TIFs.[7] Figure 5-3 uses 5 TIFs as the cut off and compares the total EV and KO

populations for either U2OS or SAOS2. By this metric, there is no significant increase in telomere

dysfunction as a result of PML loss in U2OS (figure 5-3 t-test not significant n= 600 nuclei EV or KO). An

apparent trend down in TIFs in PML KOs is apparent in SAOS2(figure 5-3).

Tables

Table 2-1

PML specific gRNA primers used with included cloning overhangs. PML sequence in red.

Primer	Target Site on Transcript	Sequence
PML Exon 2 Sense	507-485	CACCG**CAATCTGCCGGTACACCGA**C
PML Exon 2 Antisense	485-507	AAAC**GTCGGTGTACCGGCAGATTG**C

Table 2-2

PML gene sequencing in empty vector controls (EV) and PML knockout (KO) cells. CRISPR/cas9 treatment introduced insertions and deletions at the targeted cut site leading to PML knockouts in the ALT utilizing cell lines U2-OS and SAOS2. The type of mutation leading to PML disruption is also provided. Guide sequences highlighted in red.

Cell Line	Type of mutation	Unique PML Alleles Detected	Sequence
U2OS EV	n/a	1	Detected Seq TCTTTTTCGAGAGTCTGCAGCGGCGCCT**GTCGGTGTACCGGCAGATTG**TGGATGCGCAGG |||||||||||||||||||||||||||||||||||||||||||||||||||||||||||||| Refseq PML TCTTTTTCGAGAGTCTGCAGCGGCGCCT**GTCGGTGTACCGGCAGATTG**TGGATGCGCAGG
U2OS KO1	Deletion 1 bp	2	Detected Seq TCTTTTTCGAGAGTCTGCAGCGGCGCCT**GTC–GTGTACCGGCAGATTG**TGGATGCGCAGG ||||||||||||||||||||||||||||||| ||||||||||||||||||||||||||||||| Refseq PML TCTTTTTCGAGAGTCTGCAGCGGCGCCT**GTCGGTGTACCGGCAGATTG**TGGATGCGCAGG
U2OS KO1	Deletion 13 bp	2	Detected Seq TCTTTTTCGAGAGTCTGCA-------------**GTGTACCGGCAGATTG**TGGATGCGCAGG |||||||||||||||||||| |||||||||||||||||||||||||| Refseq PML TCTTTTTCGAGAGTCTGCAGCGGCGCCT**GTCGGTGTACCGGCAGATTG**TGGATGCGCAGG

U2OS KO2	Deletion 1 bp	2	Detected Seq TCTTTTTCGAGAGTCTGCAGCGGCGCCT**GTC-GTGTACCGGCAGATTG**TGGATGCGCAGG ||||||||||||||||||||||||||||||||||||||||||||||||||||||||||||||| Refseq PML TCTTTTTCGAGAGTCTGCAGCGGCGCCT**GTCGGTGTACCGGCAGATTG**TGGATGCGCAGG
U2OS KO2	Deletion 5 bp	2	Detected Seq TCTTTTTCGAGAGTCTGCAGCGGCGCCT**-----TGTACCGGCAGATTG**TGGATGCGCAGG ||||||||||||||||||||||||||||||||||||||||||||||||||||||||||||||| Refseq PML TCTTTTTCGAGAGTCTGCAGCGGCGCCTGTCGGTGTACCGGCAGATTGTGGATGCGCAGG
U2OS KO3	Insertion 1 bp	1	Detected Seq TCTTTTTCGAGAGTCTGCAGCGGCGCCT**GTCGGGTGTACCGGCAGATTG**TGGATGCGCAGG ||||||||||||||||||||||||||| |||||||||||||||||||||| Refseq PML TCTTTTTCGAGAGTCTGCAGCGGCGCCT**GTC-GGTGTACCGGCAGATTG**TGGATGCGCAGG
SAOS2 EV		1	Detected Seq TCTTTTTCGAGAGTCTGCAGCGGCGCCT**GTCGGTGTACCGGCAGATTG**TGGATGCGCAGG ||||||||||||||||||||||||||||||||||||||||||||||||||||||||||||||| Refseq PML TCTTTTTCGAGAGTCTGCAGCGGCGCCT**GTCGGTGTACCGGCAGATTG**TGGATGCGCAGG
SAOS2 KO1	Deletion 87 bp	2	Detected Seq TCTTTTTCGAGAGTCTGCAGCG------------87bp deletion------------- ||||||||||||||||||||||||||||||||||||||||||||||||||||||||||||||| Refseq PML TCTTTTTCGAGAGTCTGCAGCGGCGCCT**GTCGGTGTACCGGCAGATTG**TGGATGCGCAGG
SAOS2 KO1	Insertion 4 bp Deletion 6 bp	2	Detected Seq TCTTTTTCGAGAGTCTGCAGCGAGCAGCTCCTC--TG--C-GCCA-AGTGCTTCGAGGCACAC- |||||||||||||||||||| || || || || | | || | || | || || || Refseq PML TCTTTTTCGAGAGTCTGCAGCG-GCGCCTG-TCGGTGTACCGGCAGATTG-TG-GATGCGCAGG
SAOS2 KO2	Deletion 37 bp	2	Detected Seq TCTTTTTCGAGAGTCTGCAGCGGC----------(37 bp deletion)---------- ||||||||||||||||||||||||||||||||||||||||||||||||||||||||||||||| Refseq PML TCTTTTTCGAGAGTCTGCAGCGGCGCCT**GTCGGTGTACCGGCAGATTG**TGGATGCGCAGG
SAOS2 KO2	Insertion 4 bp Deletion 7 bp	2	Detected Seq TCTTTTTCGAGAGTCTGCAGCGAGCAGCTCCTC--TG--C-GCCA-AGTGCTTCGAGGCACAC- |||||||||||||||||||| || || || | | || | || | || || || Refseq PML TCTTTTTCGAGAGTCTGCAGCG-GCGCCTG-TCGGTGTACCGGCAGATTG-TG-GATGCGCAGG

Table 3-1

The ALT cell lines U2OS and SAOS2 are viable, grow at rates similar to parental lines. Average growth rates are given for logarithmic growth phase and determined from confluency data obtained from Incucyte monitoring (see methods for details).

Cell line	Growth rate (doubling time in hours)	Maximum population doublings
U2OS Parental Line	35	-
U2OS EV clone 1	30	700
U2OS PML knockout clone 1	30	350
U2OS PML knockout clone 2	35	400
U2OS PML knockout clone 3	35	200
SAOS2 Parental	50	-
SAOS2 EV clone 1	50	150
SAOS2 PML knockout clone 1	50	150
SAOS2 PML knockout clone 2	70	150

Table 4-1

The proteins PML, SP100 and DAXX are nuclear proteins that form numerous nuclear bodies that appear as nuclear puncta when visualized with immunofluorescence. The table indicates puncta per cell for the cell lines U2-OS (data from three separate U2-OS clonal cell lines n = 8 fields of view covering greater than 300 nuclei) and SAOS2 (one clonal population n = 8 fields of view covering greater than 300 nuclei) as one standard deviation from the mean.

Protein	U2OS	SAOS2
PML	11-18	2-5
SP100	8-17	3-7
DAXX	3-7	2-5

Figures
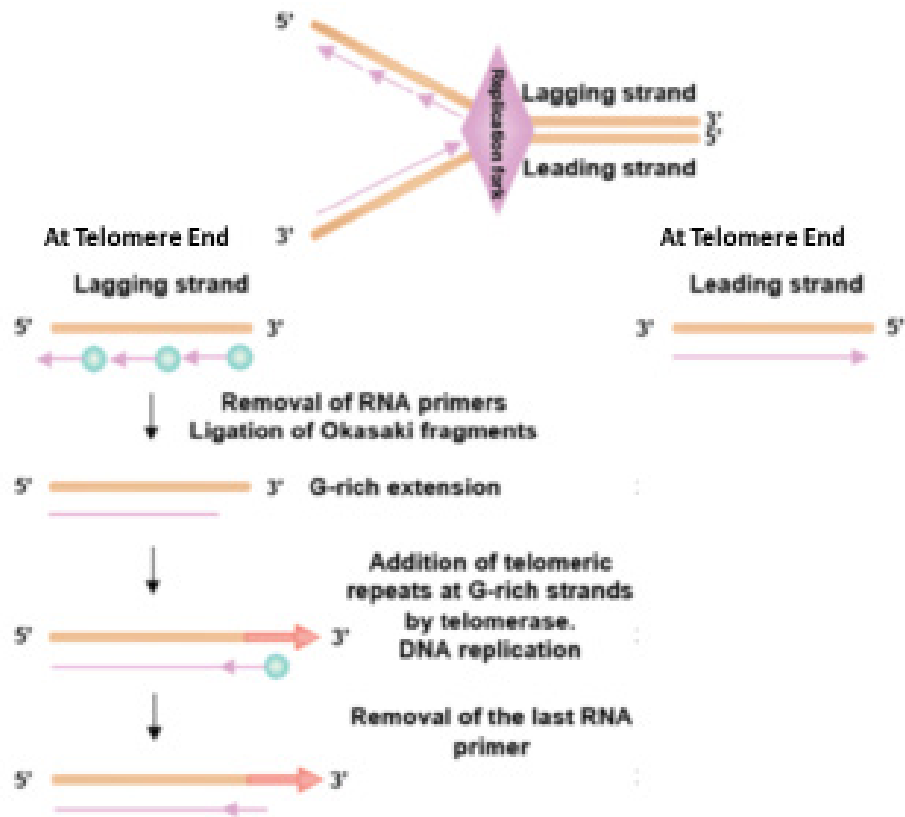
Schluth-Bolard et al.-Figure 2

Figure S1-1 See next page for description.

Figure S1-1 The end replication problem. Replication occurs from a template read in the 3'-5' DNA sequence direction and synthesized in the 5'-3' DNA sequence direction. An RNA primer is required for DNA polymerases to begin the catalysis of DNA base addition. As replication proceeds through unwinding of the template duplex DNA (referred to as a replication fork) the restriction in reading and synthesis direction results in one strand being replicated continuously (leading strand) and one strand being replicated discontinuously (lagging strand). The lagging strand has many fragments of replicated DNA referred to as Okasaki fragments. The RNA primer is degraded and the Okasaki fragments are extended such that all fragments can be ligated and the replicated strand is continuous. However, at telomere of the lagging strand there is no proximal Okasaki fragments that can be extended to fully complete replication at the terminus. This results in a protruding G rich telomere repeat sequence (AATGGG). To prevent loss of sequence the enzyme telomerase adds telomere repeats to the G-rich extension. This allows for the replication of additional complimentary sequence. A gap from the removed primer is still present (3' overhang) but the net length of the telomere is retained. Figure taken from [29]

A

B

SCE

| normal CO-FISH telomere pattern | split signal |
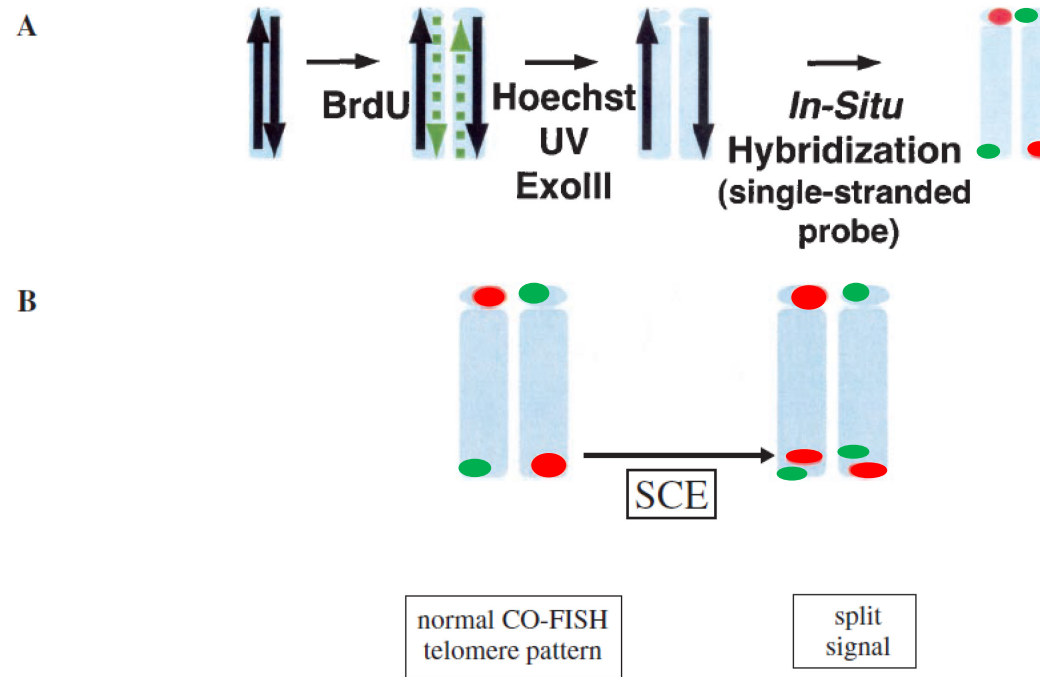
G Strand Telomere Probe   C strand telomere probe

Figure S2-1 Method for detecting homologous recombination within telomeres. (A) Mitotic cells are collected after culture in bromo-substituted nucleotides for a single cell cycle. Metaphases are prepared on microscope slides, and are then stained with the DNA-binding fluorescent dye Hoechst 33258. Exposure to UV light nicks the newly-replicated strand, and exonuclease III digests it. The process leaves behind the two parental strands that are now located on their respective sister chromatids. A single stranded telomere sequence probe hybridizes to complementary telomeric DNA on one chromatid of each chromosome arm producing a signal for each arm - either the G-strand (green) or its complement the C-stand (red) (B) The expected effect of a telomeric sister chromatid exchange (T-SCE) within telomeric DNA is to split the hybridization signal between the two arms such that both C-strand and G-strand signals are present at the terminus of the same sister chromatid. Figure taken from [112]
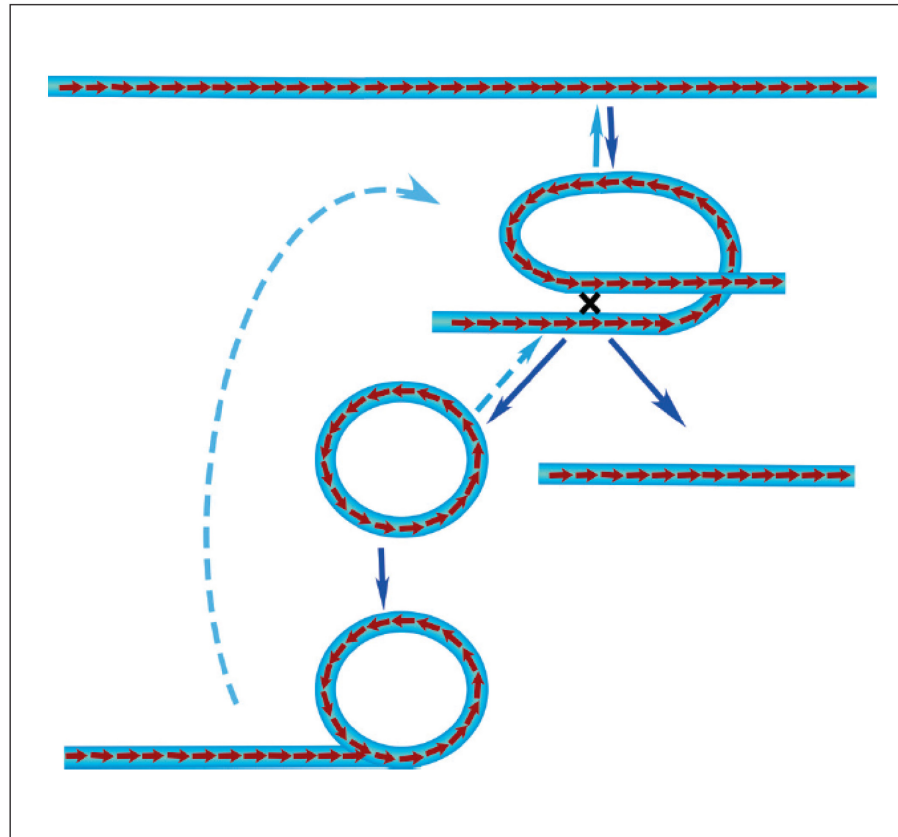
Figure S2-2 Formation of C-circles via homologous recombination. Each arrow represents a telomere repeat along a single chromosome. Repeats are capable of being aligned for homologous recombination because their sequence is identical. Intra telomere recombination can result in excision of telomere repeats by circularization. Telomere circles can potentially be used as a substrate for further homologous recombination at any telomere sequence. Figure Taken From [67]
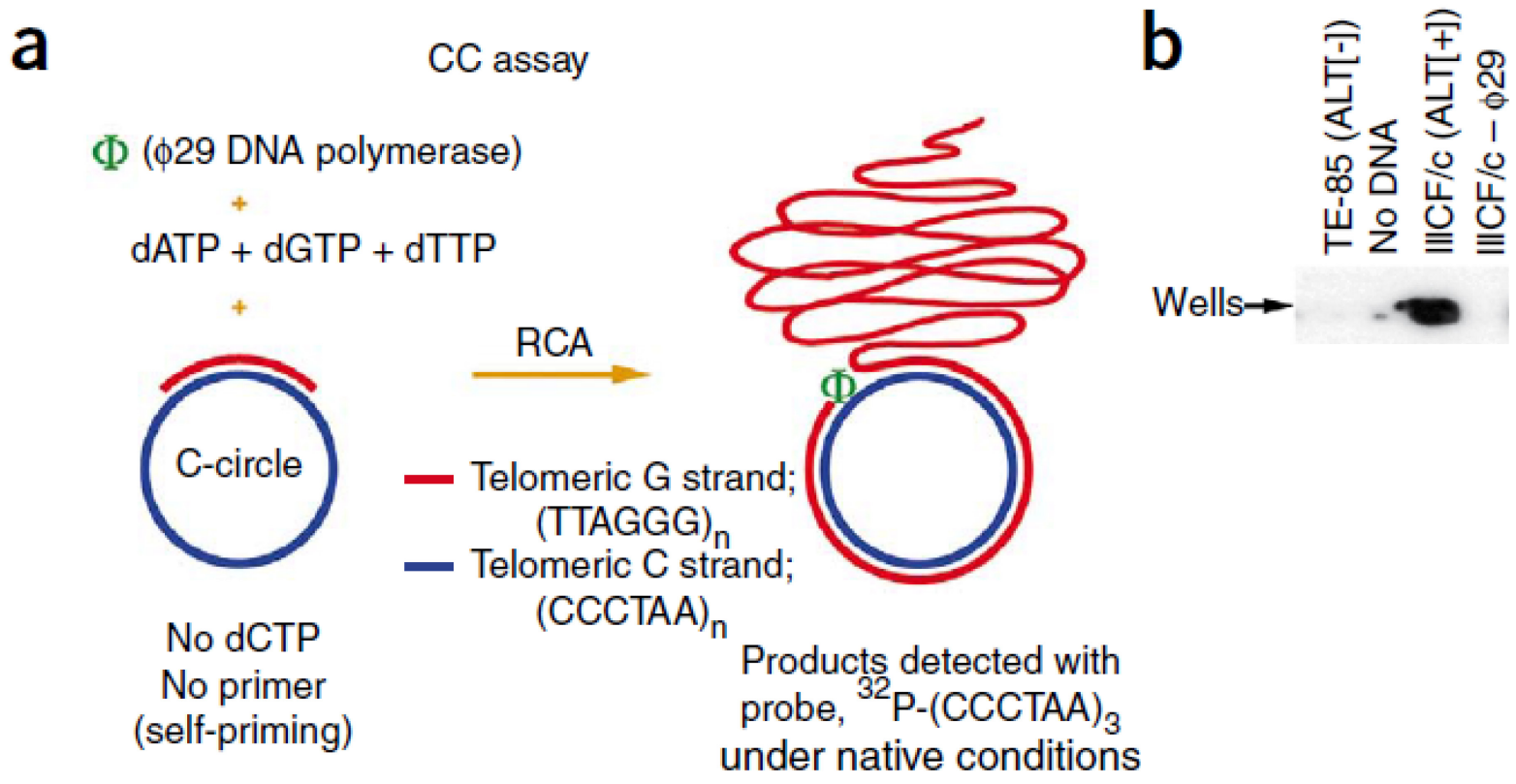
Figure S2-3 The C-circle assay. Genomic DNA is isolated from a sample that potentially contains c-circles. A small amount of this genomic DNA (here 50ng of DNA is used) is then combined with phi29 polymerase in reaction buffer and three of the four DNA nucleotides. C is excluded from the reaction to increase specificity because there are no C bases in the TTAGGG repeat being amplified. The product is the G-rich strand complementary to the c-circle CCCTAA repeat sequence. Rolling circle amplification (RCA) is primed by a naturally present fragment of telomere G strand annealed to the c-circle. RCA refers to the ability of phi29 to continuously traverse the template circle to produce a significant length of complementary sequence. The reaction products are then loaded onto a membrane and visualized with a labelled CCCTAA repeat probe. TE-85 is an ALT negative cell line. IIIFC/c is an ALT positive cell line. A phi29 negative reaction is included to ensure no detection of telomere sequence from only the genomic DNA used in the reaction. Figure taken from [116]

44
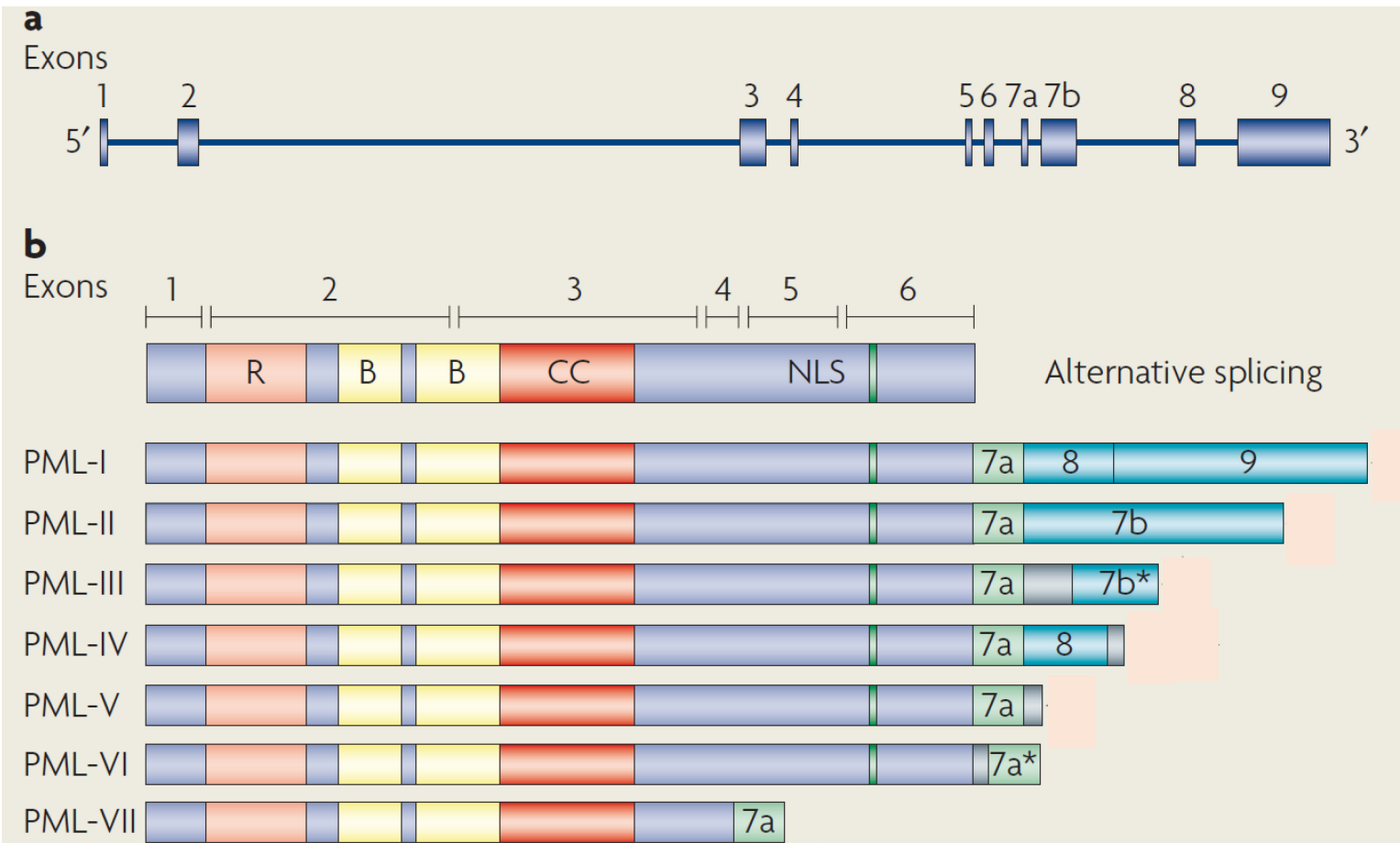
Figure S3-1 The PML gene and protein isoforms. The human promyelocytic leukemia (PML) gene is located on chromosome 15q22. **a)** It spans ~53,000 bases and contains nine exons. **b)** Alternative splicing of the C terminus generates different isoforms. All PML isoforms contain the first three exons, which encode the RBCC/TRIM motif. This is a tripartite structure that contains a zinc-finger called the RING motif (R), two additional zinc-finger motifs (B-boxes; B) and a coiled-coil domain (CC)The RBCC motif promotes homo-multimerization and the formation of macromolecular complexes. Further isoforms have been discovered after this publication. Figure taken from [88]
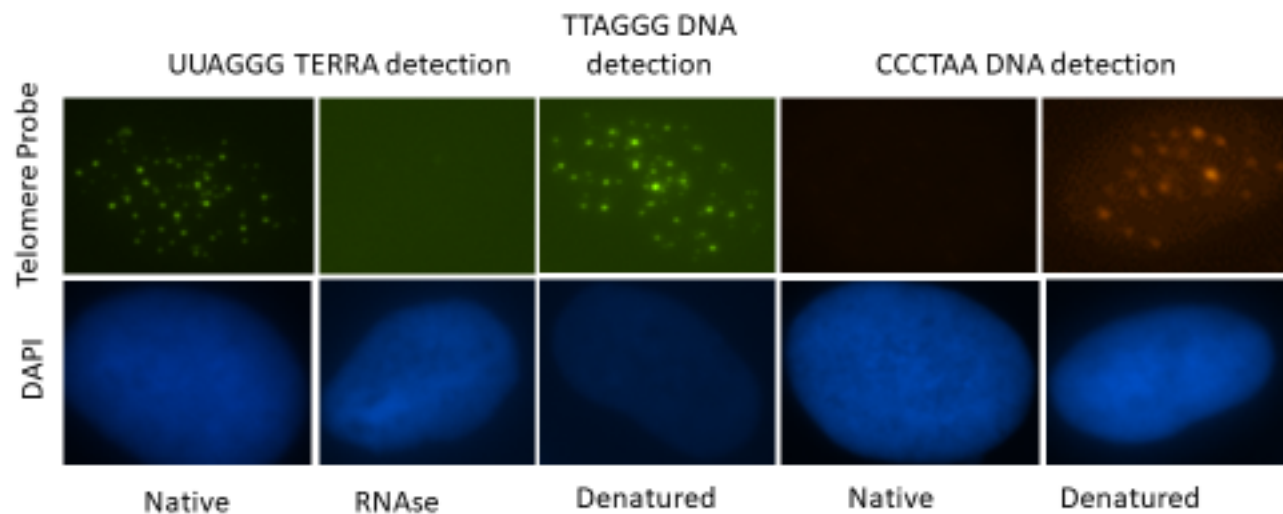
Figure 1-1 Telomeric localization of TERRA. (A) RNA-FISH with strand-specific telomeric LNA probes on U2-OS cells. Green and red signals correspond to the probes detecting TTAGGG (TERRA RNA UUAGGG) repeats or CCCTAA repeats, respectively. Experiments were performed under native conditions to detect RNA or denaturing to detect DNA4′,6′-diamidino-2-phenylindole (DAPI)–stained nuclei are in blue.

| Nucleus (DAPI) | Telomere Probe | PML | Merge |
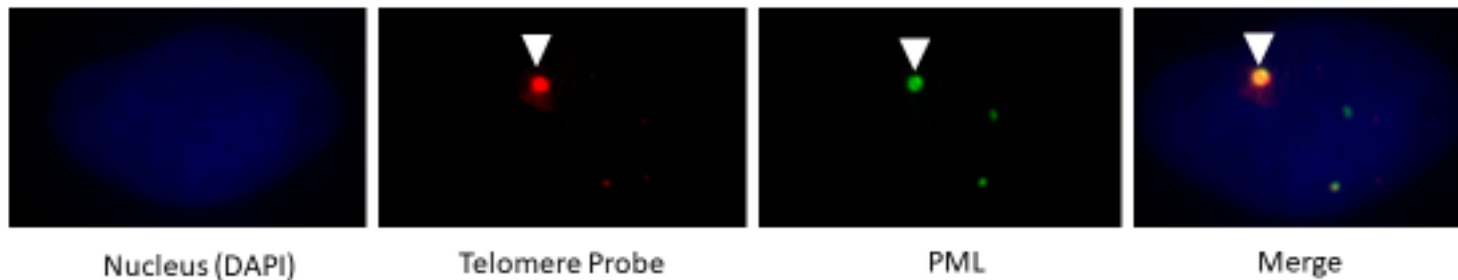
Figure 2-1 PML forms nuclear structures in association with relatively large and intense telomere DNA signals in cells that use ALT to maintain their telomeres. Here in the SAOS2 cell line co-localization of telomeres and PML was determined with combined fluorescent in situ hybridization for telomere sequences and immunofluorescence for the PML protein. Arrow indicates this co-localization
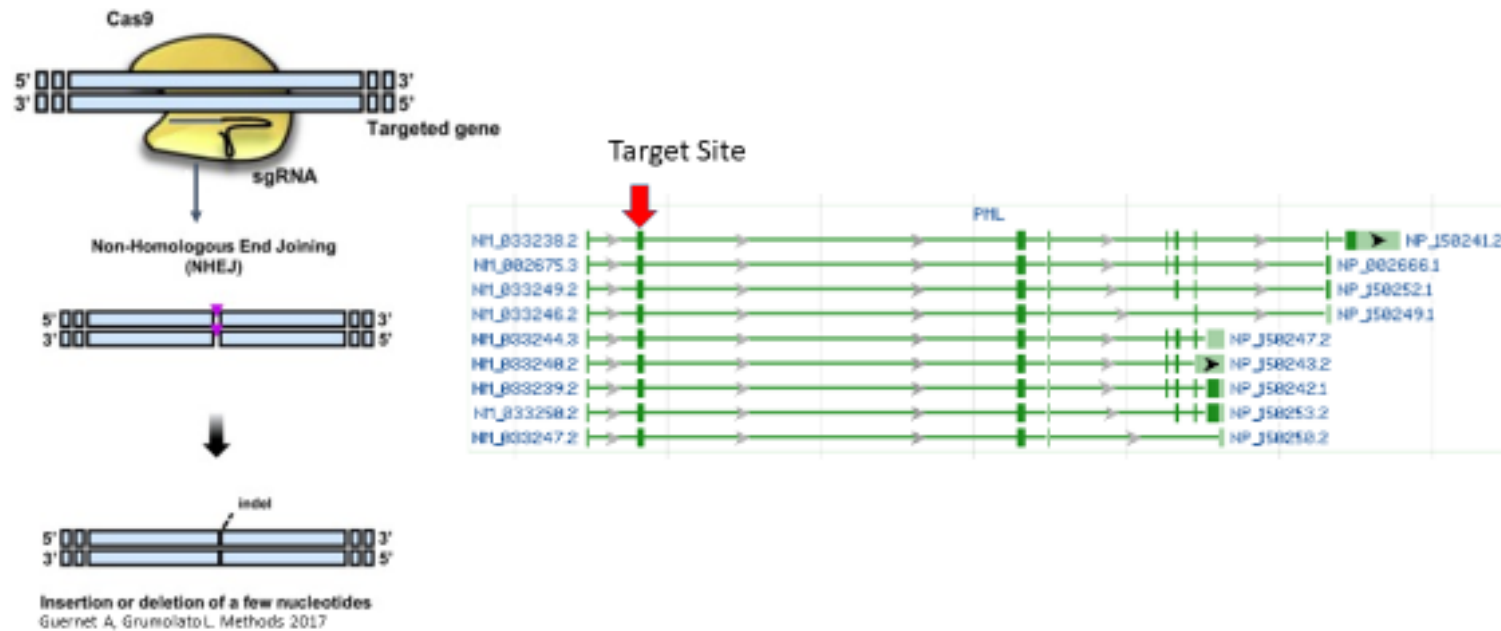
Figure 2-2 PML gene disruption strategy. Wild type CRISPR/Cas9 was used to create double strand breaks in the PML gene. Errors in repair lead to transcriptional silencing or nonsense mutations that result in loss of PML expression. A sequence specific to all known PML isoforms was selected such that all isoforms would be affected.
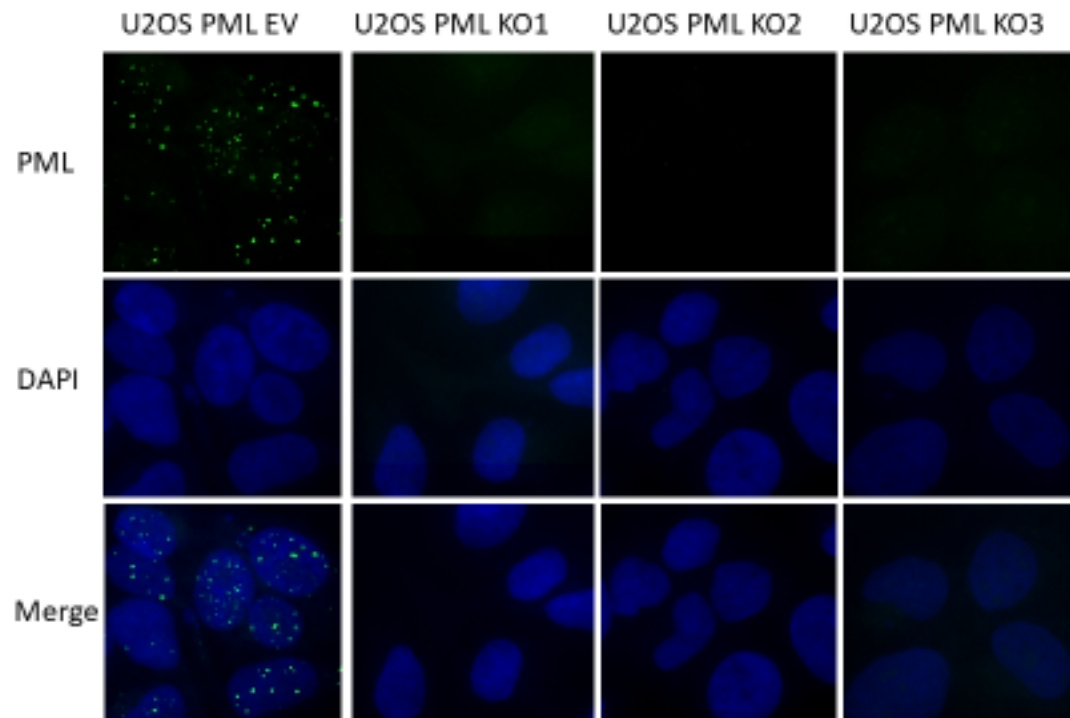
Figure 2-3 Immunofluorescence for PML (green) and DAPI (blue) in U2OS Cas9 no gRNA transfected clone (EV) and in Cas9 PML gRNA transfected PML knockout clones (KO)
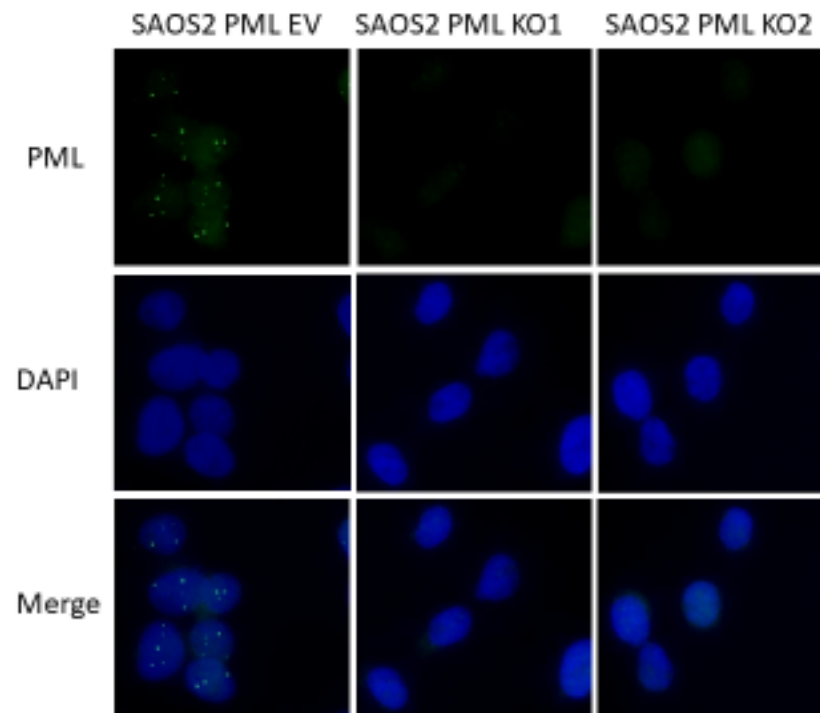
Figure 2-4 Immunofluorescence for PML (green) DAPI (blue) in SAOS2 Cas9 no gRNA transduced clone (EV) and in SOAS2 Cas9 PML gRNA transduced PML knockout clones (KO)
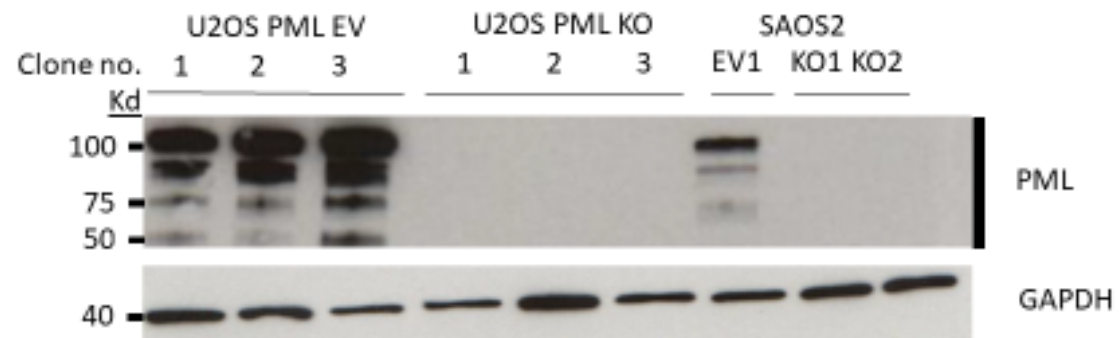
Figure 2-5 PML Protein Expression in control and Cas9 targeted clones. SDS-PAGE followed by immunoblotting for the PML protein indicates a loss of PML protein expression. PML has twelve recorded isoforms with ten of varying length thereby forming a "ladder" like effect of PML protein. Immunoblotting for GAPDH serves as a loading control.
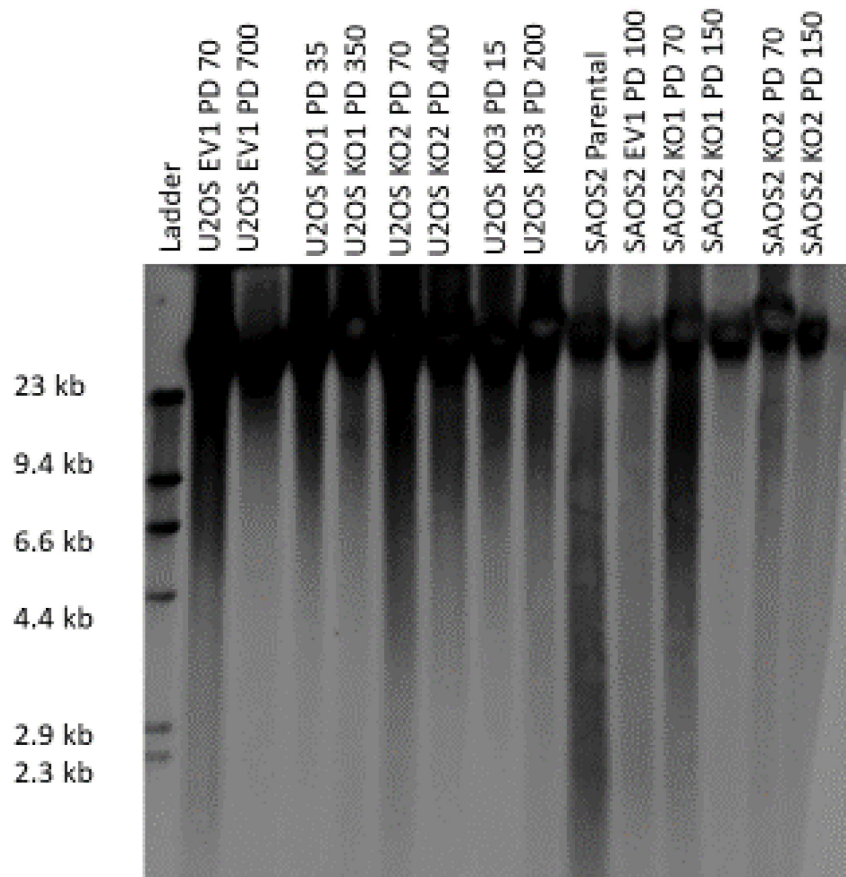
Figure 3-1 Terminal restriction length (TRF) analysis of low and high population doublings of EV control and PML knockouts (KO) showing no change in the distribution of telomere lengths. TRF analysis was done by digesting genomic DNA with restriction enzymes that do not recognize the telomeric sequence, TTAGGG, followed by agarose gel electrophoresis and transfer to membrane for hybridization with a labelled probe against TTAGGG.
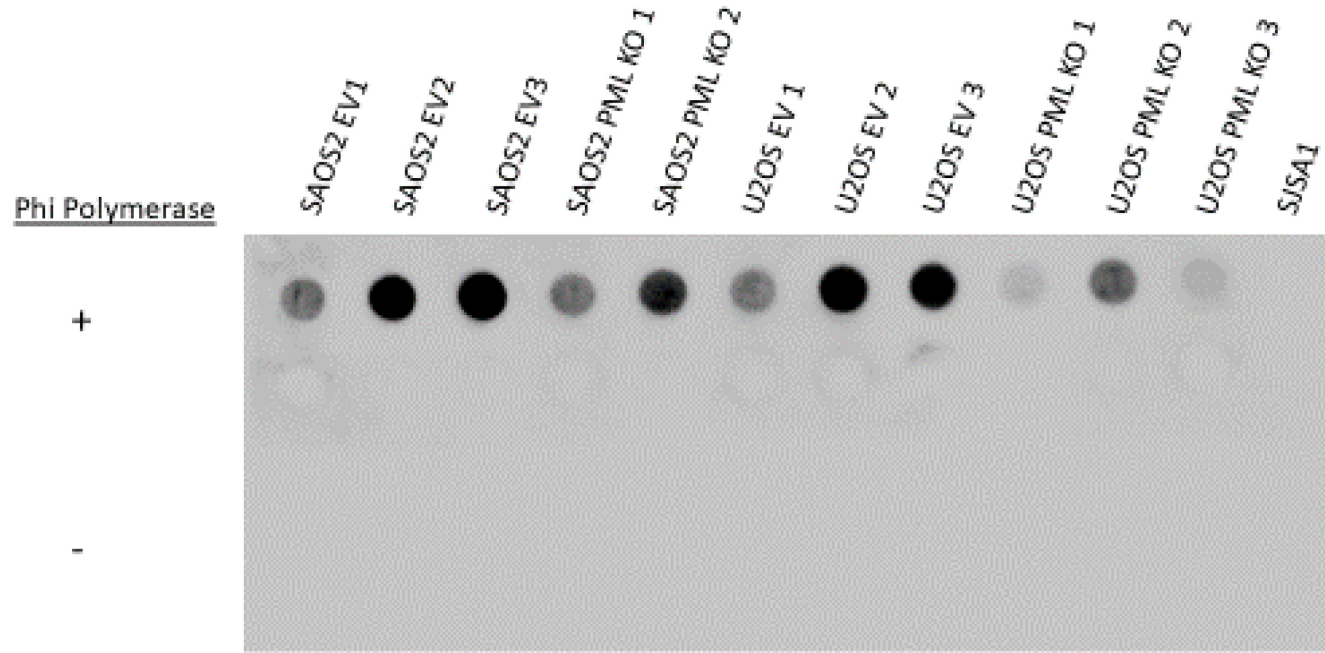
Figure 3-2 PML knockout clones are still positive for C-circles. Genomic DNA was extracted from samples and rolling circle amplification using phi polymerase was performed and transferred to a membrane via dot blot. Products are TTAGGG telomere DNA repeats and a complementary AATCCC repeat labeled probe was hybridized to the membrane. SJSA1 is a telomerase positive negative control cell line. 50 ng of DNA used in the initial reaction.

53
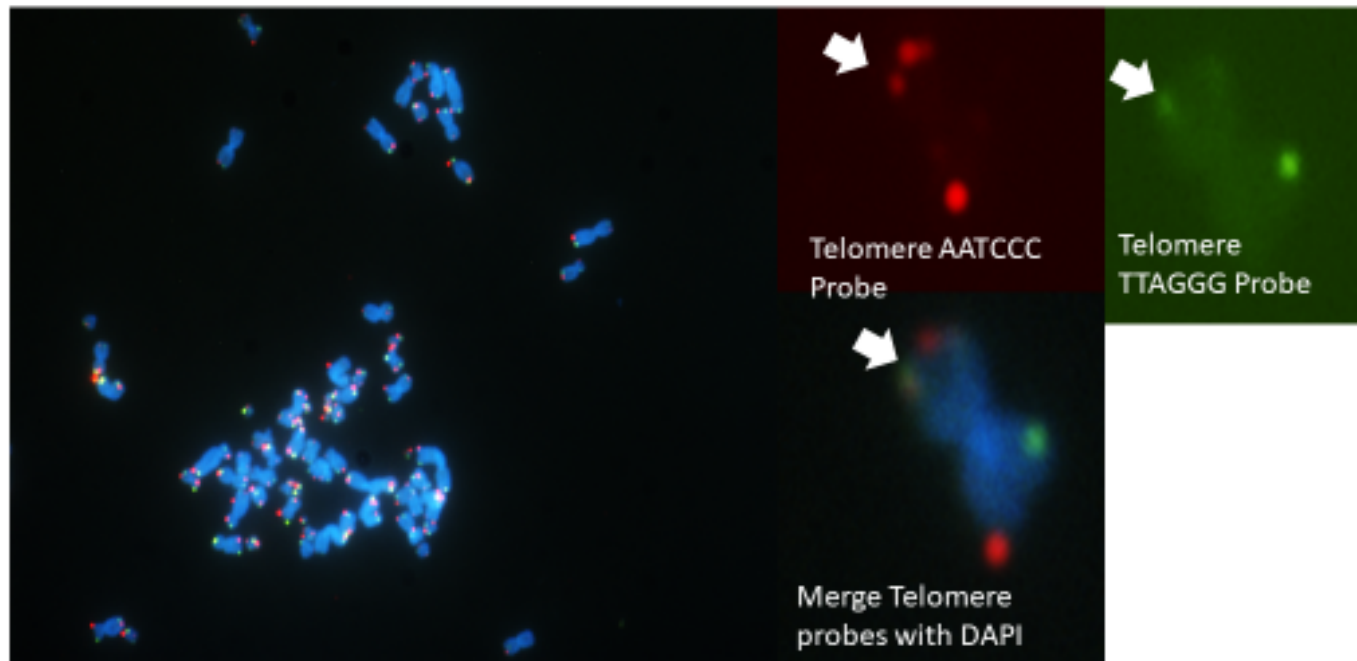
Figure 3-3 Chromosome orientation fluorescence in situ hybridization assay (CO-FISH). This assay allows for the detection of exchanges of DNA through a single cell cycle. Cellular DNA was labelled with BrdU/C, then synced by arrest at mitosis, osmotically swelled, fixed and dropped onto microscope slides. Metaphases were stained with probes specific to either telomere strand AATCCC (Red) TTAGGG (green). An exchange is indicated at the arrowhead.
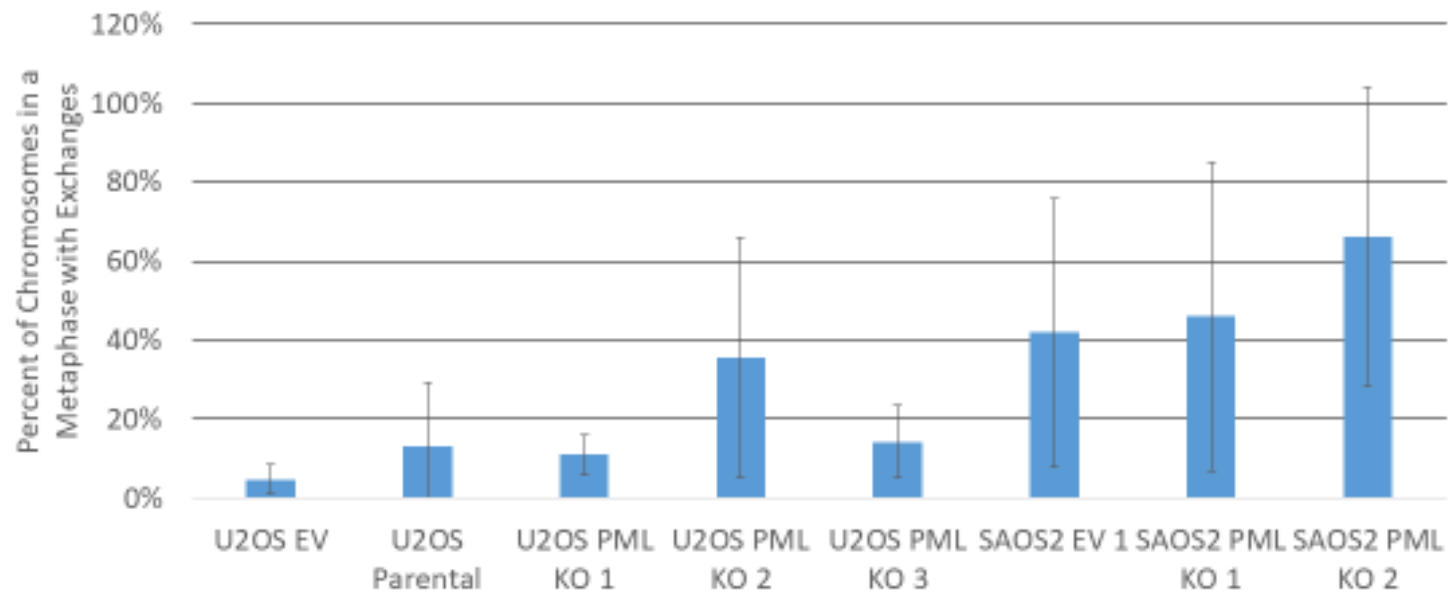
Figure 3-4 Telomere strand exchanges in PML EV and KO. Newly synthesized DNA over a single cell cycle was labelled with BrdU/C, then synced by arrest at mitosis, osmotically swelled, fixed and dropped onto microscope slides. Metaphases were stained with probes specific to either telomere strand and scored for percent of chromosomes with an exchange per metaphase. All had over 1000 chromosomes scored with n=10 metaphases for U2OS EV and n>20 for all others.
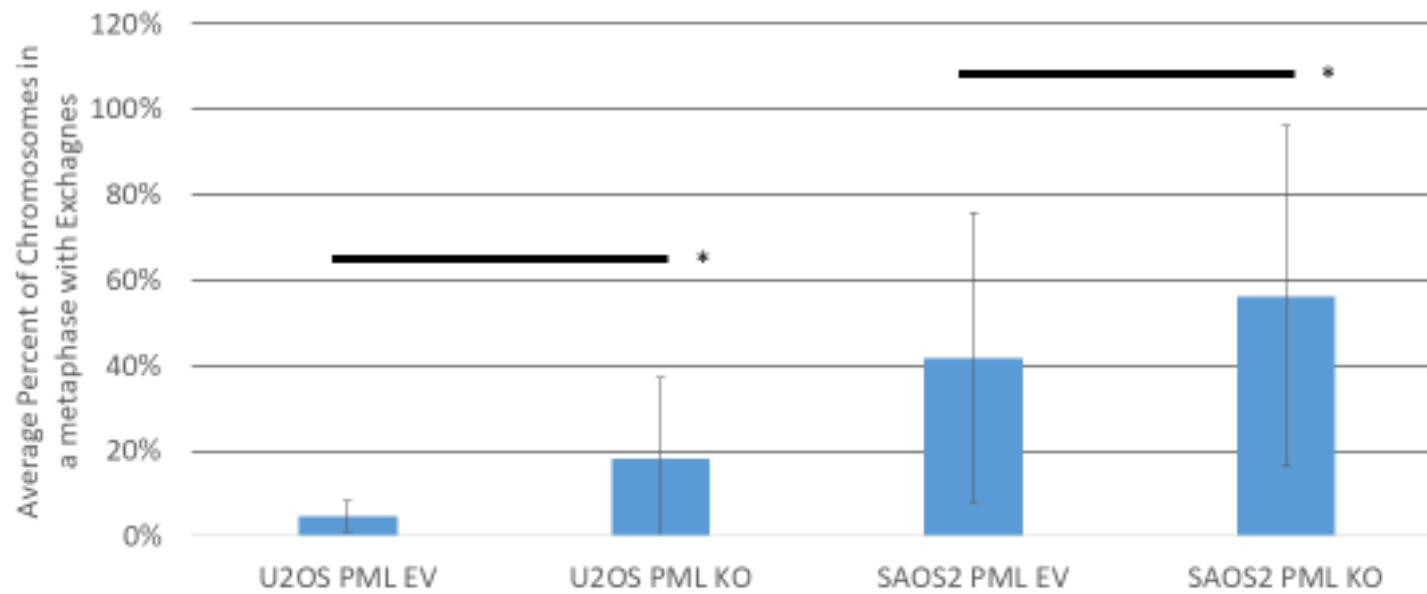
Figure 3-5 Telomere strand exchanges are increased in PML knockout cell lines over PML expressing cell lines. Data is as in fig. 3-4 but pooled by cell line and PML status. T-Test U2OS p<.01 and SAOS2 p<.05.
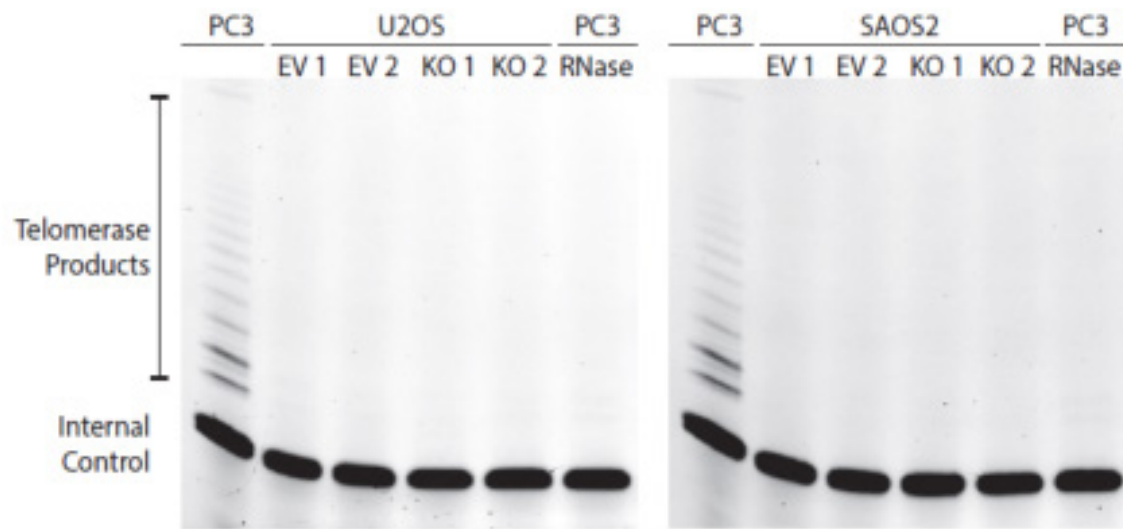
Figure 3-6 A Telomeric Repeat Amplifcation Protocol (TRAP) was performed on a selection of EV and PML KO cell lines. No activity was detected in U2OS and SAOS2. PC3 is a telomerase positive cell line as a positive control.
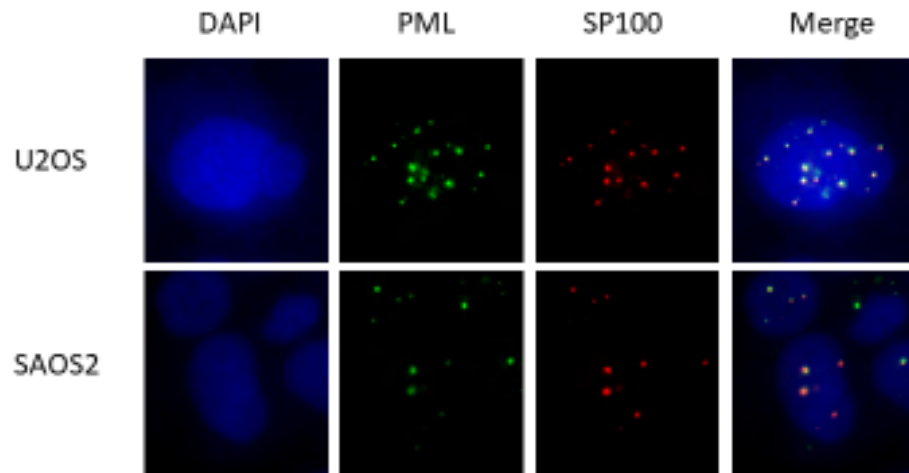
Figure 4-1 SP100 is a PML body resident protein. Combined immunofluorescence for PML (green) and SP100 (red) reveals frequent co-localizations in the nucleus (DAPI) of the cell lines U2OS and SAOS2.
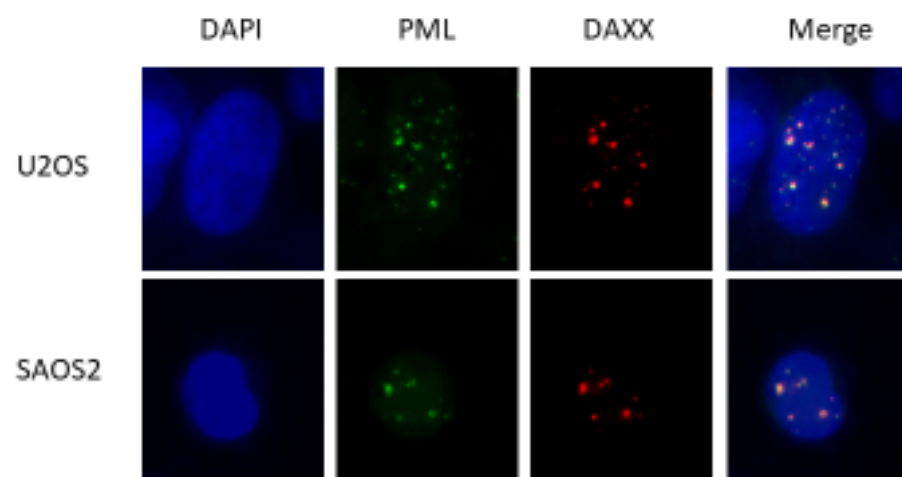
Figure 4-2 DAXX is a PML body resident protein. Combined immunofluorescence for PML (green) and DAXX (red) reveals frequent co-localizations in the nucleus (DAPI) of the cell lines U2OS and SAOS2.
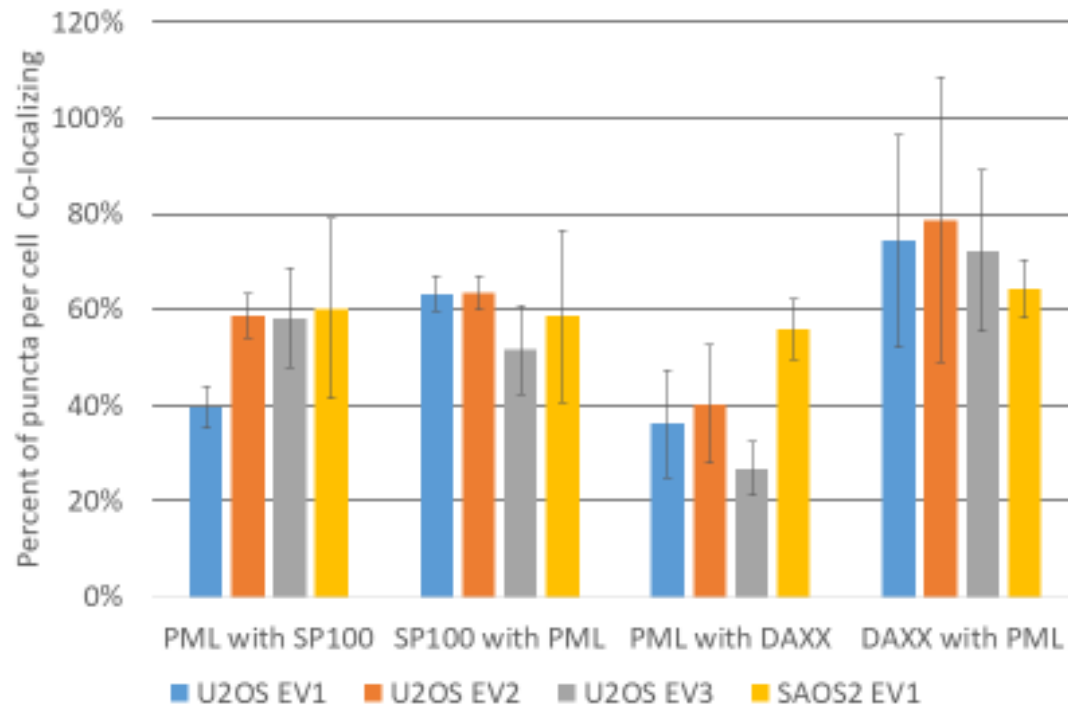
Figure 4-3 PML body resident proteins SP100 and DAXX are characterized as each having a high percent co-localization with PML. Immunofluorescence images as in figure 4-1 for SP100 and PML or figure 4-2 for DAXX and PML underwent image analysis for puncta number and co-localization status. For U2OS data is from three separate U2OS clonal cell lines with n = 8 fields of view covering greater than 300 nuclei and for SAOS2 one clonal population with n = 8 fields of view covering greater than 300 nuclei.
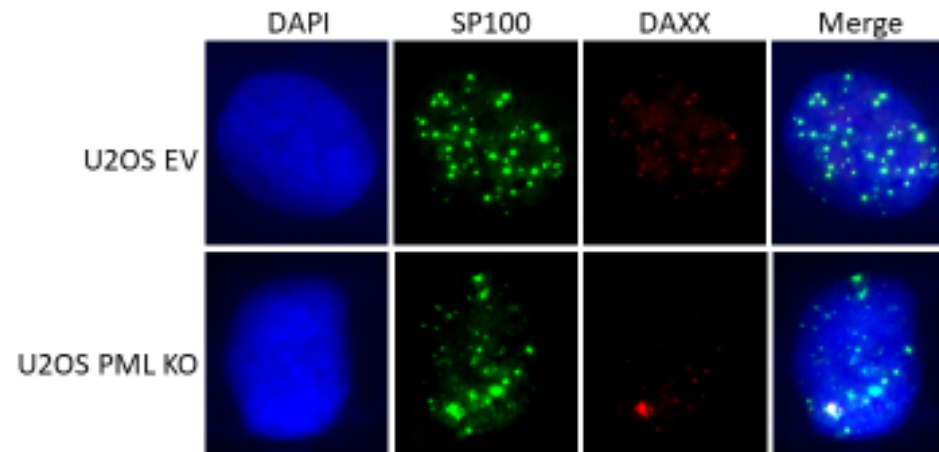
Figure 4-4 SP100 and DAXX form nuclear bodies that can co-localize independently of PML. Immunofluorescence for SP100 (green) and DAXX (red) with DAPI nuclear staining in the U2OS cell line in either control U2OS EV or in PML knockout U2OS PML KO.
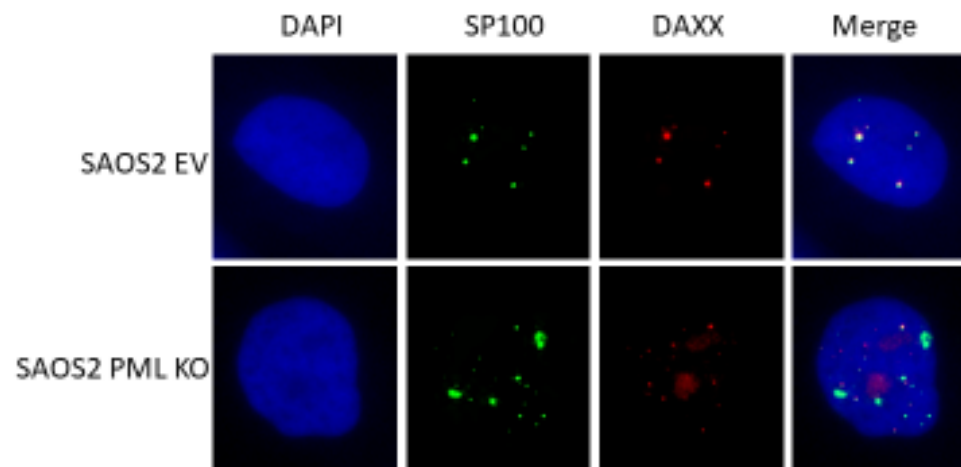
Figure 4-5 SP100 and DAXX form nuclear bodies that can co-localize independently of PML. Immunofluorescence for SP100 (green) and DAXX (red) with DAPI nuclear staining in the SAOS2 cell line in either control SAOS2 EV or in PML knockout SAOS2 PML KO.
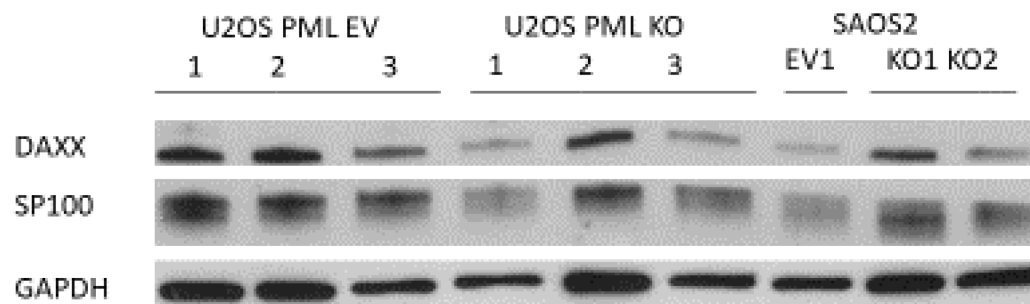
Figure 4-6 SP100 and DAXX Protein Expression in control and in Cas9 PML targeted clones. SDS-PAGE followed by immunoblotting for the SP100 and DAXX protein indicates their expression in the absence of PML on the cellular level. Immunoblotting for GAPDH as a loading control.
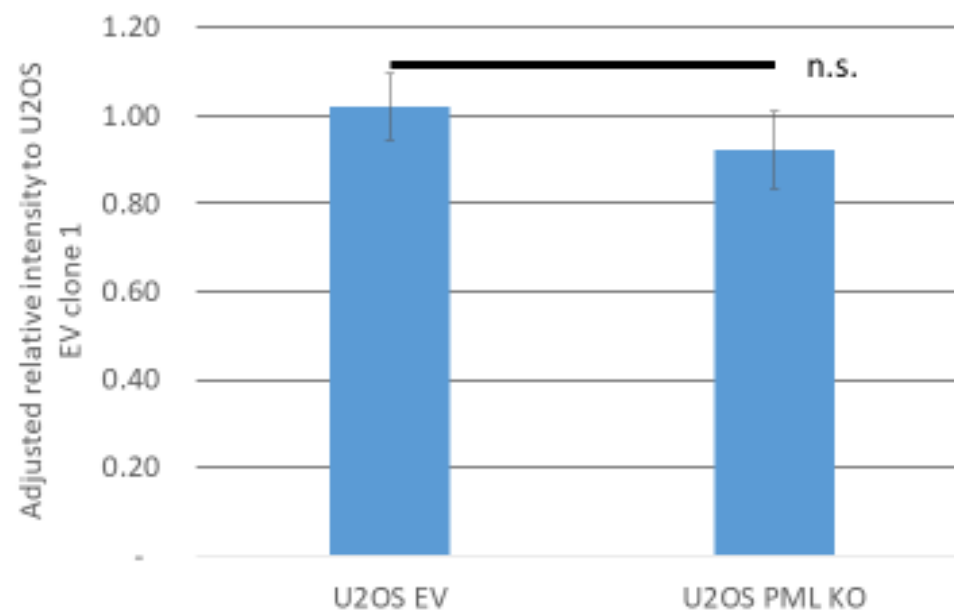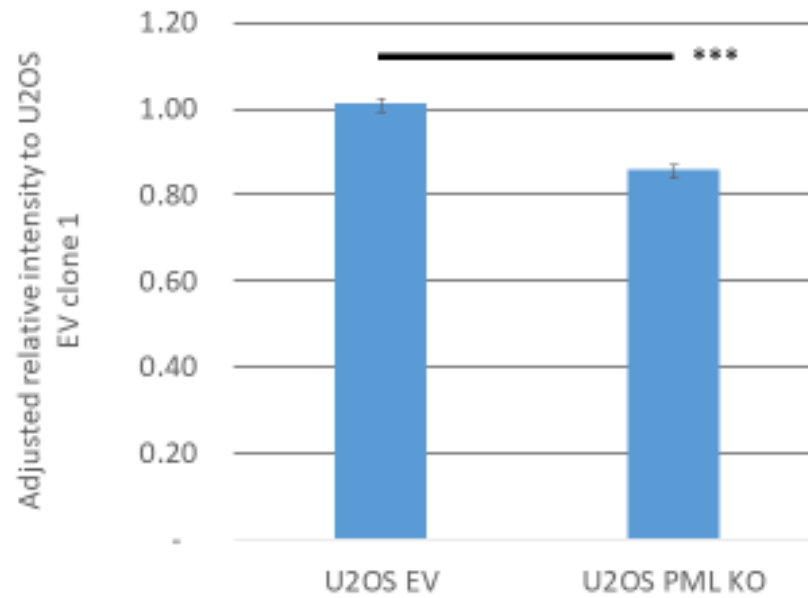
Figure 4-7 Levels of SP100 protein are unchanged after loss of PML in the U2OS cell line. Immunoblots from figure 4-6 were analyzed by densitometry and adjusted to U2OS EV 1 protein levels. The average adjusted densities were then compared between PML EV and PML KO and found to be insignificant in a t-test. (n=3 for EV and n=3 for KO)
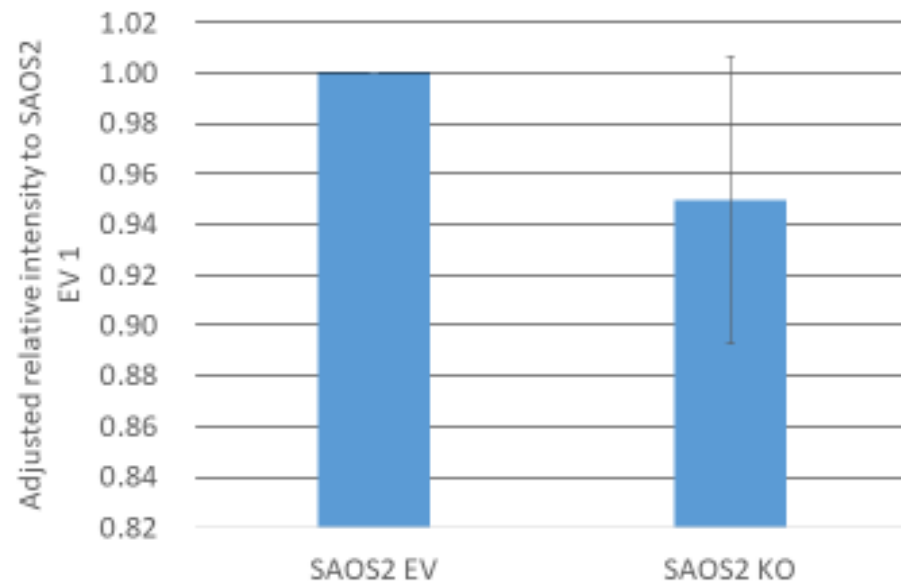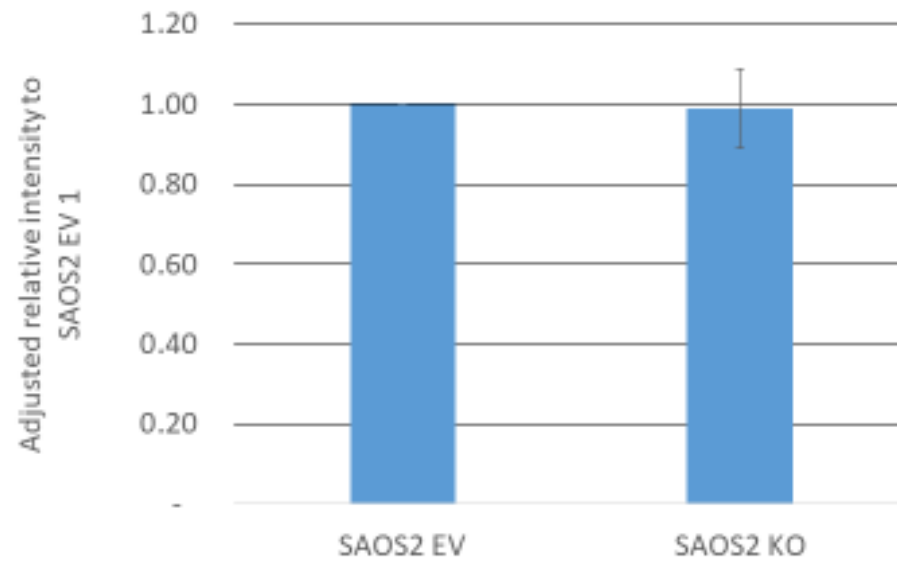
Figure 4-8 Levels of SP100 protein are similar after loss of PML in the SAOS2 cell line. Immunoblots from figure 4-6 were analyzed by densitometry and adjusted to SAOS2 EV 1 protein levels. . (n=1 for EV and n=2 for PML KO)

Figure 4-9 Levels of DAXX protein are reduced after loss of PML in the U2OS cell line. Immunoblots from figure 4-6 were analyzed by densitometry and adjusted to U2OS EV 1 protein levels. The average adjusted densities were then compared between PML EV and PML KO and found to be significant in a t-test $p < .0005$. (n=3 for EV and n=3 for KO) The change is approximately a 15% reduction in DAXX levels.
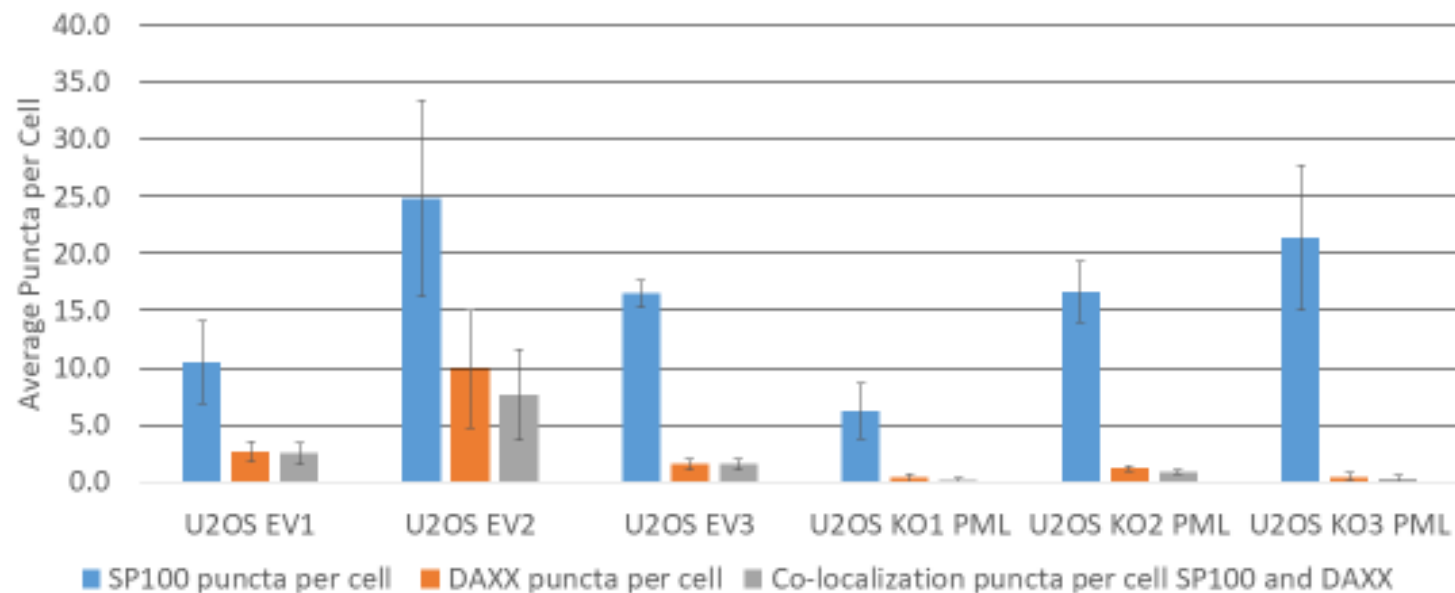
Figure 4-10 Levels of DAXX protein are similar after loss of PML in the SAOS2 cell line. Immunoblots from figure 4-6 were analyzed by densitometry and adjusted to SAOS2 EV 1 protein levels. (n=1 for EV and n=2 for PML KO)
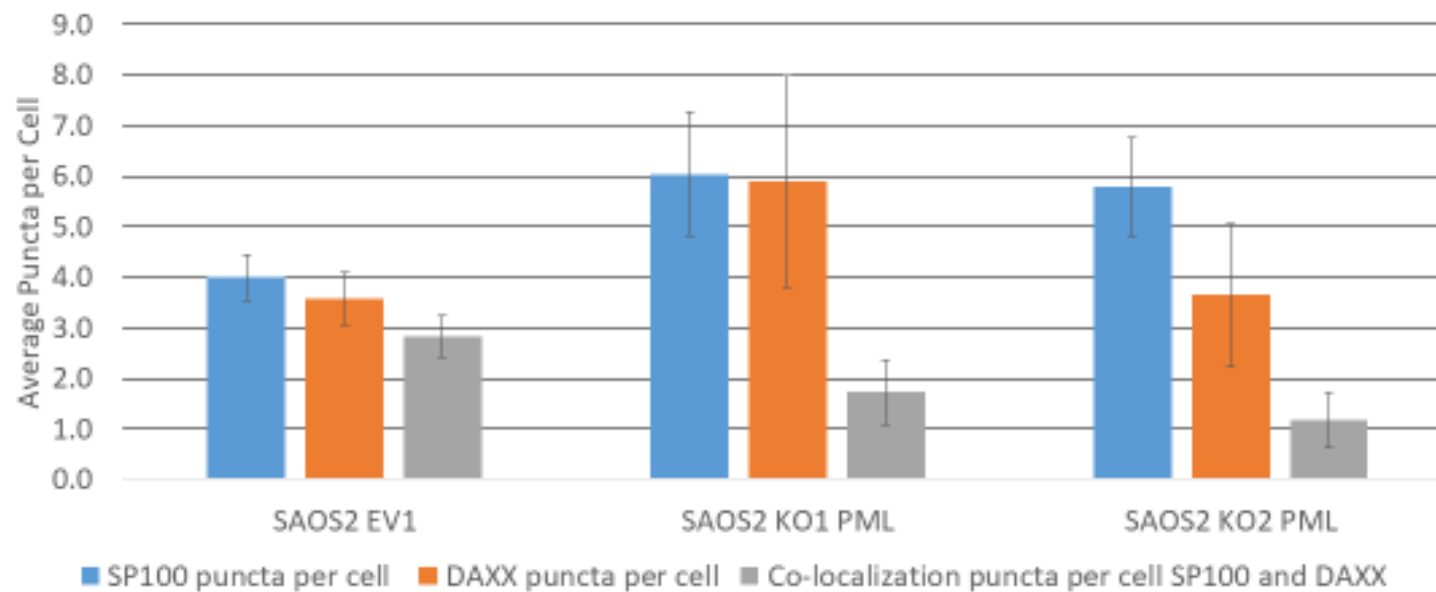
Figure 4-11 The influence of PML on nuclear SP100 and DAXX body formation in U2OS. Immunofluorescence images as in figure 4-4 for U2OS underwent image analysis for puncta number and co-localization status. For U2OS data is from three separate control PML expressing U2OS clonal cell lines with n = 8 fields of view covering greater than 300 nuclei and from three separate PML knockout U2OS clonal cell lines n = 8 fields of view covering greater than 300 nuclei.

Figure 4-12 The influence of PML on nuclear SP100 and DAXX body formation in SAOS2. Immunofluorescence images as in figure 4-5 for SAOS2 underwent image analysis for puncta number and co-localization status. For SAOS2 one control PML expressing clonal population with n = 8 fields of view covering greater than 300 nuclei was analyzed and from two PML knockout SAOS2 clones lines with n ≥ 8 fields of view covering greater than 300 nuclei.
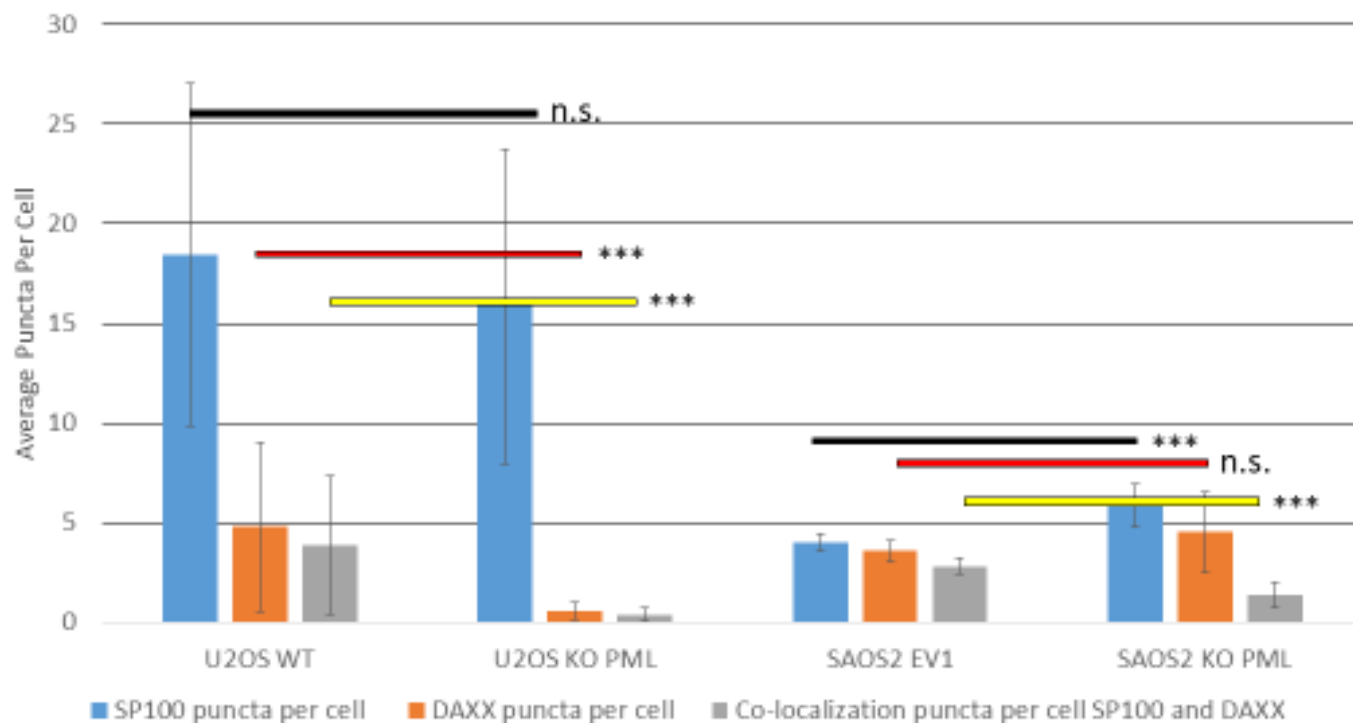
Figure 4-13 The average number of puncta for SP100, DAXX and their co-localizations compared between PML EV and KO on either cell line U2OS or SAOS2 reveals significant changes due to PML loss. Data is as in figure 4-10 and Figure 4-11 with cell line identity and PML status used as grouping. Consistent between the two cell lines is an overall decrease in co-localization events between the two proteins. T-test: n.s. = not significant *** = p< .0005, U2OS total fields of view =16 each for EV and KO, SAOS2 total fields of view = 8 EV and n=24 for KO
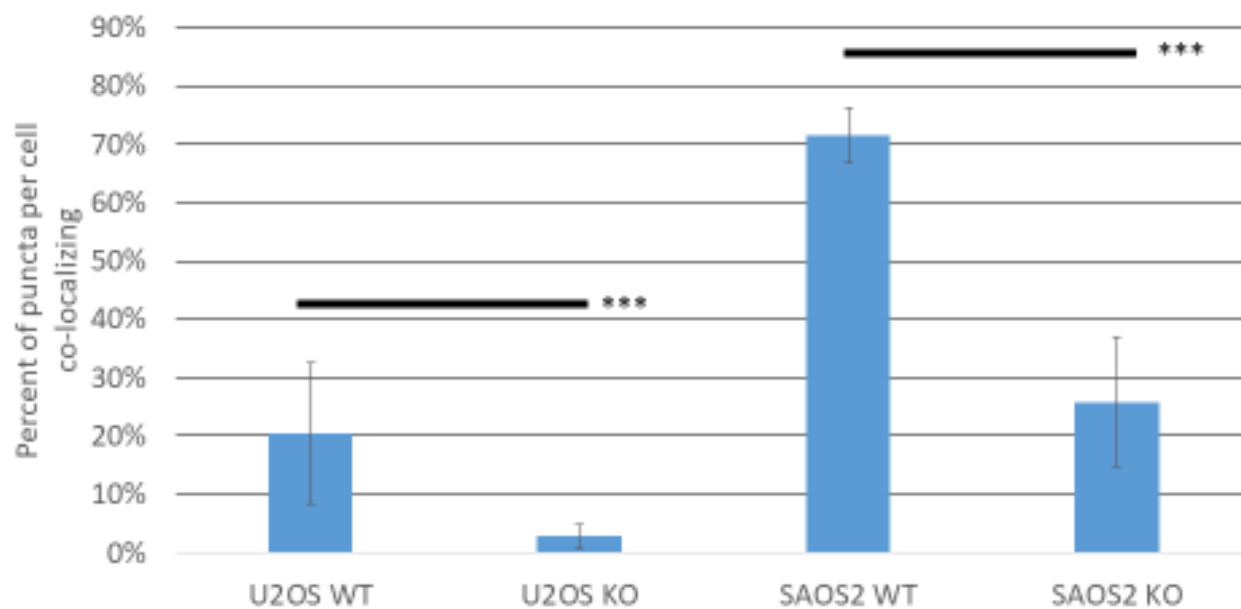
Figure 4-14 Fraction of SP100 puncta per cell that co-localize with DAXX in cell lines grouped by PML status. Data are as in figure 4-13. To partially account for changes in puncta number as a result of PML KO each field of view had their number of co-localized puncta between SP100 and DAXX calculated as a percent of the total number of SP100 puncta. There is a significant decrease in relative co-localizations for SP100 as a result of PML KO in both cell lines. T-test: *** = p< .0005
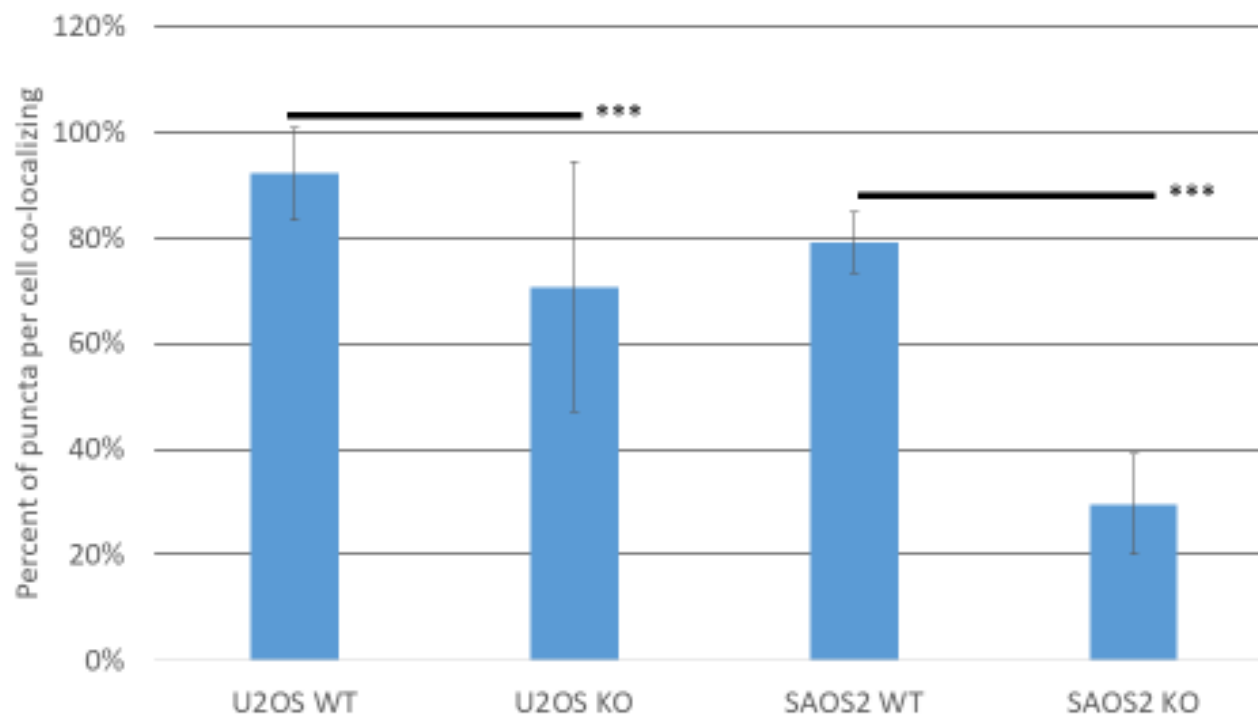
Figure 4-15 Fraction of DAXX puncta per cell that co-localize with SP100 in cell lines grouped by PML status. Data are as in figure 4-13. To partially account for changes in puncta number as a result of PML KO each field of view had their number of co-localized puncta between DAXX and SP100 calculated as a percent of the total number of DAXX puncta. There is a significant decrease in relative co-localizations for DAXX as a result of PML KO in both cell lines. T-test: *** = p< .0005
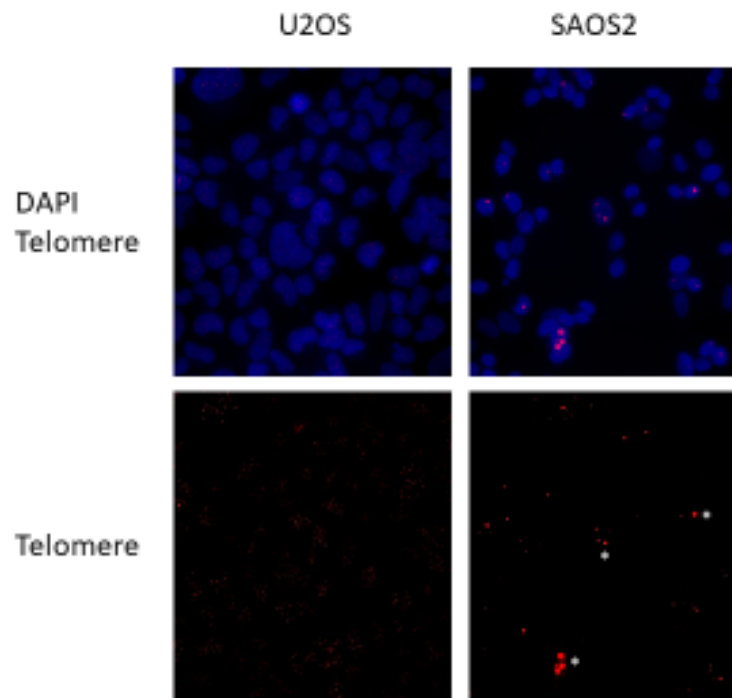
Figure 4-16 The large ultra-bright telomere DNA foci typical of ALT are readily discernable over chromosomal telomere end signals in the SAOS2 cell line while in U2OS telomere signals are closely distributed. Some SAOS2 foci are marked with *. Telomere FISH (telomeres in red) combined with DAPI (blue) staining was performed on cells grown in chamber slides.
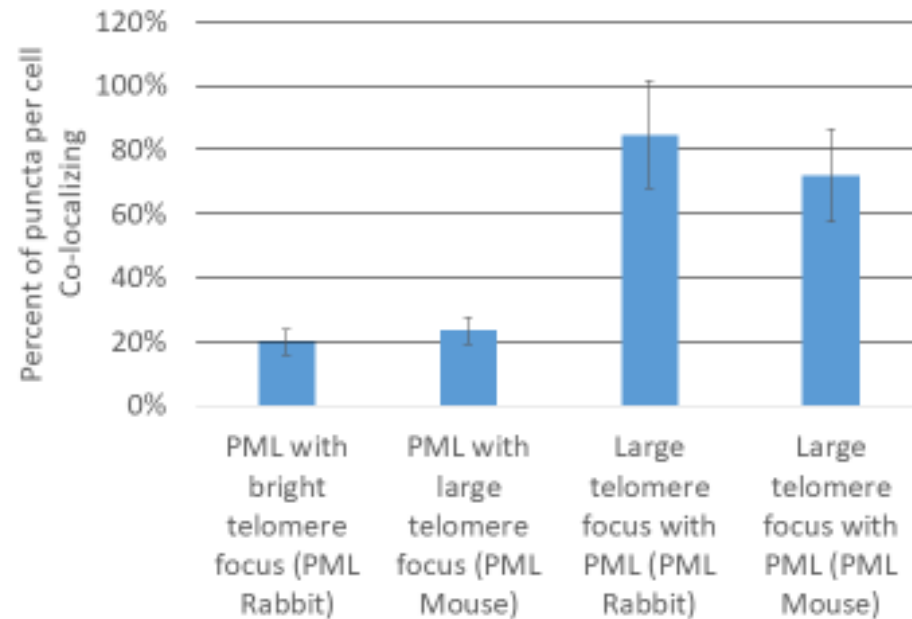
Figure 4-17 Large telomere foci often have co-localizing PML protein in SAOS2. Telomere FISH combined with immunofluorescence for PML was performed on SAOS2 EV cells grown in chamber slides. Two anti PML antibodies were utilized in two separate experiments one species rabbit and one species mouse.
Eight fields of view were captured for each condition with greater than 300 nuclei counted, processed with a high threshold for brightness to significantly exclude chromosomal telomeres and underwent image analysis for puncta number and co-localization status. Number of co-localization events were then denominated in terms of number of telomere puncta or PML puncta.
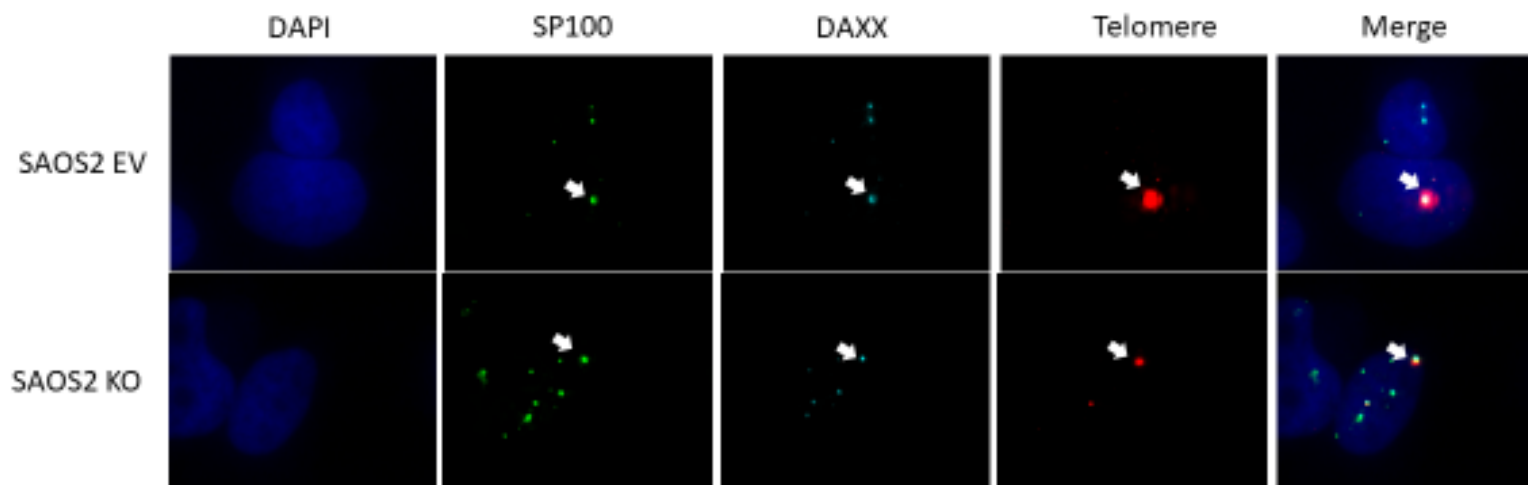
Figure 4-18 SP100 and DAXX will localize and co-localize to large telomere foci with and without PML. Combined telomere FISH (red) and immunofluorescence for SP100 (green) and DAXX (light blue). Arrowhead indicates co-localization.
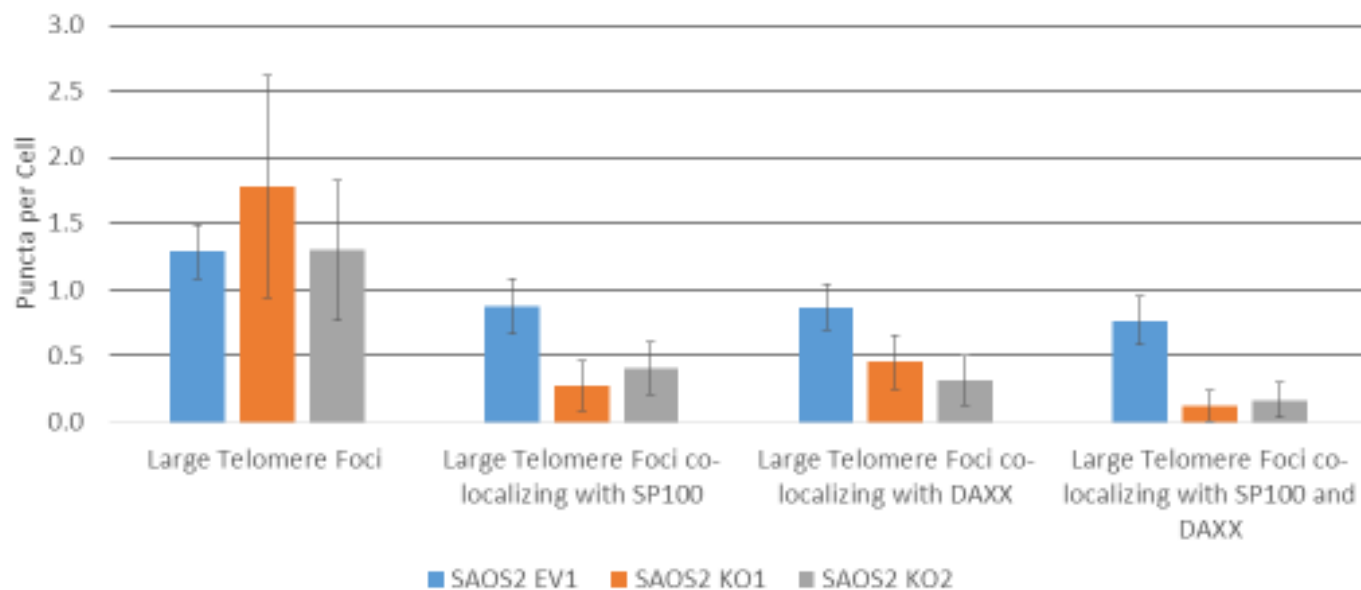
Figure 4-19 SP100 and DAXX are frequently found at large telomere foci when in the presence of PML and continue to associate with large telomere foci without PML. Telomere FISH combined with immunofluorescence for SP100 and DAXX was performed on SAOS2 cells grown in chamber slides. A minimum of eight fields of view were captured for each condition with more than 300 nuclei counted, processed with a high threshold for brightness to significantly exclude chromosomal telomeres and underwent image analysis for puncta number and co-localization status. (n=8 SAOS2 EV1, n=12 SAOS2 KO1, n=16 SAOS2 KO2)
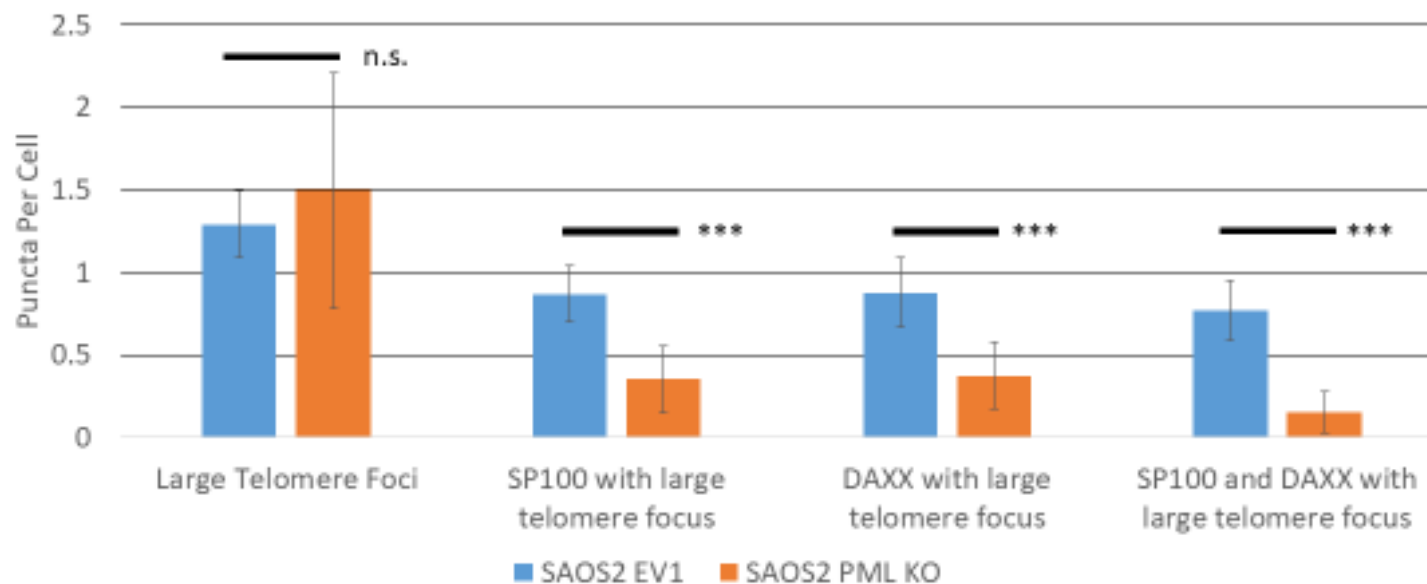
Figure 4-20 SP100 and DAXX have significantly reduced co-localizations at large telomere foci. Telomere FISH combined with immunofluorescence for SP100 and DAXX was performed on SAOS2 cells grown in chamber slides. A minimum of eight fields of view were captured for each condition with more than 300 nuclei counted, processed with a high threshold for brightness to significantly exclude chromosomal telomeres and underwent image analysis for puncta number and co-localization status. (T-test: *** = p< .0005 n=8 SAOS2 EV1, n=12 SAOS2 KO1, n=16 SAOS2 KO2)
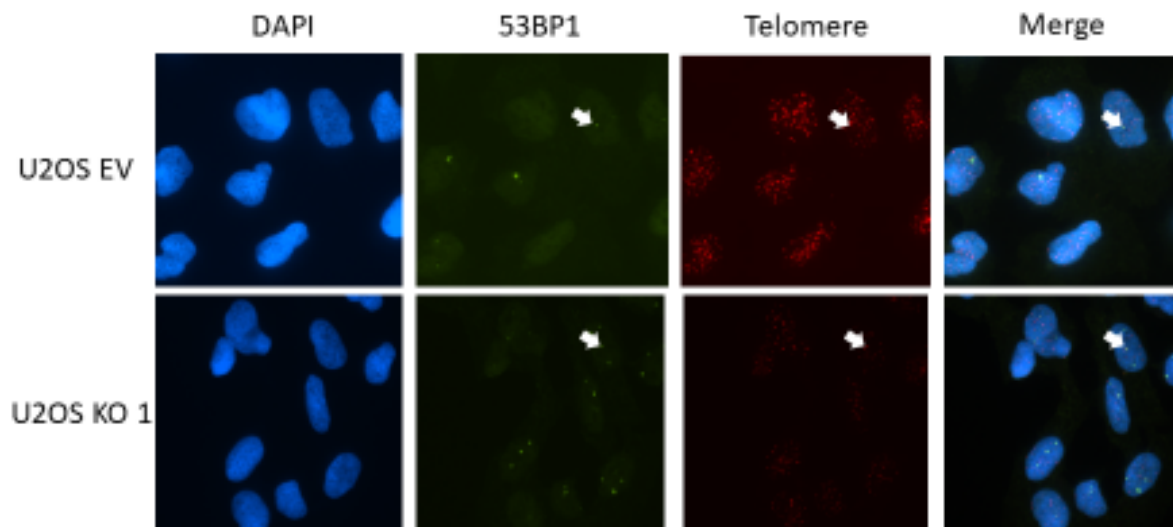
Figure 5-1 Telomere dysfunction induced foci (TIF) in U2OS. A TIF is defined as the IF co-localization of a DNA damage marker such as γH2AX or 53BP1 with a telomere. Here telomere FISH (red) is combined with IF for 53BP1. Arrowhead indicates a TIF.
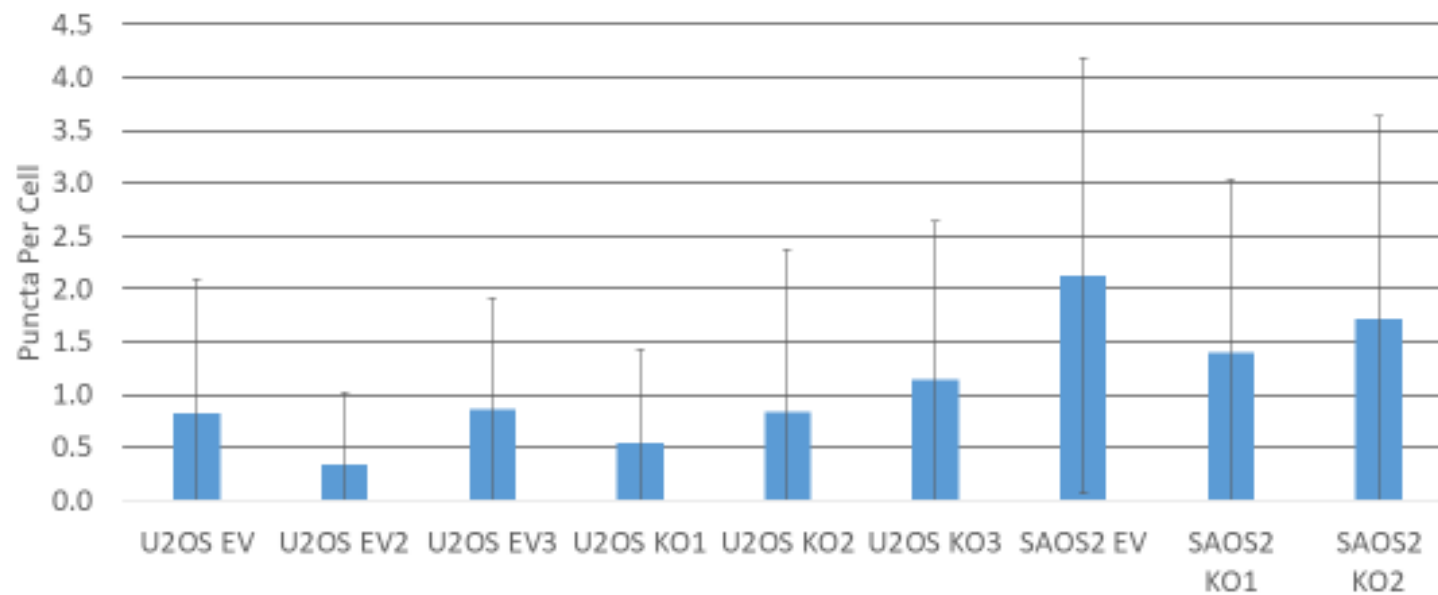
Figure 5-2 TIF across analyzed cell lines. Combined telomere FISH and IF on U2OS and SAOS2 PML EV and KO cell lines. Images were captured manually and then sent through image analysis to determine the number of co-localization events per cell between 53BP1 and telomeres. N=200 nuclei per cell line. A significant number of cells had no TIF in every cell line.
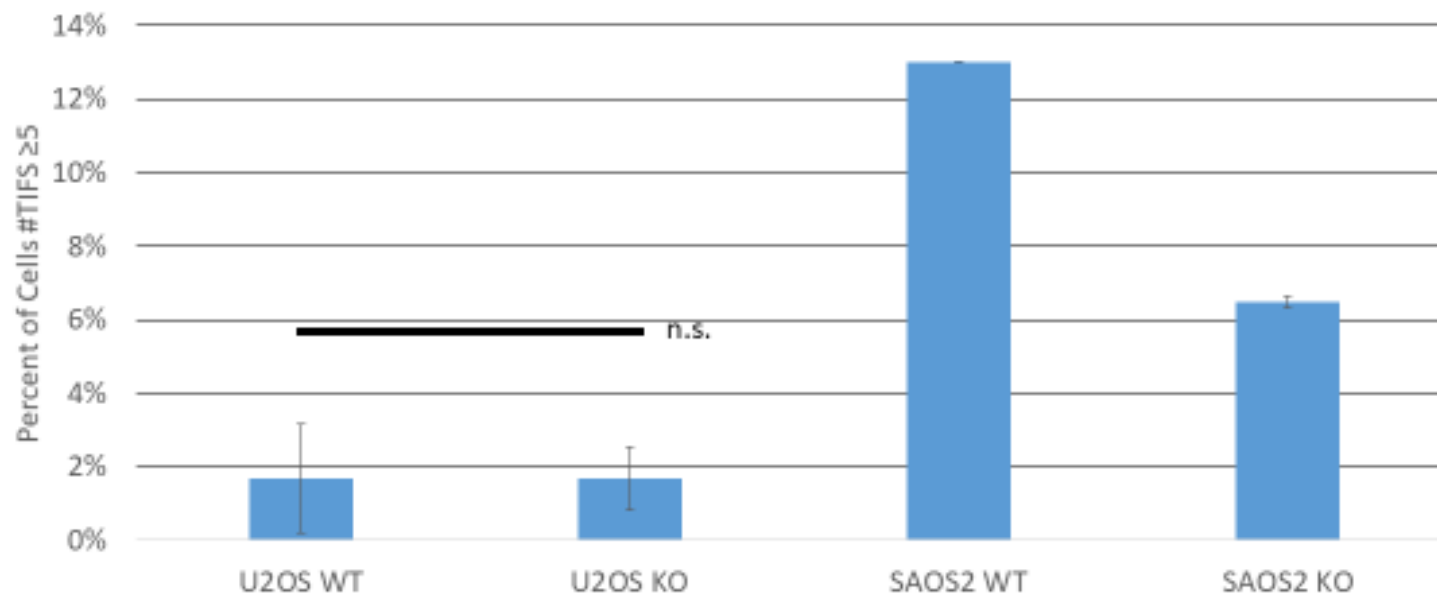
Figure 5-3 Average percent of cells with greater than 5 TIFs per cell. Samples were grouped by cell line and then by PML status. Images were collected and analyzed as in figure 5-2. Counting only cells with greater than 5 TIF limits the analysis to only cells with significant telomere dysfunction. T-Test is not significant for differences between U2OS WT and KO. In SAOS2 there is an apparent trend towards decreasing TIFs as result of PML KO.

Intended to be Blank

Discussion

The ALT pathway refers to the means by which 5-15% of cancers maintain their telomere lengths without discernible telomerase activity.[50] Finding a means to halt ALT activity presents an opportunity to potentially cure these cancers as all dividing cells need to maintain their telomeres. The probability of finding a cure will only increase as our understanding of ALT increases. What is known now about ALT is based on the examination of tumors that do not have telomerase activity. These observations allow us to list shared characteristics of cells with ALT but the causation of ALT remains unknown. The characteristics explored in this study include: no telomerase activity, heterogeneous telomere lengths, presence of extra chromosomal telomere c-circles, homologous recombination at telomeres, and the presence of APBs.[51, 54, 62, 63, 69] Within these correlated factors there may be causal factors for ALT. The examination of TERRA was in part motivated by the need to discover as many ALT associated characteristics as possible. At the time TERRA had not been characterized in ALT cells. To discern if the PML component of the APB is just correlated to ALT versus being required, the PML protein was eliminated from ALT cells and ALT activity was then assessed in these knockout cells. There are several questions that this study also sought to elucidate. Do human cells survive without the PML protein? Can ALT cells survive without PML but not maintain their telomeres? Are some characteristics of ALT dependent on the presence of PML? Are they modified by PML? Beyond this question of requirement for the ALT pathway there are data to describe the formation of ALT associated nuclear bodies. Is there TERRA in these ALT bodies? Are the large telomere foci still forming? Are there components associated with the APB that are constant and could be candidates for further study? Lastly this study presents an opportunity to learn more about the PML protein. What role is PML playing in nuclear trafficking? It is known for forming nuclear bodies but there is much to be learned regarding the functional significance of these bodies and their impact on PML body resident proteins.[82, 86, 96, 104, 106]

Part 1 TERRA

The telomeres of mammalian cells have a DNA, a protein and an RNA component.[20, 114] It is known that the RNA component is in part made up of the non-coding transcription of the C-rich strand of the telomere.[21] FISH for TERRA species in a normal human cell and in the HeLa cell line produces signals that mirror the pattern of a telomere DNA FISH.[26] Combined IF-FISH for TRF2 and TERRA indicates this pattern is the result of TERRA binding to telomere sites.[19] Since TERRA is FISH visible and the large telomere foci common to cells utilizing ALT are also FISH visible, it provided an opportunity to examine if TERRA is localized to these foci. Additionally, ALT cells could have changes in TERRA patterns versus what has been previously observed. TERRA in the U2OS cell line appears in a pattern and amount consistent with published findings on TERRA.[20, 107] There was no CCCTAA repeat RNA detected which means that no telomere transcripts are being generated from the G strand telomere sequence. While simple in nature these conclusions have significance from what they exclude as possibilities for telomere RNA biology in ALT cells. Chromosomal telomeres in ALT cells have significant spontaneous telomere dysfunction and DNA damage signaling.[115] Normal TERRA functions as a part of the shelterin complex and disruption in its function could partly explain this persistent DNA damage response signaling in ALT cells.[97, 115] Potential abnormalities in TERRA in ALT that could be tested could include changes in localization or in TERRA levels relative to telomere DNA signals. Assessing whether TERRA was in APBs was the continuation in this line of reasoning. As with many good ideas, while these studies were underway, another group published work on TERRA in ALT confirming that TERRA is indeed found in APBs, and TERRA levels relative to telomere DNA content is 1000 times more than in ALT cells than in telomerase positive cell lines.[107] On the subject of opposite strand transcription of telomeres, or anti-TERRA, if it had been found then it would have been unique to ALT, as it has not been observed in non-ALT human cells.[21] The finding of alti-TERRA would imply that hybridization of alti-TERRA to TERRA could take place, thereby potentially pulling TERRA away from the shelterin complex, contributing to

83

telomere dysfunction. TERRA is still a promising area of research with many unanswered questions having implications for telomere biology. In terms of ALT, why is TERRA over-expressed? Is this one of the steps in the development of ALT? Why is TERRA in APBs? One particularly interesting area is the development of a TERRA stain for paraformaldehyde-fixed paraffin embedded tissues. If telomere lengths are important in identifying and subtyping cancer, then the TERRA RNA component may turn out to be critical as well.

Part 2 PML and ALT

The principal connection between the PML protein and the ALT pathway is the APB.[69] What establishes the significance of the APB to the ALT pathway is that these bodies contain large amounts of telomere sequences. ALT is a telomere maintenance mechanism believed to be based on homologous recombination (HR).[63] In support of this is the observation of the localization of several DNA repair proteins e.g. RAD51, BRCA1/2, RPA to the APB and knockout of the components of HR result in a loss of viability in ALT cells.[54, 55, 58, 101, 112] HR is classically a DNA repair pathway and not necessarily a replicative process[117, 118]. It stands to reason then that these foci are potential sources of telomere sequence that are important for the ALT mechanism. PML is frequently observed at these foci even going so far as to give them a designation.[54] Just how often within or between ALT utilizing tissues APBs form has not been studied extensively. It is important to also note that neither the requirement of large telomere foci nor the PML protein for the ALT pathway has been established. This presents an excellent opportunity for examination by the current study.

As the results presented in this thesis show, human cell lines are viable without the PML protein. A similar conclusion was drawn for mice as there is a PML knockout mouse model.[71] These findings seem surprising, given the many essential pathways that PML protein has been thought to play a role in.[70-72, 75, 87, 94, 96, 106, 119] It is important to make note of this because it can help explain why

there are no PML connected genetic diseases. Promyelocytic leukemia is a disease connected to PML but it is not believed to be driven by functional loss of PML.[95] Some other pathway must be redundant with that of PML or its loss can be compensated for such as with transcriptional changes. Another possibility is that PML may interact with many proteins but have only a slight influence on each, thereby reducing the impact of its loss. PML is an interferon response gene, and if viewed through the lens of immunology this pattern seems more reasonable. Many components of the mouse immune system can be knocked out in a stable viable mouse model [120]. Another possibility is that PML is required for the viability of *normal* human cells, but the cancer-derived cell lines used here have so much disruption in their genome that they no longer depend on intact PML. PML is intimately linked to the TP53 pathway, and that pathway is knocked out in at least half of cancers.[119] TP53 status may be playing a role in the present study as well. The U2OS cell line is wild type for TP53 and SAOS2 is a knockout for TP53 and it has been observed to have a significant impact on DNA damage signaling in these cell lines.[115] This may help explain the recorded differences in this study in telomere recombination or TIF formation between the two cell lines. Lastly on a similar note to the TP53 pathway, the PML knockout phenotype may be more apparent in stress induction experiments. It is intimately linked to the SUMO ubiquitin pathway which are known to respond to stress.[77, 91, 92, 121, 122] Thus, in order to fully investigate the impact of PML loss on general cellular viability further work is needed.

As shown in this thesis, cancer-derived ALT cell lines are viable without the PML protein. Whatever role it had, if it had any, in the pathogenesis of these ALT-utilizing cancers, PML is either no longer necessary, or is able to be compensated for at this snapshot in time of cancer. The results in this thesis also indicate that PML is not absolutely required for multiple ALT characteristics (putative ALT biomarkers) that are used to identify a cell as ALT-positive. Notably, no single assay or analysis is enough to give a definitive answer as to whether or not a cell, or cell population, is ALT-positive.[123] Experts in the field may have their favorite biomarker to identify ALT, but ALT is functionally defined: ALT-positive

85

cells maintain their telomeres in the absence of telomerase by fundamentally altering their telomere biology.[58] Biomarkers that have been associated with ALT include; telomere recombination, telomere c-circles, extreme telomere length heterogeneity and comparatively giant masses of telomere RNA and DNA sequence in discrete foci within their nucleus. All of this is present in PML expressionless ALT cells. In keeping with the maintenance of ALT features, PML knockouts maintain their telomere lengths in the long term and do not have a net increase in telomere dysfunction as measured by TIFs. The work presented here, by complete deletion of PML definitively show that PML is not required for maintenance of pre-existing ALT in human cancer-derived cell lines.

The data generated in this thesis support the existing designation of SP100 and DAXX as PML body resident proteins. In both SAOS2 and U2OS, across an asynchronously grown population of cells, SP100 and DAXX spend more time in PML bodies than out of them, as indicated by co-localization studies. It would be reasonable then to believe that there could be functional connections between these 3 proteins. The data is somewhat inconsistent between the two cell lines in terms of the total puncta and protein levels. Despite clone-to-clone and cell line-to-cell line variations observed in the cells studied here, PML does act to increase interactions between SP100 and DAXX which is consistent in both cell lines. PML could then be acting as a regulator of intra-nuclear trafficking of these proteins. Here, there are a number of possible mechanisms of action. PML could be acting like a storage depot for nuclear proteins, or at least SP100 and DAXX, although it is not possible to draw conclusions on the purpose of such a storage site from the presently available data. It could be a nuclear vesicle for transport of these proteins to specific sites in the nucleus such as sites of DNA damage. The data is a fixed snapshot and this would require further investigation in live cells. The drop in co-localizations of SP100 and DAXX could be explained also by a decrease in the residency time of these two proteins at a specific site, without PML acting to "hold" proteins there. The concept of PML acting as a mediator of interactions between proteins provides a link to our understanding of the nature of the APB.

The data obtained here are consistent with previous observations of APBs for the SAOS2 cell line.[69] These observations are critical to understanding the significance of this thesis. Time and again the large telomere foci in different ALT cell lines have been presumed to be synonymous with the APB. This assumption stems from the frequent co-localizations of PML with these foci. A dogmatic approach to APBs is potentially harmful for studying ALT, because even in a cell line where 85% of large telomere foci have PML there are still 15% of them that do not. As shown in this thesis, these large telomere foci are still present even in complete PML knockouts. What does this mean then for discerning the role of PML in ALT? Could it be that PML is not required for ALT because APBs or ALT bodies still form without it? This would be consistent with the theory that these large foci are the site of the mechanism of action of ALT but this has not been conclusively proven.[103] SP100 and DAXX each still co-localize with large telomere foci and even all three occur together without PML. The theorized role of PML as a mediator of nuclear traffic remains consistent when examining ALT bodies. PML loss decreases the number of times SP100 and DAXX interact but also the number of times these proteins interact with large telomere foci. The continued interactions of these proteins after PML loss with the foci may have other implications for ALT. Mutations in DAXX have been linked to the presence of ALT in tumors and it may be possible that mutations in SP100 will also be significantly linked to occurrence of ALT.[46, 50] One particular observation worth examining is the determination of ALT activity by the c-circle assay. The results here demonstrate continued ALT activity in all clones, but there is noticeable variability between EV and PML KOs. C-circle levels have been used to quantify ALT "activity".[66] There is also the increase in homologous recombination in PML KO. Are these two observations linked? C-circles may be the excision product of homologous recombination. There is also the alternate viewpoint that PML is acting to inhibit ALT and prolonged presence and assembly of the ALT body does not directly lead to telomere length maintenance.

Although PML is not required for the maintenance of ALT, this does not mean that it may not be a useful therapeutic target in ALT-positive cancers. Rescue experiments on PML KO clones could help determine the quantity of change in the characteristics of ALT by reducing clonal variability. The generalizability of the findings regarding the loss of PML and phenotypes such as focus formation and co-localizations of PML body resident proteins, such as SP100 and DAXX, could be furthered by investigating telomerase-positive/ALT-negative cancers using Cas9 against PML. Clinical ALT-positive cancer samples can be examined for PML expression levels and co-localizations between PML and PML-interacting/PML body resident proteins. Discerning the impact of PML on extrachromosomal telomere DNA versus chromosomal telomere DNA could further our understanding of just what is in an APB and give possible clues to its function (if one indeed exists) in ALT-positive cells. Reintroduction of PML labelled with GFP could allow for in vivo imaging of the formation of ALT bodies.

A number of significant findings that advance our understanding of the ALT phenomenon are presented in this thesis. TERRA localization in U2OS occurs in a pattern consistent with its previously described residency at telomere DNA sequences. The PML protein is not required for cell growth and the maintenance of telomere lengths in cells utilizing the ALT pathway. PML is also not required for the ALT biomarkers of telomere recombination, c-circles and does not reactivate telomerase. This work also makes several conclusions that may redefine the way we describe the APB. Large telomere foci do not require PML to form and these foci can still co-localize with the PML body resident proteins SP100 and DAXX. Does this imply that we should refer to these as just ALT bodies and drop the PML designation? Just what is required then for the definition of an ALT body? Are they even necessary? This work also informs our understanding of PML body resident proteins. PML is not required for these proteins to form nuclear bodies but it does however change their frequency. PML is therefore important for these proteins localization which may also impact the function of these proteins. Interestingly their overall expression is almost unaffected which leads to wonder of the impact of their diffusion in the cell.

Telomere dysfunction is also not increased in PML knockouts so PML may not be important for telomere

stability. Both PML and ALT are complex in function and this study raises more questions than answers

but this study could represent a blueprint for determination of the factors that are necessary for ALT.

Protein by protein find a cure for ALT cancers.

References

1. Moyzis, R.K., et al., *A highly conserved repetitive DNA sequence, (TTAGGG)n, present at the telomeres of human chromosomes.* Proc Natl Acad Sci U S A, 1988. **85**(18): p. 6622-6.
2. Palm, W. and T. de Lange, *How shelterin protects mammalian telomeres.* Annu Rev Genet, 2008. **42**: p. 301-34.
3. Makarov, V.L., Y. Hirose, and J.P. Langmore, *Long G tails at both ends of human chromosomes suggest a C strand degradation mechanism for telomere shortening.* Cell, 1997. **88**(5): p. 657-66.
4. Nikitina, T. and C.L. Woodcock, *Closed chromatin loops at the ends of chromosomes.* J Cell Biol, 2004. **166**(2): p. 161-5.
5. Stansel, R.M., T. de Lange, and J.D. Griffith, *T-loop assembly in vitro involves binding of TRF2 near the 3' telomeric overhang.* EMBO J, 2001. **20**(19): p. 5532-40.
6. Wang, R.C., A. Smogorzewska, and T. de Lange, *Homologous recombination generates T-loop-sized deletions at human telomeres.* Cell, 2004. **119**(3): p. 355-68.
7. Sfeir, A., et al., *Mammalian telomeres resemble fragile sites and require TRF1 for efficient replication.* Cell, 2009. **138**(1): p. 90-103.
8. Konishi, A., T. Izumi, and S. Shimizu, *TRF2 Protein Interacts with Core Histones to Stabilize Chromosome Ends.* J Biol Chem, 2016. **291**(39): p. 20798-810.
9. Zhou, X.Z., K. Perrem, and K.P. Lu, *Role of Pin2/TRF1 in telomere maintenance and cell cycle control.* J Cell Biochem, 2003. **89**(1): p. 19-37.
10. Martinez, P., et al., *Increased telomere fragility and fusions resulting from TRF1 deficiency lead to degenerative pathologies and increased cancer in mice.* Genes Dev, 2009. **23**(17): p. 2060-75.
11. Dimitrova, N. and T. de Lange, *Cell cycle-dependent role of MRN at dysfunctional telomeres: ATM signaling-dependent induction of nonhomologous end joining (NHEJ) in G1 and resection-mediated inhibition of NHEJ in G2.* Mol Cell Biol, 2009. **29**(20): p. 5552-63.
12. Celli, G.B., E.L. Denchi, and T. de Lange, *Ku70 stimulates fusion of dysfunctional telomeres yet protects chromosome ends from homologous recombination.* Nat Cell Biol, 2006. **8**(8): p. 885-90.
13. Konishi, A. and T. de Lange, *Cell cycle control of telomere protection and NHEJ revealed by a ts mutation in the DNA-binding domain of TRF2.* Genes Dev, 2008. **22**(9): p. 1221-30.
14. Martinez, P., et al., *Mammalian Rap1 controls telomere function and gene expression through binding to telomeric and extratelomeric sites.* Nat Cell Biol, 2010. **12**(8): p. 768-80.
15. Hockemeyer, D., et al., *POT1 protects telomeres from a transient DNA damage response and determines how human chromosomes end.* EMBO J, 2005. **24**(14): p. 2667-78.
16. Hockemeyer, D., et al., *Telomere protection by mammalian Pot1 requires interaction with Tpp1.* Nat Struct Mol Biol, 2007. **14**(8): p. 754-61.
17. Kibe, T., et al., *Telomere protection by TPP1 is mediated by POT1a and POT1b.* Mol Cell Biol, 2010. **30**(4): p. 1059-66.
18. Liu, D., et al., *PTOP interacts with POT1 and regulates its localization to telomeres.* Nat Cell Biol, 2004. **6**(7): p. 673-80.
19. Deng, Z., et al., *TERRA RNA binding to TRF2 facilitates heterochromatin formation and ORC recruitment at telomeres.* Mol Cell, 2009. **35**(4): p. 403-13.
20. Azzalin, C.M., et al., *Telomeric repeat containing RNA and RNA surveillance factors at mammalian chromosome ends.* Science, 2007. **318**(5851): p. 798-801.
21. Feuerhahn, S., et al., *TERRA biogenesis, turnover and implications for function.* FEBS Lett, 2010. **584**(17): p. 3812-8.
22. Nergadze, S.G., et al., *CpG-island promoters drive transcription of human telomeres.* RNA, 2009. **15**(12): p. 2186-94.

23. Martadinata, H. and A.T. Phan, *Structure of human telomeric RNA (TERRA): stacking of two G-quadruplex blocks in K(+) solution.* Biochemistry, 2013. **52**(13): p. 2176-83.

24. Poulet, A., et al., *The N-terminal domains of TRF1 and TRF2 regulate their ability to condense telomeric DNA.* Nucleic Acids Res, 2012. **40**(6): p. 2566-76.

25. Arora, R., C.M. Brun, and C.M. Azzalin, *Transcription regulates telomere dynamics in human cancer cells.* RNA, 2012. **18**(4): p. 684-93.

26. Flynn, R.L., et al., *TERRA and hnRNPA1 orchestrate an RPA-to-POT1 switch on telomeric single-stranded DNA.* Nature, 2011. **471**(7339): p. 532-6.

27. Porro, A., et al., *Functional characterization of the TERRA transcriptome at damaged telomeres.* Nat Commun, 2014. **5**: p. 5379.

28. Frenck, R.W., Jr., E.H. Blackburn, and K.M. Shannon, *The rate of telomere sequence loss in human leukocytes varies with age.* Proc Natl Acad Sci U S A, 1998. **95**(10): p. 5607-10.

29. Schluth-Bolard, C., A. Ottaviani, and F. Magdinier, *Dynamics and plasticity of chromosome ends: consequences in human pathologies* Atlas of Genetics and Cytogentics in Oncology and Haematology, 2009.

30. Ozturk, M.B., Y. Li, and V. Tergaonkar, *Current Insights to Regulation and Role of Telomerase in Human Diseases.* Antioxidants (Basel), 2017. **6**(1).

31. Kamranvar, S.A. and M.G. Masucci, *Regulation of Telomere Homeostasis during Epstein-Barr virus Infection and Immortalization.* Viruses, 2017. **9**(8).

32. Schmidt, J.C., A.J. Zaug, and T.R. Cech, *Live Cell Imaging Reveals the Dynamics of Telomerase Recruitment to Telomeres.* Cell, 2016. **166**(5): p. 1188-1197 e9.

33. Xi, L. and T.R. Cech, *Inventory of telomerase components in human cells reveals multiple subpopulations of hTR and hTERT.* Nucleic Acids Res, 2014. **42**(13): p. 8565-77.

34. Broccoli, D., J.W. Young, and T. de Lange, *Telomerase activity in normal and malignant hematopoietic cells.* Proc Natl Acad Sci U S A, 1995. **92**(20): p. 9082-6.

35. Bisht, K., et al., *Structural and functional consequences of a disease mutation in the telomere protein TPP1.* Proc Natl Acad Sci U S A, 2016. **113**(46): p. 13021-13026.

36. Chen, R., et al., *Telomerase Deficiency Causes Alveolar Stem Cell Senescence-associated Low-grade Inflammation in Lungs.* J Biol Chem, 2015. **290**(52): p. 30813-29.

37. *Telomerase gene expression*. 2017 [cited 2017 2017]; Telomerase Gene Expression]. Available from: http://www.proteinatlas.org/ENSG00000164362-TERT/tissue.

38. Hayflick, L., *The Limited in Vitro Lifetime of Human Diploid Cell Strains.* Exp Cell Res, 1965. **37**: p. 614-36.

39. Heaphy, C.M., et al., *Prevalence of the alternative lengthening of telomeres telomere maintenance mechanism in human cancer subtypes.* Am J Pathol, 2011. **179**(4): p. 1608-15.

40. Peifer, M., et al., *Telomerase activation by genomic rearrangements in high-risk neuroblastoma.* Nature, 2015. **526**(7575): p. 700-4.

41. Rachakonda, P.S., et al., *TERT promoter mutations in bladder cancer affect patient survival and disease recurrence through modification by a common polymorphism.* Proc Natl Acad Sci U S A, 2013. **110**(43): p. 17426-31.

42. Li, Y. and V. Tergaonkar, *Telomerase reactivation in cancers: Mechanisms that govern transcriptional activation of the wild-type vs. mutant TERT promoters.* Transcription, 2016. **7**(2): p. 44-9.

43. Calvello, C., et al., *Alternative splicing of hTERT: a further mechanism for the control of active hTERT in acute myeloid leukemia.* Leuk Lymphoma, 2017: p. 1-8.

44. Rampazzo, E., et al., *Role of miR-15a/miR-16-1 and the TP53 axis in regulating telomerase expression in chronic lymphocytic leukemia.* Haematologica, 2017. **102**(7): p. e253-e256.

45. Cheng, et al., *Repression of telomerase gene promoter requires human-specific genomic context and is mediated by multiple HDAC1-containing corepressor complexes.* FASEB J, 2017. **31**(3): p. 1165-1178.

46. Singhi, A.D., et al., *Alternative Lengthening of Telomeres and Loss of DAXX/ATRX Expression Predicts Metastatic Disease and Poor Survival in Patients with Pancreatic Neuroendocrine Tumors.* Clin Cancer Res, 2017. **23**(2): p. 600-609.

47. Dilley, R.L. and R.A. Greenberg, *ALTernative Telomere Maintenance and Cancer.* Trends Cancer, 2015. **1**(2): p. 145-156.

48. de Wilde, R.F., et al., *Loss of ATRX or DAXX expression and concomitant acquisition of the alternative lengthening of telomeres phenotype are late events in a small subset of MEN-1 syndrome pancreatic neuroendocrine tumors.* Mod Pathol, 2012. **25**(7): p. 1033-9.

49. Lovejoy, C.A., et al., *Loss of ATRX, genome instability, and an altered DNA damage response are hallmarks of the alternative lengthening of telomeres pathway.* PLoS Genet, 2012. **8**(7): p. e1002772.

50. Heaphy, C.M., et al., *Altered telomeres in tumors with ATRX and DAXX mutations.* Science, 2011. **333**(6041): p. 425.

51. Henson, J.D., et al., *Alternative lengthening of telomeres in mammalian cells.* Oncogene, 2002. **21**(4): p. 598-610.

52. Bryan, T.M., et al., *Evidence for an alternative mechanism for maintaining telomere length in human tumors and tumor-derived cell lines.* Nat Med, 1997. **3**(11): p. 1271-4.

53. Londono-Vallejo, J.A., et al., *Alternative lengthening of telomeres is characterized by high rates of telomeric exchange.* Cancer Res, 2004. **64**(7): p. 2324-7.

54. Jiang, W.Q., et al., *Identification of candidate alternative lengthening of telomeres genes by methionine restriction and RNA interference.* Oncogene, 2007. **26**(32): p. 4635-47.

55. Zhong, Z.H., et al., *Disruption of telomere maintenance by depletion of the MRE11/RAD50/NBS1 complex in cells that use alternative lengthening of telomeres.* J Biol Chem, 2007. **282**(40): p. 29314-22.

56. Henson, J.D. and R.R. Reddel, *Assaying and investigating Alternative Lengthening of Telomeres activity in human cells and cancers.* FEBS Lett, 2010. **584**(17): p. 3800-11.

57. O'Sullivan, R.J. and G. Almouzni, *Assembly of telomeric chromatin to create ALTernative endings.* Trends Cell Biol, 2014. **24**(11): p. 675-85.

58. Pickett, H.A. and R.R. Reddel, *Molecular mechanisms of activity and derepression of alternative lengthening of telomeres.* Nat Struct Mol Biol, 2015. **22**(11): p. 875-80.

59. Mender, I. and J.W. Shay, *Telomere Restriction Fragment (TRF) Analysis.* Bio Protoc, 2015. **5**(22).

60. Nguyen, D.N., et al., *Molecular and morphologic correlates of the alternative lengthening of telomeres phenotype in high-grade astrocytomas.* Brain Pathol, 2013. **23**(3): p. 237-43.

61. Mender, I. and J.W. Shay, *Telomerase Repeated Amplification Protocol (TRAP).* Bio Protoc, 2015. **5**(22).

62. Bryan, T.M., et al., *Telomere elongation in immortal human cells without detectable telomerase activity.* EMBO J, 1995. **14**(17): p. 4240-8.

63. Dunham, M.A., et al., *Telomere maintenance by recombination in human cells.* Nat Genet, 2000. **26**(4): p. 447-50.

64. Conomos, D., R.R. Reddel, and H.A. Pickett, *NuRD-ZNF827 recruitment to telomeres creates a molecular scaffold for homologous recombination.* Nat Struct Mol Biol, 2014. **21**(9): p. 760-70.

65. Acharya, S., et al., *Association of BLM and BRCA1 during Telomere Maintenance in ALT Cells.* PLoS One, 2014. **9**(8): p. e103819.

66. Henson, J.D., et al., *The C-Circle Assay for alternative-lengthening-of-telomeres activity.* Methods, 2017. **114**: p. 74-84.

67.   Cohen, S.B. and D. Segal, *Extrachromosomal Circular DNA in Eukaryotes: Possible Involvement in the Plasticity of Tandem Repeats.* Cytogenetic and Genome Research, 2009(124): p. 327-338.

68.   Komosa, M., H. Root, and M.S. Meyn, *Visualization and quantitative analysis of extrachromosomal telomere-repeat DNA in individual human cells by Halo-FISH.* Nucleic Acids Res, 2015. **43**(4): p. 2152-63.

69.   Yeager, T.R., et al., *Telomerase-negative immortalized human cells contain a novel type of promyelocytic leukemia (PML) body.* Cancer Res, 1999. **59**(17): p. 4175-9.

70.   Fasching, C.L., et al., *DNA damage induces alternative lengthening of telomeres (ALT) associated promyelocytic leukemia bodies that preferentially associate with linear telomeric DNA.* Cancer Res, 2007. **67**(15): p. 7072-7.

71.   Wang, Z.G., et al., *Role of PML in cell growth and the retinoic acid pathway.* Science, 1998. **279**(5356): p. 1547-51.

72.   Wang, Z.G., et al., *PML is essential for multiple apoptotic pathways.* Nat Genet, 1998. **20**(3): p. 266-72.

73.   Topcu, Z., et al., *The promyelocytic leukemia protein PML interacts with the proline-rich homeodomain protein PRH: a RING may link hematopoiesis and growth control.* Oncogene, 1999. **18**(50): p. 7091-100.

74.   Salomoni, P., et al., *The promyelocytic leukemia protein PML regulates c-Jun function in response to DNA damage.* Blood, 2005. **105**(9): p. 3686-90.

75.   Shen, T.H., et al., *The mechanisms of PML-nuclear body formation.* Mol Cell, 2006. **24**(3): p. 331-9.

76.   Palibrk, V., et al., *Promyelocytic leukemia bodies tether to early endosomes during mitosis.* Cell Cycle, 2014. **13**(11): p. 1749-55.

77.   Ivanschitz, L., et al., *PML IV/ARF interaction enhances p53 SUMO-1 conjugation, activation, and senescence.* Proc Natl Acad Sci U S A, 2015. **112**(46): p. 14278-83.

78.   Hadjimichael, C., et al., *Promyelocytic Leukemia Protein Is an Essential Regulator of Stem Cell Pluripotency and Somatic Cell Reprogramming.* Stem Cell Reports, 2017. **8**(5): p. 1366-1378.

79.   Huang, D., et al., *Annexin A2-S100A10 heterotetramer is upregulated by PML/RARalpha fusion protein and promotes plasminogen-dependent fibrinolysis and matrix invasion in acute promyelocytic leukemia.* Front Med, 2017. **11**(3): p. 410-422.

80.   Iaccarino, L., et al., *Comparative genomic analysis of PML and RARA breakpoints in paired diagnosis/relapse samples of patients with acute promyelocytic leukemia treated with all-trans retinoic acid and chemotherapy.* Leuk Lymphoma, 2017: p. 1-3.

81.   Doucas, V., et al., *The PML-retinoic acid receptor alpha translocation converts the receptor from an inhibitor to a retinoic acid-dependent activator of transcription factor AP-1.* Proc Natl Acad Sci U S A, 1993. **90**(20): p. 9345-9.

82.   Grignani, F., et al., *The acute promyelocytic leukemia-specific PML-RAR alpha fusion protein inhibits differentiation and promotes survival of myeloid precursor cells.* Cell, 1993. **74**(3): p. 423-31.

83.   Borden, K.L., et al., *Two RING finger proteins, the oncoprotein PML and the arenavirus Z protein, colocalize with the nuclear fraction of the ribosomal P proteins.* J Virol, 1998. **72**(5): p. 3819-26.

84.   Song, M.S., et al., *The deubiquitinylation and localization of PTEN are regulated by a HAUSP-PML network.* Nature, 2008. **455**(7214): p. 813-7.

85.   *PML Gene*. Gene Database 2017 [cited 2017 2017]; Available from: https://www.ncbi.nlm.nih.gov/gene/5371.

86.   Reymond, A., et al., *The tripartite motif family identifies cell compartments.* EMBO J, 2001. **20**(9): p. 2140-51.

87.   Nisole, S., et al., *Differential Roles of PML Isoforms.* Front Oncol, 2013. **3**: p. 125.

88. Bernardi, R. and P.P. Pandolfi, *Structure, dynamics and function of promyelocytic leukaemia nuclear bodies* Nature Review Molecular Cell Biology, 2007. **8**: p. 1006-1016.

89. Seker, H., et al., *UV-C-induced DNA damage leads to p53-dependent nuclear trafficking of PML.* Oncogene, 2003. **22**(11): p. 1620-8.

90. Conlan, L.A., C.J. McNees, and J. Heierhorst, *Proteasome-dependent dispersal of PML nuclear bodies in response to alkylating DNA damage.* Oncogene, 2004. **23**(1): p. 307-10.

91. He, X., et al., *Characterization of the loss of SUMO pathway function on cancer cells and tumor proliferation.* PLoS One, 2015. **10**(4): p. e0123882.

92. Sahin, U., H. de The, and V. Lallemand-Breitenbach, *PML nuclear bodies: assembly and oxidative stress-sensitive sumoylation.* Nucleus, 2014. **5**(6): p. 499-507.

93. Sahin, U., et al., *Oxidative stress-induced assembly of PML nuclear bodies controls sumoylation of partner proteins.* J Cell Biol, 2014. **204**(6): p. 931-45.

94. Salsman, J., et al., *Myogenic differentiation triggers PML nuclear body loss and DAXX relocalization to chromocentres.* Cell Death Dis, 2017. **8**(3): p. e2724.

95. Melnick, A. and J.D. Licht, *Deconstructing a disease: RARalpha, its fusion partners, and their roles in the pathogenesis of acute promyelocytic leukemia.* Blood, 1999. **93**(10): p. 3167-215.

96. Xu, P. and B. Roizman, *The SP100 component of ND10 enhances accumulation of PML and suppresses replication and the assembly of HSV replication compartments.* Proc Natl Acad Sci U S A, 2017. **114**(19): p. E3823-E3829.

97. Chu, H.P., et al., *TERRA RNA Antagonizes ATRX and Protects Telomeres.* Cell, 2017. **170**(1): p. 86-101 e16.

98. Sidorova, J.M., et al., *Distinct Functions of human RECQ helicases WRN and BLM in replication fork recovery and progression after hydroxyurea-induced stalling.* DNA repair, 2013. **12**: p. 128-139.

99. McKusick-Nathans Institute of Genetic Medicine, J.H.U.B., MD). *Online Mendelian Inheritance in Man, OMIM*. [cited 2017; Available from: https://omim.org/.

100. Potts, P.R. and H. Yu, *The SMC5/6 complex maintains telomere length in ALT cancer cells through SUMOylation of telomere-binding proteins.* Nat Struct Mol Biol, 2007. **14**(7): p. 581-90.

101. Draskovic, I., et al., *Probing PML body function in ALT cells reveals spatiotemporal requirements for telomere recombination.* Proc Natl Acad Sci U S A, 2009. **106**(37): p. 15726-31.

102. Osterwald, S., et al., *PML induces compaction, TRF2 depletion and DNA damage signaling at telomeres and promotes their alternative lengthening.* J Cell Sci, 2015. **128**(10): p. 1887-900.

103. Cho, N.W., M.A. Lampson, and R.A. Greenberg, *In vivo imaging of DNA double-strand break induced telomere mobility during alternative lengthening of telomeres.* Methods, 2017. **114**: p. 54-59.

104. Brouwer, A.K., et al., *Telomeric DNA mediates de novo PML body formation.* Mol Biol Cell, 2009. **20**(22): p. 4804-15.

105. Cesare, A.J. and R.R. Reddel, *Alternative lengthening of telomeres: models, mechanisms and implications.* Nat Rev Genet, 2010. **11**(5): p. 319-30.

106. Chung, I., H. Leonhardt, and K. Rippe, *De novo assembly of a PML nuclear subcompartment occurs through multiple pathways and induces telomere elongation.* J Cell Sci, 2011. **124**(Pt 21): p. 3603-18.

107. Balk, B., et al., *Telomeric RNA-DNA hybrids affect telomere-length dynamics and senescence.* Nat Struct Mol Biol, 2013. **20**(10): p. 1199-205.

108. Perrem, K., et al., *Repression of an alternative mechanism for lengthening of telomeres in somatic cell hybrids.* Oncogene, 1999. **18**(22): p. 3383-90.

109. Seluanov, A., et al., *DNA end joining becomes less efficient and more error-prone during cellular senescence.* Proc Natl Acad Sci U S A, 2004. **101**(20): p. 7624-9.

110.   Shekhani, M.T., et al., *High-resolution telomere fluorescence in situ hybridization reveals intriguing anomalies in germ cell tumors.* Hum Pathol, 2016. **54**: p. 106-12.

111.   Arnoult, N., A. Van Beneden, and A. Decottignies, *Telomere length regulates TERRA levels through increased trimethylation of telomeric H3K9 and HP1alpha.* Nat Struct Mol Biol, 2012. **19**(9): p. 948-56.

112.   Bailey, S.M., M.A. Brenneman, and E.H. Goodwin, *Frequent recombination in telomeric DNA may extend the proliferative life of telomerase-negative cells.* Nucleic Acids Res, 2004. **32**(12): p. 3743-51.

113.   Takai, H., A. Smogorzewska, and T. de Lange, *DNA damage foci at dysfunctional telomeres.* Curr Biol, 2003. **13**(17): p. 1549-56.

114.   Kim, H., et al., *Systematic analysis of human telomeric dysfunction using inducible telosome/shelterin CRISPR/Cas9 knockout cells.* Cell Discov, 2017. **3**: p. 17034.

115.   Cesare, A.J., et al., *Spontaneous occurrence of telomeric DNA damage response in the absence of chromosome fusions.* Nat Struct Mol Biol, 2009. **16**(12): p. 1244-51.

116.   Henson, J.D., et al., *DNA C-circles are specific and quantifiable markers of alternative-lengthening-of-telomeres activity.* Nat Biotechnol, 2009. **27**(12): p. 1181-5.

117.   Quinet, A., D. Lemacon, and A. Vindigni, *Replication Fork Reversal: Players and Guardians.* Mol Cell, 2017. **68**(5): p. 830-833.

118.   Hustedt, N. and D. Durocher, *The control of DNA repair by the cell cycle.* Nat Cell Biol, 2016. **19**(1): p. 1-9.

119.   Kastenhuber, E.R. and S.W. Lowe, *Putting p53 in Context.* Cell, 2017. **170**(6): p. 1062-1078.

120.   Mak, T.W., J.M. Penninger, and P.S. Ohashi, *Knockout mice: a paradigm shift in modern immunology.* Nat Rev Immunol, 2001. **1**(1): p. 11-9.

121.   Full, F., et al., *Gammaherpesviral Tegument Proteins, PML-Nuclear Bodies and the Ubiquitin-Proteasome System.* Viruses, 2017. **9**(10).

122.   Chang, H.R., et al., *The functional roles of PML nuclear bodies in genome maintenance.* Mutat Res, 2017.

123.   Sobinoff, A.P. and H.A. Pickett, *Alternative Lengthening of Telomeres: DNA Repair Pathways Converge.* Trends Genet, 2017. **33**(12): p. 921-932.

WALTER BARRY

2725 North Charles St. Apt 3 Baltimore, MD • waltertbarry@gmail.com • 508-494-9406

Present position: Johns Hopkins School of Medicine, Baltimore MD

Cellular and Molecular Medicine PhD program

Doctoral Thesis with Dr. Alan K. Meeker

Aim to cure 10% of cancers by Cas9 targeting of the promyelocytic leukemia protein (PML) component of the alternative lengthening of telomeres pathway   2013-Present

Experience:

Johns Hopkins School of Medicine, Baltimore MD

Cellular and Molecular Medicine PhD program

Doctoral Work with the laboratories of Dr. Stephen Baylin, Dr. Elias Zambidis

Induced pluripotent stem cell (iPS) generation as a model of oncogenesis   2011-2013

The Rockefeller University, New York City NY

Laboratory of Charles Rice, Hepatitis C center

Research Assistant and mouse colony manager

Generation of a mouse model for hepatitis C infection   2009-2011

PUBLICATIONS

Expression of paramyxovirus V proteins promotes replication and spread of hepatitis C virus in cultures of primary human fetal liver cells. Andrus L, Marukian S, Jones CT, Catanese MT, Sheahan TP, Schoggins JW, **Barry WT**, Dustin LB, Trehan K, Ploss A, Bhatia SN, Rice CM. Hepatology. 2011 Dec;54(6):1901-12

A genetically humanized mouse model for hepatitis C virus infection. Dorner M, Horwitz JA, Robbins JB, **Barry WT**, Feng Q, Mu K, Jones CT, Schoggins JW, Catanese MT, Burton DR, Law M, Rice CM, Ploss A. Nature. 2011 Jun 8;474(7350):208-11

Development of human CD4+FoxP3+ regulatory T cells in human stem cell factor-, granulocyte-macrophage colony-stimulating factor-, and interleukin-3-expressing NOD-SCID IL2Rγ(null) humanized mice. Billerbeck E**, Barry WT**, Mu K, Dorner M, Rice CM, Ploss A. Blood. 2011 Mar 17;117(11):3076-86

A humanized mouse model to study hepatitis C virus infection, immune response, and liver disease. Washburn ML, Bility MT, Zhang L, Kovalev GI, Buntzman A, Frelinger JA, **Barry W**, Ploss A, Rice CM, Su L. Gastroenterology. 2011 Apr;140(4):1334-44

PRESENTATIONS

National

"The promyelocytic leukemia (PML) protein is dispensable for the alternative lengthening of telomeres (ALT) pathway and its loss leads to an increased rate of recombination at telomeres" Poster, American Association for Cancer Research, Washington DC 2017

"The promyelocytic leukemia (PML) protein is dispensable for the alternative lengthening of telomeres (ALT) pathway and its loss leads to an increased rate of recombination at telomeres" Poster, Cold Spring Harbor Laboratory, Cold Spring Harbor, NY

Regional

"Characterization of ALT Associated PML bodies" Poster, Baltimore Area Repair Symposia, Baltimore, MD 2016

<u>**Industry experience**</u>

Sirtris Pharmaceuticals Cambridge, MA   2006- 2007

Assistant Compound Manager

Determined solubility of new chemical entities (NCE's) by HPLC and UPLC.

<u>**Education**</u>

Tufts University, Medford MA   2005-2009

Bachelor of Science in Biochemistry

Summa Cum Lade with Highest Thesis Honors

3.84 GPA

UNDERGRADUATE AWARDS/HONORS

Dean's List all Semesters

Phi Beta Kappa Member

The Paula Frazier Poskitt Honor (for Biological Research)

The Durkees Scholarship (For Chemical Research)

UNDERGRADUATE RESEARCH EXPERIENCE

Cold Spring Harbor Laboratories, Cold Spring Harbor, NY   Summer 2008

Laboratory of Dr. Bruce Stillman

Summer Undergraduate Researcher, Summer Undergraduate Research Program

The impact of mutations in the origin recognition complex (ORC) on replication origin firing

Tufts University, Department of Chemistry, Somerville, MA   2007- 2009

Head Teaching Assistant, Introductory Chemistry

Tufts University, Department of Chemistry, Somerville, MA   2007-2009

Laboratory of Dr. David H. Lee Undergraduate Researcher

Sulfonation of proteins as a chemical mimic of phosphorylation